Fabrication and Characterization of Hydroxyapatite Based Biocompatible Composite Scaffold for Bone Tissue Engineering.

M.S. THESIS-2017

SUBMITTED BY

Poulomi Das

EXAMINATION ROLL-14276002

DEPARMENT OF MATHEMATICS AND NATURAL SCIENCES

BRAC UNIVERSITY

DHAKA, BANGLADESH

Fabrication and Characterization of Hydroxyapatite Based Biocompatible Composite Scaffold for Bone Tissue Engineering.

M.Sc. THESIS-2017

A DISSERTATION SUBMITTED TO THE DEPARMENT OF MATHEMATICS AND NATURAL SCIENCES, BRAC UNIVERSITY, IN PARTIAL FULFILLMENT OF THE REQUIREMENT FOR THE DEGREE OF MASTER OF SCIENCE IN BIOTECHNOLOGY.

DEPARMENT OF

MATHEMATICS AND NATURAL SCIENCES

BRAC UNIVERSITY

DHAKA, BANGLADESH

SUBMITTED BY

Poulomi Das

EXAMINATION ROLL-14276002

DEDICATED

TO

MY BELOVED PARENTS

Declaration

I hereby solemnly declare that the research work embodying the results reported in this thesis entitled "**Fabrication and Characterization of Hydroxyapatite Based Biocompatible Composite Scaffold for Bone Tissue Engineering**" submitted by undersigned candidate in partial fulfillments of the requirements for the degree of Master of Science in Biotechnology under the Department of Mathematics and Natural Sciences (MNS), BRAC University, Mohakhali, Dhaka was carried out under the joint supervision of Professor Dr. Naiyyum Choudhury, Chairman of the Bangladesh Atomic Energy Regulatory Authority (BAERA) and the former coordinator of Biotechnology Program, MNS Department, BRAC University and Dr. S. M. Asaduzzaman, Principal Scientific Officer and Director, Institute of Tissue Banking and Biomaterial Research, Atomic Energy Research Establishment, Savar, Dhaka. It is further declared that the research work presented here is original and has not been submitted to any other institution for any degree or diploma.

Poulomi Das
Candidate

Professor Dr. Naiyyum Choudhury
Supervisor
Chairman
Bangladesh Atomic Energy Regulatory Authority
Agargaon, Dhaka
&
Former coordinator
Department of Mathematics and Natural Sciences
BRAC University, Dhaka.

S. M. Asaduzzaman, Ph.D.
Supervisor
Principal Scientific Officer & Director
Institute of Tissue Banking and Biomaterial Research
Atomic Energy Research Establishment
Savar, Dhaka.

ACKNOWLEDGMENT

First of all, I would like to thank the Almighty.

I would like to express my special thanks of gratitude to my supervisor Professor Dr. Naiyyum Choudhury, Chairman of the Bangladesh Atomic Energy Regulatory Authority (BAERA) and the former coordinator of Biotechnology Program, MNS Department, BRAC University. Without his contribution I would not be able to get the chance to pursue my thesis work at Institute of Tissue Banking and Biomaterial Research (ITBBR) of Atomic Energy Research Establishment (AERE), Savar, Dhaka.

I offer my profound reverence to my supervisor Dr. S.M. Asaduzzaman, Principal Scientific Officer and Director of ITBBR, AERE, Savar, Dhaka for providing me the chance to do my thesis work in ITBBR.

I am very much grateful to Naznin Akhtar, Senior Scientific Officer of ITBBR, AERE, Savar, Dhaka. She always helped me to develop my thesis work with dynamic, guidance, effective encouragement, cordial co-operation, purposeful and valuable advices in performing the work and preparation of this thesis.

I am grateful to Professor A. A. Ziauddin Ahmed, Chairperson, Department of Mathematics and Natural Sciences (MNS), BRAC University for allowing me to undertake my M.Sc. program in the Department of MNS and encouraging me in all my academic activities.

I am thankful to all of my fellows and lab mates of ITBBR, AERE, Savar, Dhaka for helping me and providing mental support and encouragement.

Most importantly, none of this would have been possible without the love and patience of my family. I would like to express my heart-felt gratitude to my family. I warmly appreciate the generosity and understanding of family. Many friends have helped me to stay sane through this difficult time. Their support and care helped me overcome setbacks and stay focused on my thesis. I greatly value their friendship and I deeply appreciate their belief in me.

Poulomi Das
Department of Mathematics and Natural Sciences
BRAC University
Dhaka, Bangladesh.

List of Figure

List of Tables

Abstract

Bone tissue engineering with cells and synthetic extracellular matrix represents a new approach for the regeneration of mineralized tissue for the transplantation of bone. Hydroxyapatite and its composite with biopolymers are extensively developed and applied in bone tissue regeneration. The main aim of this study was to fabricate and characterize a biomimetic scaffolds through thermal inducing phase separation technique and cross-linked using physical and chemical method. In this regard, two biomimetic [Hydroxyapatite/chitosan-alginate (HCA) and Hydroxyapatite/collagen-chitosan (HCC)] scaffolds were fabricated and characterized by porosity & density, swelling kinetics, biodegradability, fourier transform infrared spectroscopy (FTIR), scanning electron microscope (SEM) analysis and also compared with human bone allograft (HBA).

Following the freeze drying technique, HCA scaffold was prepared in two different ratios (2:1 and 1:1). A cross linker agent, 2-Hydroxylmethacrylate (HEMA) was added at different percentage (0.5% - 2%) into the selected composition and irradiated at 5 kGy - 25 kGy to optimize the proper mixing of components in the presence of HEMA. Porosity of the prepared scaffold was nearly similar to the Human Bone Allograft (HBA) and the value was 62% to 86%. However, density of the scaffold was comparatively lower (0.004 g/cm^3 - 0.076 g/cm^3) than HBA. Nonetheless, in-vitro biodegradation analysis showed that the remaining weight of scaffold was lower (10% - 50%) than HBA. FTIR analysis depicted the intermolecular interaction between components in the scaffold. Pore size of a scaffold was nearly comparable (162 µm - 510 µm) with HBA.

Again, another scaffold HCC was fabricated through freeze drying method and cross-linked using chemical cross-linker (HEMA & glutaraldehyde solution) and physical cross linker (de-hydrothermal treatment). In this study, porosity and density of the prepared scaffold were 90.64% to 96.21% and 0.004 g/cm^3 to 0.076g/cm^3 respectively. In contrast, scaffold had nearly similar biodegradation rate (10% - 55%) than HBA. FTIR analysis showed intermolecular interaction between components in the scaffold. Pore size of a scaffold was nearly comparable (111.80 µm - 212.60 µm) with HBA.

Finally, scaffold (HCA and HCC) samples were compared with HBA to determine the best scaffolds that mimic the human bone. The porosity of HBA was found 96%; comparing with the

other two samples (HCA and HCC), it was 86% and 91%, which is closely enough to the HBA. Then density properties showed huge difference among three samples; i.e, for HBA, it showed 0.625 g/cm^3 and HCC sample showed 0.183 g/cm^3 but HCA sample showed 0.076 g/cm^3, which was very poor comparing to the HBA. In the contrast, the water uptaking rate varied drastically, in which HCA showed highest water absorption rate 354.61% and HCC showed 307.23% but water absorption rate for HBA was 51.30%. Further, comparing the degradation properties among HBA, HCA and HCC; it was found that the remaining weight of sample HCA and HCC for day 1 & day 7 were 78.57 & 50% and 90 & 87% consequently; whilst remaining weight of HBA was found to be 89% for day 1 and 80.82% for day 7, which is closely related with HBA. Pore size of the scaffold was nearly comparable (162 µm - 510 µm) and (111.80 µm - 212.60 µm) for HCA and HCC with HBA (420 µm - 623µm). Above results suggest that the porous bone scaffolds that were fabricated in this study might be a potential bone substitute to be used in reconstructive surgery.

Introduction

1.1 Background

Human body is a complex network of different organs and tissues with specific functions. 8% of healthcare spending globally accounts for organ replacement and nearly a quarter of patients die before receiving their transplant. Risk of disease transmission and immune-rejection in allogeneic transplantation also limit the transplantations. Therefore, alternative biomedical solutions need to be developed to address the above serious issues in health care systems. Tissue engineering offers to bypass these difficulties by replacing and restoring various tissues through delivering the cells derived from the patient into an engineered platform to pre-engineer custom tissue construct for implantation (Naderi *et al*., 2011). Although, classical cell culture on two dimensional (2D) environment are widely used to understand secrets in cell biology, the cells reside, proliferate, differentiate and mature in three dimensional (3D) microenvironment in body; thus, this research focuses on biomaterial based 3D microenvironment. The general approach is usually to seed the cells within a 3D structural scaffold that outlines the geometry of replacement tissue. In 3D scaffold, cell fate and functions extremely depend on the cell microenvironment, in which coordination among spatial, temporal, mechanical and chemical cues is vital to produce complex functional tissue construct (Naderi *et al*., 2011).

Thus the design and selection of materials in scaffold fabrication is the first important step for intended tissue engineering. While structural design depends on various fabrication methods including phase separation, freeze-drying, foaming, particle leaching, electrospinning, and sintering, material selection dictates the material's biocompatibility and biodegradability, support for cell adhesion, proliferation, migration and differentiation, and finally, adaptability to scaffold manufacturing techniques (Kim *et al*., 2011). Some other criteria such as chemistry, molecular weight, solubility, hydrophobicity/ hydrophilicity, surface energy, water absorption etc. also play role in material selection process. Among all, natural materials are more biocompatible, easily available in abundance and can be processed easily compared to others. On the other hand, the properties (e.g. mechanical properties, porosity, biodegradability, density, swelling kinetics etc.) of synthetic biomaterials can be tailored for specific applications. In some cases, synthetic

biomaterials are cheaper than natural ones and can be produced in large quantities with uniform properties, have long shelf life (Dhandayuthapani *et al*., 2011).

Despite all these, natural biomaterials are preferable in tissue engineering due to their superior biological properties. Most commonly used natural biomaterials in tissue engineering are collagen, gelatin, alginate, chitosan, hyaluronic acid and fibrins - all of which are polymers (Kim *et al.,* 2011). Among them, chitosan has higher mechanical properties and easily available in abundance and can be processed easily compared to others. Commonly produced from crab shells, chitosan is non-toxic and biodegradable; its hydrophilic surface promotes cell adhesion and proliferation (Bhattarai *et al*., 2010, Kean *et al*., 2010) unlike the natural polymers derived from costly mammalian proteins and chitosan evokes minimal foreign body response and fibrous encapsulation. (Jayakumar *et al*., 2010, Bhattarai *et al*., 2005, Lee *et al*., 2009, Kim *et al*., 2008) Moreover, chitosan is a semi-crystalline polymer, so, mechanical properties can be tailored according to requirement in scaffold fabrication. Alginate is a naturally occurring anionic and hydrophilic polysaccharide. It is one of the most abundant biosynthesized materials (Narayanan *et al*., 2012, Skjak-Braerk *et al*., 1989) and is derived primarily from brown seaweed and bacteria. Alginate is of particular interest for a broad range of applications as a biomaterial and especially as the supporting matrix or delivery system for tissue repair and regeneration. Due to its outstanding properties in terms of biocompatibility, biodegradability, non-antigenicity and chelating ability, alginate has been widely used in a variety of biomedical applications including tissue engineering, drug delivery and in some formulations preventing gastric reflux (Stevens *et al*., 2004, Kuo *et al*., 2001).Type I collagen also another important structural protein factor that is widely used in clinically as scaffold due to its hydration properties such as swelling and solubility. Collagen generally obtained either from cultured cells or extracted from native tissues. In this experiment type I collagen was extracted from bovine derived epidermal cells. Another crucial biomaterial for scaffold fabrication is hydroxyapatite (HA). HA has a chemical composition similar to human mineral tissue and can be synthesized from many natural sources with calcium-based structures, such as bovine bone, mollusk shell and coral (Vecchio *et al*., 2007, Barakat *et al*., 2008).

This study focuses on fabricating and characterizing composite scaffold, synthesized from three natural-based materials – chitosan, alginate, collagen and HA for bone tissue engineering. In

combination of right amount of chitosan-alginate and chitosan-collagen concentration and in-situ co-precipitation method, we prepared high strength porous HA scaffolds with wide range of properties including pore size, density, and mechanical strength and thus could be suitable for bone tissue regeneration as well as other biomedical applications.

1.2 Literature Review

1.2.1 Tissue engineering

Tissue engineering is the use of a combination of cells, engineering and materials methods, and suitable biochemical and physicochemical factors to improve or replace biological functions. Tissue engineering involves the use of a scaffold for the formation of new viable tissue for a medical purpose. While it was once categorized as a sub-field of biomaterials, having grown in scope and importance, it can be considered as a field in its own right.

While most definitions of tissue engineering cover a broad range of applications, in practice the term is closely associated with applications that repair or replace portions of or whole tissues (i.e., bone, cartilage, blood vessel, bladder, skin, muscle etc.). Often, the tissues involved require certain mechanical and structural properties for proper functioning. The term has also been applied to efforts to perform specific biochemical functions using cells within an artificially-created support system (e.g. an artificial pancreas, or a bio artificial liver). A schematic overview of tissue engineering is shown in the Figure 1.1.

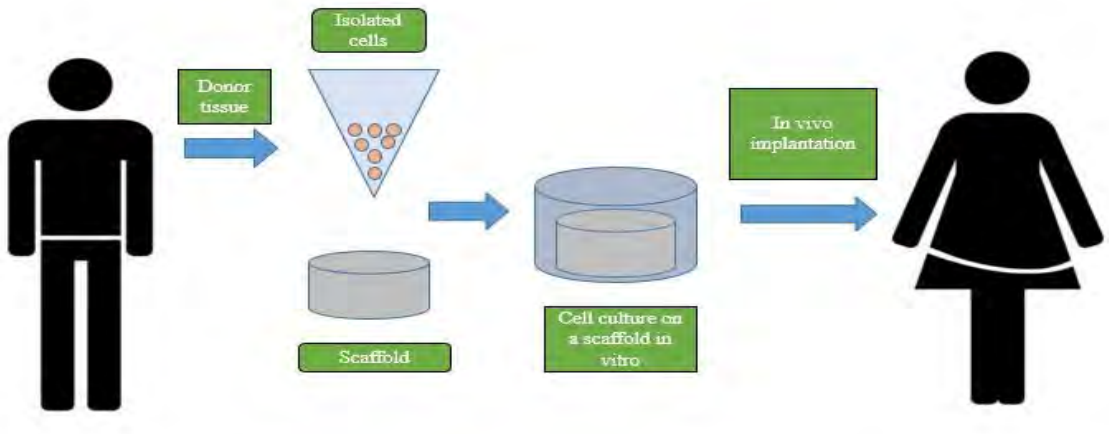

Figure 1.1: Schematic of tissue engineering principle

1.2.2 Bone tissue engineering

The main role of bone is to provide structural support to the body (Salgado *et al*., 2004). It also supports muscular contraction resulting in motion and withstands load bearing and protects internal organs (Sommerfeldt *et al*., 2001). Due to injury or disease in bone, the structure of bone can be altered; thus affecting the body equilibrium and quality of life. Current therapies such as bone grafting have limitation due to lack of supply, morbidity and immunogenicity. As an alternative, tissue engineering for bone regeneration has got importance in last 10 years.In adult skeleton, bone tissue is organized in two structural forms: spongy or trabecular bone consisted of 20% of total skeleton and compact or cortical bone consisted of 80% of total skeleton (Sikavitsas *et al*., 2001). Trabecular bone shows a porosity of 50-90% whereas cortical bone has the porosity only 10%. The modulus and strength of trabecular bone are 20 times lower than cortical bone. Trabecular bone is arranged with honeycomb of branching bars, plates and rods of various sizes. Cortical bone has three types: long bone (femur and tibia), short bones (wrist and ankle), and flat bones (skull vault and irregular bones). There are three types of cells responsible for elaboration, maintenance and resorption of bone tissue from their interactions and they are osteoblast, osteocytes and osteoclasts (Ducy *et al*., 2000, Aubin *et al*., 1996). They have defined tasks and very crucial for healthy bone tissue maintenance. A schematic of cortical and trabecular bone is shown in Figure 1.2.

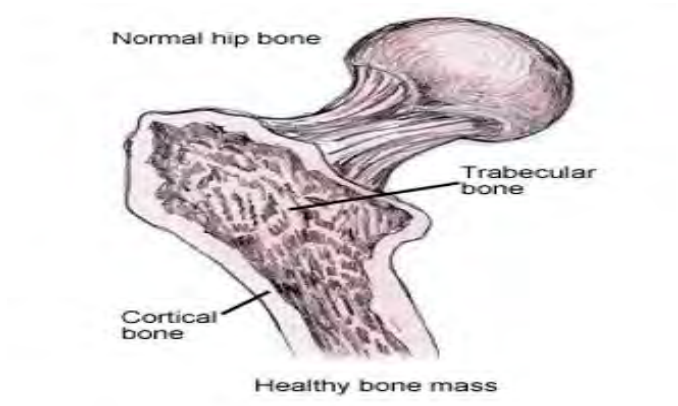

Figure 1.2: Schematic diagram of cortical and trabecular bone (Einhorn *et al*., 2007)

Most of bone properties depend on the composition of matrix, which has two components: a mineral part, made of hydroxyapatite and an organic part, composed of glycoproteins, proteoglycans, sialoproteins and glaproteins. Mineral part contributes 65-70% of the matrix, whereas organic part consists of remaining 30-35% of the matrix (Aubin *et al*., 1996). With very limited damage or fracture, bone has unique capacity to heal and remodel without leaving any scar. For larger damage or diseases, tissue engineering is the only option as conventional grafting methods face difficulties.

1.2.3 Requirements of bone grafting

Bone replacements, compact structure provides good mechanical strength while a porous structure is suitable for cell attachment and blood supply (Cai *et al*., 2009). Bone tissue engineering creates a biological material that provides the option for implantation and/or prosthesis. Bone tissue engineering has three main requirements: osteoconductive biomaterial scaffolds, osteogenic cells and osteoinductive molecules (Vachiraroj *et al*., 2009).

Osteoinduction: This term means that primitive, undifferentiated and pluripotent cells are somehow stimulated to develop into the bone-forming cell lineage. One proposed definition is the process by which osteogenesis is induced (Wilson and Hench, 1987).

Osteoconduction: This term means that bone grows on a surface. An osteoconductive surface is one that permits bone growth on its surface or down into pores, channels or pipes. Wilson-Hench (Wilson and Hench, 1987) has suggested that osteoconduction is the process by which bone is directed so as to conform to a material's surface. However, Glantz (Glantz, 1987) has pointed out that this way of looking at bone conduction is somewhat restricted, since the original definition bears little or no relation to biomaterials.

Osteogenesis: It occurs when vital osteoblasts originating from bone graft material contributes to the growth of new bone along with bone formation.

Graft is performed as a medical procedure to repair a damage tissue. Three different type of graft exist depending on their sources .Those include autografts, allografts and xenografts.

Autograft: Autologous or autogenous bone grafting involves utilizing bone obtained from same individual receiving the graft. Bone can be harvested from nonessential bones, such as from iliac crest, mandibular symphysis (chin area), and anterior mandibular ramus (coronoid process). When a block graft will be performed, autogenous bone is the most preferred, because there is less risk of graft rejection as the graft is originated from the patient′s body (Conrad *et al*., 1995). It would be osteoinductive and osteogenic, as well as osteoconductive. Disadvantage of autologous grafts is that additional surgical site is required, another potential location for postoperative pain and complications (Conrad *et al*., 1995).

All bones require blood supply in the transplanted site. Depending on where the transplant site is and size of the graft, an additional blood supply may be required. For these types of grafts, extraction of the part of the periosteum and accompanying blood vessels along with the donor bone is required. This kind of graft is known as a free flap graft.

Allograft: Allograft is derived from humans. The difference is that allograft is harvested from an individual other than the one receiving the graft. Allograft bone is taken from cadavers that have donated their bone so that it can be used for living people who are in need of it; it is typically sourced from a bone bank.

There are three types of bone allograft available: (Florida and Louisiana, 2001)

1. Fresh or fresh-frozen bone
2. Freeze-dried bone allograft (FDBA)
3. Demineralized freeze-dried bone allograft (DFDBA)

The use of allografts for bone repair often requires sterilization and deactivation of proteins normally found in healthy bone. Contained in the extracellular matrix of bone tissue are the full cocktail of bone growth factors, proteins, and other bioactive materials necessary for osteoinduction and successful bone healing; the desired factors and proteins are removed from the mineralized tissue by using a demineralizing agent, such as hydrochloric acid. The mineral content of the bone is degraded, and the osteoinductive agents remain in a demineralized bone matrix (DBM).

Xenograft: Xenograft bone substitute has its origin from a species other than human, such as bovine bone (or recently porcine bone), which can be freeze dried or demineralized and deproteinized. However, the bioactive properties of xenografts are weaker than allografts and autografts. To improve xenografts, a new treatment technique has been introduced for bone or tissue repair called bone tissue engineering. Different types of graft are shown in Figure 1.3.

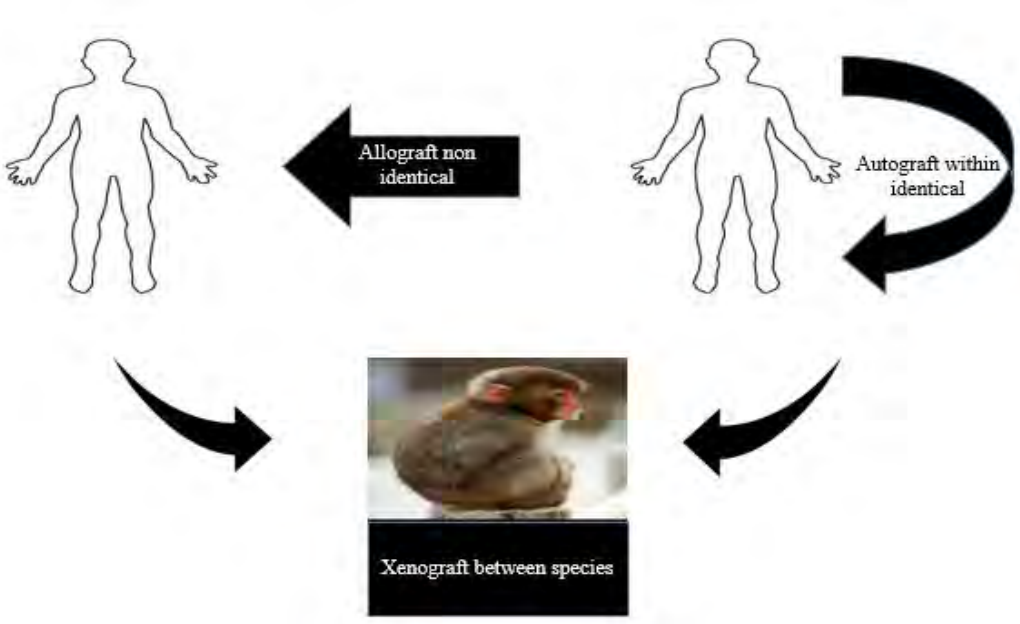

Figure 1.3: Different types of graft

Synthetic variants: Flexible hydrogel-hydroxyapatite composite, which has a mineral to organic matrix ratio, approximating that of human bone.

Artificial bone can be created from ceramics, such as calcium phosphates (e.g., HA and tricalcium phosphate), bioglass, and calcium sulphate are biologically active depending on solubility in physiological environment. These materials combine with growth factors, ions, such as strontium or mixed with bone marrow aspirate to increase biological activity. The presence of elements, such as strontium can result in higher bone mineral density (BMD) and enhanced osteoblast proliferation.

Alloplastic grafts: Alloplastic grafts may be made from HA, a naturally occurring mineral (main mineral component of bone), made from bioactive glass. HA is a synthetic bone graft, which is the

most used now due to its osteoconduction, hardness, and acceptability by bone. Some synthetic bone grafts are made of calcium carbonate, which start to decrease in usage, because it is completely resorbable in short time and makes breaking of the bone easier. Finally used is the tricalcium phosphate in combination with HA and thus giving effect of both, osteoconduction and resorbability.

1.2.3.1 Cell

Primary cells are retrieved from natural tissues. They have been widely used in tissue engineering and are commercially available (Vacanti *et al*., 1999). It is important to choose an effective cell source so that sufficient cells can be available and the cells can maintain certain phenotype to obtain functional tissues. All cell sources have advantages and disadvantages. As for example, progenitor cells are non-immunogenic and show required phenotype; however, harvesting appropriate cell number is difficult. Their differentiated cells don't grow further in long-term cell culture and instead display diverse phenotype with the change of culture condition. Thus, immortal cell lines have been developed and they are commercially available too. These cells have unlimited expansion capabilities in an appropriate microenvironment. On the other hand, cell lines from tumor cells induce mortality through cell mutation (Li *et al*., 2010). Therefore, choosing of special cell type for controlled expression of phenotype to mimic the natural tissue is important.

Stem cells have the potential for self-renewal and differentiation into different lineages depending on microenvironment and thus have emerged as prospective cell source (Reya *et al*., 2001). One of them is embryonic stem cell (ESC) line which has least commitment and can be differentiated into any type of tissue. However, ethical issues restrict their application. Alternatively, adult stem cells (ASCs) harvested from mature tissues, such as bone marrow, mammary gland, small and large intestine can differentiate into several types of tissues including bone, liver, and muscle etc. (Prabhakaran *et al*., 2009, Miyazaki *et al*., 2002, Dezawa *et al*., 2005). They are not controversial in terms of ethical issues. However, they don't possess unlimited self-renewal as of ESC and have low harvesting density (Barry *et al*., 2003, Ulloa-Montoya *et al*., 2005). Most immortal cells raise immune response in in-vivo applications, although they are sufficient in in vitro characterization for tissue engineering.

1.2.3.2 Growth factor

Growth factors (GFs) are polypeptides that send signals to stimulate or inhibit moderate cellular activities, such as proliferation, differentiation, gene expression, adhesion and migration. Same GF can be applied to different cell types with same or different effects and different cell types can produce same GF. GFs first bind to specific receptors on the surface of target cells and then initiate their actions. Depending on sites of actions, GF can be classified as endocrine (target cell is distant), paracrine (target cell is nearby), autocrine (target cell is the same cell that secreted the growth factor) and intracrine (growth factor is internalized). There are hundreds of GFs that have been identified, characterized and grouped based on structural homologies (McKay *et al*., 1993). Common osteogenic GFs are transforming growth factor-β1 (TGF-β1), bone morphogenetic protein-2 (BMP-2), and osteogenic protein (OP-1 or BMP-2) (Babensee *et al*., 2000). For muscle tissue engineering, generally used GFs are insulin-like growth factors (IGFs) and muscle specific microRNAs. For nerve regeneration, nerve growth factor (NGF), glial cell line-derived neurotropic factor (GDNF) and ciliaryneurotrophic factor (CNTF) are generally used. For potential efficacy, GFs need to be released over an extended time period and this can be achieved by incorporation of GFs into polymer carriers (Vasita *et al*., 2006). These carriers could be macroscale scaffold, hydrogel, micro or nanoscale particles and fibers etc. Polymeric carrier will degrade slowly in tissue engineering environment and GFs will be released. The release of GFs may occur through diffusion process or combination of diffusion and biomaterials degradation. Schematic illustration of methods for immobilization of bioactive factor molecules (growth factors) and cross linkers into hydrogels scaffolds is shown in Figure 1.4.

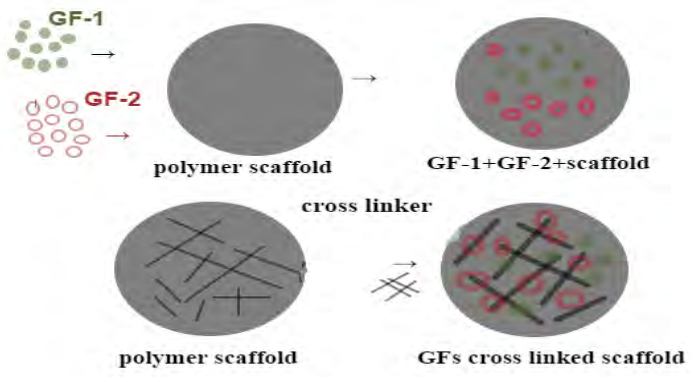

Figure 1.4: Schematic illustration of methods for immobilization of bioactive factor molecules (growth factors) and cross linkers into hydrogels scaffolds

A number of growth factors, which can be incorporated in polymer hydrogels and scaffolds to promote tissue regeneration, are given in Table 1.1.

Table 1.1: A number of growth factors, which can be incorporated in polymer hydrogels and scaffolds to promote tissue regeneration, are given below

Growth factors	Tissue engineering application	Function	Reference
Ang-1	Blood vessel, heart, and muscle	Promote maturation and stability of blood vessel.	(Lee *et al*., 2011)
Ang-2	Blood vessel	Destabilize, regress and disassociate ECs from surrounding tissues.	(Lee *et al*., 2011)
BMP-2	Bone and cartilage	Promote differentiation and migration of osteoblasts.	(Gautschi *et al.,* 2007, Nagai and Embil, 2002, Kempen *et al*.,2009)
BMP-7	Bone, cartilage and kidney	Enhance differentiation and migration of osteoblasts, as well as renal development	(Lee *et al*., 2011, Gautschi *et al.*, 2007)
BMP-9	Bone	Enhance osteogenic differentiation and bone formation.	(Chen *et al*.,2010)
EGF	Blood vessel, bone, skin, nerve, spine, and muscle	Maintaining epithelial cell growth, proliferation and differentiation.	(Lee *et al*., 2011)
FGF-2	Blood vessel, bone, skin, nerve, spine, and muscle	Induce angiogenesis; enhance the formation of blood vessels; migration, proliferation and survival of ECs; inhibition of differentiation of embryonic stem cells.	(Lee *et al*., 2011)
NGF	Nerve, spine, and brain	Survival and proliferation of neural cells.	(Lee *et al*., 2011)
PDGF	Blood vessel, muscle, bone, cartilage, and skin	Function for embryonic development, proliferation, migration, growth of ECs.	(Lee *et al*., 2011)
TGF-α	Brain and skin	Assisting proliferation of basal cells or neural cells.	(Lee *et al*., 2011)
TGF-β	Bone and cartilage	Enhancing proliferation and differentiation of bone-forming cells, anti-proliferative factor for epithelial cells.	(Lee *et al*., 2011)

1.2.3.3 Scaffolds

Scaffold is a well-designed three dimensional structure that guide tissue formation both in vivo and in vitro. Degradable porous materials integrated with biological cell or molecules to regenerate tissue are an advanced approach to the tissue engineering that utilizes synthetic implants and tissue graft (Hollister *et al*., 2005). Consequently, the selection of scaffold is important that enable the cells to behave in the desired manner so that the regeneration of tissue and organs has desired shape and size.

1.2.3.3.1 Requirements of scaffold

Within tissue engineering one of the major research themes id scaffold design. A scaffold serves as a temporary support for isolated cells to grow into new tissue before transplantation back to the host. The design scaffold determines the functionality of the construct to a high extent. Although the final requirements depends on the specific purpose of the scaffold, several general characteristics and requirements needed to be consider for all designed. (Hutmacher, 2000, Kretlow *et al*., 2008, Liu *et al*., 2007, Moroni *et al*., 2008).

The scaffold should be/have:

- **Biodegradable-** The scaffold materials should degrade in tandem with tissue regeneration and remodeling of the extracellular matrix (ECM) into smaller nontoxic substances without interfering with the function of the surrounding tissue (Hutmacher, 2011).
- **Promote cell attachment, spreading and proliferation-** Vital for the regulation of cell growth and differentiation (Ito *et al*., 1997).
- **Suitable mechanical strength**- Its strength should be comparable to in vivo tissue at the site of implantation as evidently, a scaffold requires more flexibility or rigidity depending on the application in e.g., cardiovascular versus bone prostheses (Mitragotri *et al*., 2009).
- **Good transport properties-** To ensure sufficient nutrient transport towards the cells and removal of waste products the scaffold should be highly porous with good pore connectivity, however, it should maintain sufficient mechanical strength implying optimization of porosity (Hutmacher, 2011, Agrawal *et al*., 2001, Karageorgiou *et al*., 2005, Karande *et al*., 2004).

- **Easy to connect to the vascularization system of the host-** To ensure good nutrient supply throughout the scaffold post implantation, the scaffold should be connected to the natural nutrient supplying system (Hutmacher, 2011, Agrawal *et al*., 2001, Kannan *et al*., 2005).
- **Suitable surface characteristics-** Apart from optimal physiochemical properties, research suggests that the introduction of e.g., surface topography into the scaffold improves tissue organization leading to increased tissue function (Dunn *et al*., 1976, Falconnet *et al*., 2006, Flemming *et al*., 1999, Papenburg *et al*., 2007).

1.2.3.3.2 Biomaterials

Biomaterials are originated from a wide range of natural as well as synthetic sources. This section only describes the selection of widely used materials and focuses more on the materials used in this thesis. Many biomaterials have been used as scaffold for cell culture and they can be divided into four main categories: natural polymers, synthetic polymers, bio ceramics and composites (Garg *et al*., 2012, Zanetti *et al*., 2013).

1.2.3.3.2.1 Natural polymers

Natural polymers have been and continued to be the materials most used for scaffold fabrication because of their great similarity to the extracellular matrix structure and their biocompatibility and biodegradability (Garg *et al*., 2012). In fact, they can easily be modified, degraded and absorbed in vivo by enzymes naturally present in the human body (Gaalen, 2008). Natural polymers are derived mainly from animal sources, but vegetable sources have also been investigated (Kohf *et al*., 2010, Khan *et al*., 2012). Among the large number of natural polymers of animal origin some have attracted particular interest in recent years, namely: collagen, gelatin silk and chitosan. Instead, cellulose, alginate, agarose and cornstarch have been explored as potential scaffolds of vegetable origin.

Chitosan: Chitosan is an N-deacetylated (Figure 1.5) form of chitin produced by exposure to a highly basic solution (such as sodium hydroxide) or enzymatic degradation of chitin, resulting in an N-acetylglucosamine and N-glucosamine copolymer. Chitosan is a widely used natural cationic polymer in biomedicine (Agrawal *et al*., 2010). Commonly produced from crab shells, chitosan is non-toxic and biodegradable; its hydrophilic surface promotes cell adhesion and proliferation (Bhattarai *et al*., 2010, Kean *et al*., 2010). Chitosan has a chemical structural analogous to

glycosaminoglycans (GAGs), which make up a portion of natural tissue Extra cellular matrix (ECM), indicating its potential bioactivity.

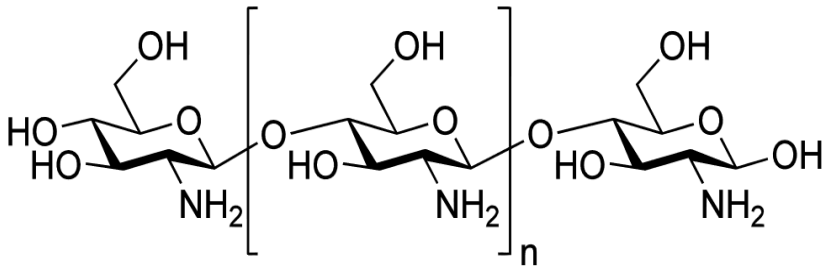

Figure 1.5: Chemical structure of Chitosan

Unlike the natural polymers derived from costly mammalian proteins, chitosan evokes minimal foreign-body response and fibrous encapsulation, (Jayakumar *et al*., 2010, Kim *et al*., 2008) and has unlimited material sources and excellent reproducibility. It is a semcrystaline polymer and its crystallinity depends on degree of deacetylation with the highest crystallization at 100% deacetylation and minimum crystallization at intermediate deacetylation values due to the increased random interactions between polymer chains. Chitosan has amine groups in it molecule with a pKa value of ~6.3 and are susceptible to variations in pH that are affected by the degree of acetylation, average molecular weight, and spacing of acetyl units (Yi *et al*., 2005) At slightly acidic pH values, the amine groups on the chitosan become protonated, resulting in the chitosan acting as a water-soluble polyelectrolyte. When the pH increases above 6, the amino groups are deprotonated and the chitosan becomes more insoluble. Chitosan shows antibacterial and antimicrobial characteristics (Raafat *et al*., 2008). The cationic moieties of chitosan molecules interact with anionic cell wall of bacteria/micro-organisms causing ruptures of their cell wall that reduces the bacteria attachment and survivability. Thus chitosan based scaffold produces antibacterial environment in tissue engineering. The cationic nature of the chitosan attracts negatively charged molecules, including GAGs and proteins, which affect cell attachment, migration, proliferation, and differentiation. Due to this cationic property, chitosan is chemo-attractant to neutrophils and macrophages, which induces immune response. However, it does not trigger any inflammatory response. Thus, it is often treated as non-toxic and biocompatible. The degree and rate of degradation of chitosan-based biomedical material or scaffold depend on degree of deacetylation and molecular weight (Xu *et al*., 1996). With the increase of both these

parameters, degradation rate decreases. With degree of deacetylation of ~ 80%, the degradation rate in vivo is ~5% per week 48.

Collagen: Collagen is probably the most widely used natural polymer for TE applications (Figure 1.6). Many types of collagen are available, and they differ in terms of their animal source (i.e. bovine, equine, etc.) and zone of extraction (i.e. derma, tendon etc.). Collagen offers numerous advantages; first of all, it is present in most natural tissues, being the main component of connective tissue and the most abundant protein in the body, but it has the disadvantage of degrading very fast and at a quite uncontrolled rate, which reduces its mechanical strength (Zanetti *et al*., 2013). Crosslink treatments, thermal or chemical, can be performed in order to extend its durability in body fluids and increase its mechanical performance. Alternatively, composites made of collagen and a reinforcing phase, such as hydroxyapatite, has been widely proposed to improve the mechanical strength of the material (Zhou *et al*., 2011, Prosecká *et al*., 2011, Sionkowska *et al*., 2013).

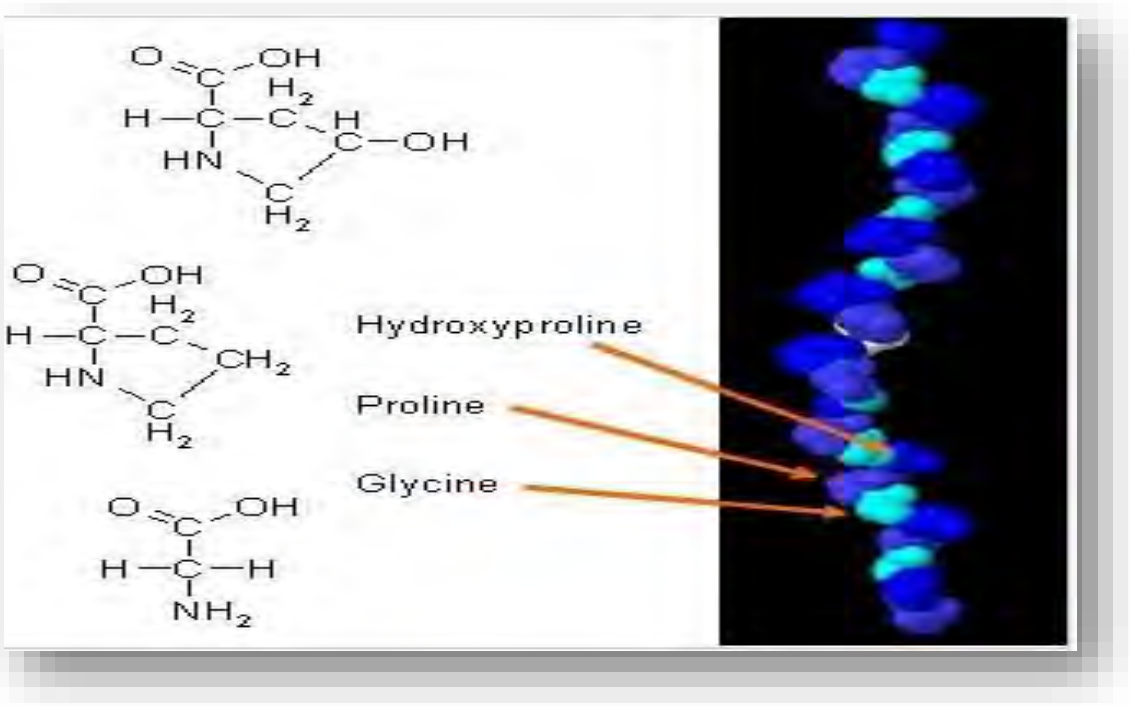

Figure 1.6: Amino Acid residues in collagen. Glycine, Proline and Hydroxyproline residues present in a collagen molecule (Yamazaki *et al*., 2010).

Alginate: Alginate is a naturally occurring anionic polymer typically obtained from brown seaweed which has been used for many biomedical applications, due to its biocompatibility, low toxicity, relatively low cost, and mild gelation by addition of divalent cations, such as Ca^{2+} (David, 2012). Figure 1.7 represents the structure of sodium alginate.

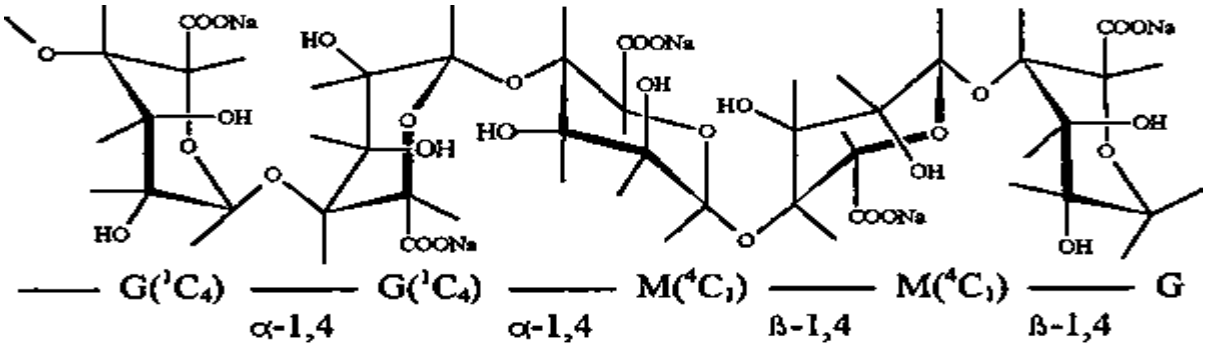

Figure 1.7: Chemical Structure of Sodium Alginate

Commercially available alginate is extracted from brown algae by treatment with aqueous alkali solutions, typically with NaOH. The extract is filtered, and either sodium or calcium chloride is added to the filtrate in order to precipitate alginate. After further purification and conversion, water-soluble sodium alginate powder is produced (Kuen and David, 2012). Alginate is typically used in the form of a hydrogel in biomedicine, including wound healing, drug delivery and tissue engineering. Applications Figure 1.8 represents the structure of calcium alginate.

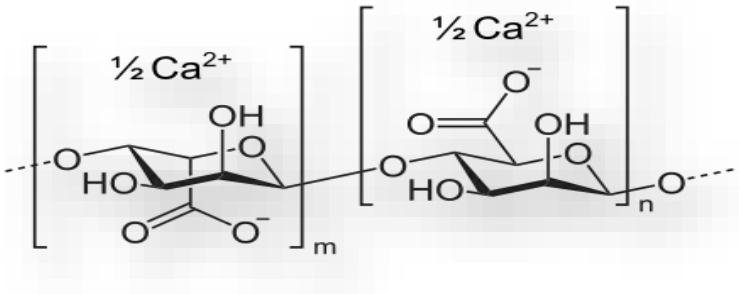

Figure 1.8: Chemical Structure of Calcium Alginate

These are biocompatible, being structurally similar to the macro molecular-based components in the body, and can often be delivered into the body via invasive administration. Cross-linking is usually done by chemical or physical cross-linking. The most common method to prepare hydrogels is to combine the solution with ionic cross-linking agents, such as divalent cations

(i.e.,Ca^{2+}). Calcium chloride ($Cacl_2$) is the most frequently used agent to cross-link alginate though it leads to rapid and poorly controlled gelation. Alginate has been used in many biomedical applications including pharmaceutical fields like serving as thickening, gel forming or stabilizing agents for drug delivery applications.

1.2.3.3.2.2 Synthetic polymers

Although natural polymers are currently the materials most extensively used in the fabrication of scaffolds, synthetic polymers have been and continue to be widely used since they have good mechanical strength, reproducible/controllable mechanical-chemical properties, and controllable biodegradation rates. Synthetic polymers can be divided in two classes: biodegradable, such as poly (glycolic), poly (lactic) acid and copolymers, polycaprolactone, polydioxanone, and polyurethanes, and non-biodegradable, such as polyvinyl alcohol, polyhydroxyethymethacrylate, and poly (N-isopropylacrylamide). However, because the most common synthetic polymers have a hydrophobic nature, they show poor wetting properties that result in poor cell distribution and poor cell adhesion. Moreover, synthetic polymers can cause systemic or local reactions caused by acidic degradation products. In order to improve the cell affinity of these materials, surface treatments have recently been proposed and are currently under examination by numerous investigators (Poncin-Epaillard *et al*., 2013, Ajiro *et al*., 2012).

1.2.3.3.2.3 Bio ceramics

A ceramic material used in a biomedical application can be defined a bioceramic material. Bioceramics is the science governing the production of solid ceramic bodies, porous or dense, by the melting of raw inorganic material (Garg *et al*., 2012) the main application field of bioceramic materials is orthopedics, because of the great affinity of the chemical composition of some ceramic materials with the mineral constituent of bones. The bioceramic materials can be grouped into three classes according to their behavior in the physiological environment: (a) bioresorbable, i.e. calcium and tri-calcium phosphates (TCP), (b) bioactive or surfaceactive, i.e. hydroxyapatite, (c) non-resorbable or inert, i.e. alumina and zirconia. The main disadvantages of these materials are their low mechanical resistance and high brittleness; their main advantages are their high biocompatibility and good osteconductivity.

Hydroxyapatite

Hydroxyapatite is the main bio-mineral component found in human hard tissues, i.e. tooth and bone. Its stoichiometry is represented by the formula [Ca_{10} $(PO_4)_6(OH)_2$]. It is comprised of calcium and phosphorus present in the ratio (Ca/P) of 1.67. (Oliveira *et al*., 2007) It is the main mineral component of the enamel, comprising of more than 60% of tooth dentine by weight.

HA is manufactured in many forms and can be prepared as a dense ceramic (Kong *et al*., 2002) powder (Kweh *et al*., 1999), ceramic coating (Nissan *et al*., 2004) or porous ceramic (Ozgur *et al*., 1999) as required for the particular applications. However, in recent years, nanosized hydroxyapatite (nHA) with appropriate stoichiometry, morphology and purity have stimulated great interest in scientific research. It is believed that nHA with grain size <100 nm in at least one direction has a high surface activity and ultrafine structure similar to the mineral found in hard tissues.

HA has attracted much interest as a biomaterial for use in prosthetic applications due to its similarity in crystallography and chemical composition to that of human hard tissue (Ramli *et al*., 2011) On account of its outstanding properties like biocompatibility, bioactivity, osteoconductivity, non-toxicity and non-inflammatory nature (Liu *et al*., 1997) this bio ceramic has got a variety of applications which include: Bone tissue engineering; restoration of periodontal defects; (Meffert *et al*., 1985, Yukna *et al*., 1985) edentulous ridge augmentation; (Piecuch, 1986) orthopedic and dental implant coating (Munting *et al*., 1990,Chang *et al*., 1997,Rigo *et al*., 2004) endodontic treatment like pulp‐ capping, desensitizing agent post bleaching ; (Browning *et al*., 2012) for treating early carious lesions (Li *et al*., 2008, Huang *et al*., 2011, Huang *et al*., 2010) and as a remineralizing agent in toothpastes (Tschoppe *et al*., 2011). A crystalline structure of HA has been shown in the Figure 1.9.

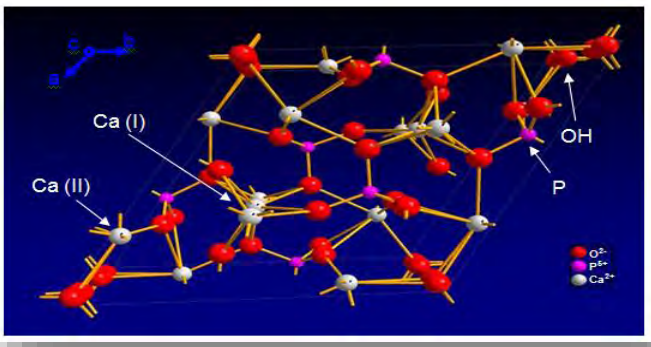

Figure 1.9: Crystalline structure of hydroxyapatite.

The mechanical properties of HA are greatly determined by the morphology and crystallography of the particles, which in turn demands on the mode of fabricating HA.

1.2.1.3.2.4 Composites

One of the most interesting solutions currently under evaluation in order to overcome some of the disadvantages of the single-phase materials described above is the combination of different materials to obtain a composite. A composite material should increase the performance of the single-phase materials that compose it. Among the possible combinations, we cite: (a) natural or synthetic polymer-ceramic, and (b) polymer-polymer, both natural and synthetic. The main advantage of a composite is that it can provide tailored mechanical properties and degradation rates. The main disadvantage is that the scaffold fabrication techniques can be quite complicated.

1.2.1.3.3 Techniques for fabrication

In the body, cells and tissues are organized into three-dimensional architecture. Scaffolds have to be fabricated by different methodology to engineer these functional tissue and organs to facilitate the cell distribution and guide their growth into three-dimensional space. There are many techniques for scaffold fabrication among them main techniques for scaffolds fabrication are mentioned here.

1.2.3.3.3.1 Solvent casting

Solvent casting property for the scaffolds preparation is very simple, easy and inexpensive. It does not require any large equipment; it is totally based upon the evaporation of some solvent in order to form scaffolds by one of the two routes. One method is to dip the mold into polymeric solution and allow sufficient time to draw off the solution; as a result, a layer of polymeric membrane is created. Other method is to add the polymeric solution into a mold and provide the sufficient time to evaporate the solvent that create a layer of polymeric membrane, which adhere to the mold (Mikos *et al*., 2004).

One of the main drawbacks of this technique, the toxic solvent denatures the protein and may affect other solvents. There is a possibility that the scaffolds designed by these techniques may also retain some of the toxicity. To overcome these problems scaffolds are fully dried by vacuum process to remove toxic solvent. However, this is very time consuming technique and to overcome these

problems some researchers have combined it with particulate leaching techniques (Mikos *et al*., 1993a, Mikos *et al*., 1993b, Mikos *et al.,* 1996) for the fabrication of scaffolds.

1.2.3.3.3.2 Particulate-leaching techniques

Particulate leaching is one of the popular techniques that are widely used to fabricate scaffolds for tissue engineering applications (Ma and Langer, 1999; Lu *et al*, 2000). Salt, wax or sugars known as porogens are used to create the pores or channels. Here salt is grounded into small particles and those particles that have desired size are poured into a mold and filled with the porogen. A polymer solution is then cast into the salt-filled mold. After the evaporation of the solvent, the salt crystals are leached away using water to form the pores of the scaffold.

The process is easy to carry out. The pore size can be controlled by controlling the amount of porogen added, the size and shape of the porogen (Plikk *et al*., 2009). The particulate leached scaffold possesses pore size (~500 μm), percentage porosity (around 94-95%) and desired crystallinity. The advantage of this method is the requirement of very less amount of polymer to fabricate the scaffold. However, certain critical variables, such as pore shape and inter-pore openings are not controlled. To conquer this drawback new technologies are being developed.

1.2.3.3.3.3 Gas foaming

Many of the fabrication techniques require use of organic solvents and high temperature. The residues that remains after completion of process can damage cells and nearby tissues. This may also denature the biologically active molecules incorporated within the scaffolds. The gas foaming scaffold fabrication techniques does not require the utilization of organic solvents and high temperature.

This technique uses high pressure carbon dioxide gas for the fabrication of highly porous scaffolds. The porosity and porous structure of the scaffolds depend upon the amount of gas dissolved in the polymer. This process involves exposing highly porous polymer with carbon dioxide at high pressure (800 psi) to saturate the polymer with gas (Sachlos and Czernuszka, 2003). Under this condition, dissolved carbon dioxide becomes unstable and will phase separates from the polymer. The carbon dioxide molecule becomes cluster to minimize the free energy; as a result, pore nucleation is created. These pores cause the significant expansion of polymeric volume and

decrease in polymeric density. A three dimensional porous structure (scaffolds) is formed after completion of foaming process.

The porosity of the scaffolds is controlled by the use of porogens like sugar, salts and wax (Ikada, 2006). The polymer e.g., PLGA that expands in foaming process fused together around the porogen to create a continuous polymeric matrix, and also entrap any other molecule, which is present in the mixture. The mix polymer and porogen are exposed to high pressure until they have completed its saturation with carbon dioxide, followed by foaming process porogen is removed and a highly interconnected pore structure is formed (Huang and Mooney, 2005).

1.2.3.3.3.4 Membrane lamination

Membrane lamination is another SFF-like technique used for constructing three-dimensional biodegradable polymeric foam scaffolds with precise anatomical shapes. Membrane lamination is prepared by solvent casting and particle leaching and introducing peptide and proteins layer by layer during the fabrication process. The membranes with appropriate shape are soaked with solvent, and then stacked up in three-dimensional assemblies with continuous pore structure and morphology (Maquet and Jerome, 1997). The bulk properties of the final 3D scaffolds are identical to those of the individual membrane. This method generates the porous 3D polymer foams with defined anatomical shape, since it is possible to use the computer assisted modeling to design the template with desired implant shape. The disadvantage of this technique is that layering of porous sheets, result in lesser pore interconnectivity (Hutmacher *et al*., 2000) and other disadvantage of this technique is that it is a time consuming process since only thin membrane can be used in this process.

1.2.3.3.3.5 Electrospinning

The electrospinning technique for the scaffolds designing utilizes the electrostatic force for the production of polymeric fiber ranging from nanoscale to micro scale. This process is control by high intensity electric field between two electrodes having electric charges of opposite polarity. One electrode is placed in the polymer solution and other is placed in collector. Generally, polymer solution is pumped as result in forming a drop of solution. Afterwards, electric field is generated, which intends to produce a force, due to this the droplets results to overcome the surface tension

of the solution. A jet of polymer is ejected, which produces the fibers, same instant the solvent starts evaporating due to jet formation and continues after the nanofibers are deposited to collector.

More than 200 polymers are used for electrospinning like silk fibroin (Zarkoob *et al*., 2004; Sukigara *et al*., 2003; Jin *et al*., 2004), collagen (Mathews *et al*., 2002), chitosan (Ohkawa *et al*., 2004), gelatin (Ma *et al*., 2005) etc. In the field of tissue engineering electrospinning technique is applied for the preparation of nanofiber scaffold design. The process is very versatile in terms of use of polymers, non-invasive and does not require the use of coagulation chemistry or high temperature for fiber generation. Basically, in this process, a high voltage is used to create an electrically charged jet of polymer solution or melt, which forms polymer fiber after drying or solidification (Reneker and Chun, 1996; Doshi and Reneker, 1995). One of the main advantages of this technique is that it can produce the scaffold with main structural feature suitable for growth of the cell and subsequent tissue organization (Li and Tuan, 2009; Liang *et al*., 2007; Leong *et al*., 2008). It can produce the ultra-fine fibers with special orientation, high aspect ratio, high surface area, and having control over pore geometry. These characteristics are favorable for better cellular growth for in vitro and in vivo, because they directly influence the cell adhesion, cell expression, and transportation of oxygen, nutrients to the cells. This provides spatial environment for the growth of new tissue with appropriate physiological functions. Cell seeding is the main problem of electrospinning technology. This is overcome by sacrificial biopolymer or cryospinning, which allows creating the hole of desired size in electro spun matrices (Baker *et al*., 2008; Leong *et al*., 2008). The nano fibrous scaffolds are widely used in biomedical application for scaffolds preparation for tissue engineering (Ma *et al*., 2005; Yang *et al*., 2005), wound dressing (Kim *et al*., 2000), artificial blood vessels (Ma *et al*., 2005), protective clothing material (Lu and Ding , 2008), drug release membrane (Katti *et al*., 2004, Chew *et al*., 2005; Venugopal *et al*., 2008), nanotube material, chemical catalytic apparatus, bio-transplant material, and hydrogen storage tank for fuel cell (Cho *et al*., 2003). The nano fibrous scaffolds are prepared for the biomedical application, such as hydrophilicity, mechanical strength, biodegradability, biocompatibility, interaction of cells, which are controlled by chemical composition of the material (Madurantakam *et al*., 2009). On the basis of that by selecting and adjusting the combination of proper component ratio, property of electrospinning scaffolds can be customized with desired function.

1.2.3.3.3.6 Porogen leaching

Porogen leaching is one of the most common methods used for preparation of scaffolds with controlled porosity. The particulate leaching method is totally based upon the dispersion of porogen (salt, sugar and wax) either in liquid particulates or powdered materials (Hou *et al*., 2003; Lee *et al*., 2004, Nazarov *et al*., 2004 Vepari and Kaplan, 2007) by the process of evaporation, cross linking or other reaction liquid may be solidified. These porogens act as place holder for pore and interconnection of the pores in the actual scaffolds fabrication technique. Highly porous scaffold with porosity up to 93 % and pore diameter up to 500 micrometers can be prepared by using this technique (Mikos *et al*., 1993 a, b). Main objective of this technique is the realization of bigger pore size and increase pore interconnectivity. Main advantage of this technique is its simplicity, versatility and easy to control the pore size and geometry. Pore geometry is control by the selection of the shape for specific porogen agent, whereas pore size is control by sieving the porogen particle to the specific dimensional range (Mano *et al*., 2007). One of the main drawbacks of this technique is that it can only produce thin wafers or membrane up to 3 mm thick and very difficult to design the scaffolds with accurate pore inter-connectivity (Moore *et al*., 2004).

1.2.3.3.3.7 Fiber mesh

Fiber mesh technique for scaffold fabrication consists of individual fiber either woven or interweave into three dimensional pattern of variable pore size (Martins *et al*., 2009). PGA is the first biocompatible and biodegradable polymer to spun into the fiber and used as a synthetic suture thread. It is prepared by the deposition of polymer solution over a nonwoven mesh of another polymer followed by subsequent evaporation (Ikada, 2006). Main advantage of this technique is to provide the large surface area for cell attachment and rapid diffusion of nutrient that is favorable for cell survival and growth (Chen *et al*., 2002). However, one of the main drawbacks of this technique is lack of structural stability which can partly be overcome by hot drying of PLLA fiber to improve the structure orientation and crystallinity**.**

1.2.3.3.3.8 Fiber bonding

Fiber bonding technique for scaffold fabrication is developed by Mikos and his coworkers (Mikos *et al*., 1993a). Synthetic polymer (PLLA) was dissolved in chloroform followed by non-woven mesh of PGA fiber had added. Subsequently solvent was removed by evaporation as a result a

composite material, which consists of non-bonded PGA fiber, embedded in PLLA matrix is formed (Chen *et al*., 2002). The scaffolds were fabricated by bonding a collagen matrix to PGA polymers with threaded collagen fiber stitches (Eberli *et al*., 2009). Fiber bonding occurs during post treatments at a temperature above the melting temperature of PGA. As a result, PLLA matrix of the composite has removed by dissolving in methylene chloride agent (Sachlos and Czernuszka, 2003) utilizing the fact that PGA is insoluble in this solvent. This process yields the scaffolds of PGA fiber that is bonded together by heat treatment. PGA mesh provides the high porosity and surface area to polymer mass ratio (Mooney *et al*., 1996). This provides the mechanical stability and allows the tissue ingrowths. One of the main advantages of using the fiber is its large surface area, which is suitable for scaffolds applications. Therefore, it provides the more surface area for cells attachment and sufficient space for the regeneration of extracellular matrix (Moroni *et al*., 2008)

1.2.3.3.3.9 Self assembly

Self-assembly is the spontaneous organization of the molecule into well defines into an ordered structure required for specific function (Zhang, 2003). Self-assembly of natural or synthetic molecule produced nanoscale fibers known as nanofibers. Amphiphilic peptide sequence is a common method for the fabrication of 3D nanofibrous structure for tissue engineering. In aqueous solution the hydrophobic and hydrophilic domains within these peptides interact together with the help of weak non covalent bonds (Joshi *et al*., 2009; Zhang *et al*., 2006) (e.g., Hydrogen bond, Van der Waals interactions, Ionic bond and Hydrophobic interaction) this produces distinct fast recovering hydrogel, with the hydrophobic interactions as the molecules come together. Instead of peptides synthetic polymer nanofibers are also prepared by self-assembly of di-block polymers (AxBy) when the two blocks separate from one another in bulk due to their incompatibility, the volume formation of A and B can be controlled to obtain B domain of cylindrical shape with nanoscale diameter that is embedded into matrix A. Polymeric dendrimers can also self-assemble into nanofibers (Liu *et al*., 1996). The di- and tri-block peptide ampholites (PAs) are designed that are self-assembled into a rod-like architecture. So a new technique for the self-assembly of PAs into nanofibers by controlling pH and by engineering the peptide head group of the PAs is developed (Hartgerink *et al*., 2001). According to Hartgerink *et al*., (2002) and Tambralli *et al*., (2009) the salient features for synthesis of the PA involve the following:

1. Phosphoserine residue incorporation to increase hydroxyapatite mineralization.

2. RGD (Arg-Gly-Asp) peptide incorporation to enhance integrin-mediated cell adhesion.

3. Four consecutive cysteine residues incorporation forming inter-molecular disulfide bonds that polymerizes to provide improved structural stability.

4. Flexible linker region incorporation consisting of three glycine residues to provide flexibility to the head group.

By virtue of the modifications in the structure of the PA enables a variety of self-assemblies including layered and lamellar structures and by its reversibility properties provides flexibility to the system. Therefore, the self-assembly technique shows designing potential novel scaffolds for tissue engineering applications Self-assembly shows several advantages over the electrospinning, because it produces the much thinner nanofiber with very thin diameter (Ma, 2008). The fabricated nanofibers have amino acid residues that may be chemically modified by the addition of bioactive moieties. Other advantage of this technique is to avoid the use of organic solvent and reduce the cytotoxicity, because, it is carried out in aqueous salt solution or physiological media (Ma *et al*., 2005). Main disadvantage of this technique is its complicated and elaborated process.

1.2.3.3.3.10 Rapid prototyping (RP)

RP is also called as solid free-form technique. This technique is more advanced technique for scaffold fabrication. It is computer controlled fabrication technique. It can rapidly produce 3D object by using layer manufacturing method. RP technique generally comprises the design of scaffold model by using the computer added design (CAD) software, which is then expressed as a series of cross section (Lin *et al*., 2008, Woodfield *et al*., 2009). Corresponding to each cross section RP machine lays down a layer of material starting from the bottom and moving up a layer at a time to create the scaffolds. In typical example, image of bone defect in a patient can be taken and develop 3D CAD computer model. The computer then can have reduced the model to slice or layers. The 3D objects are constructed layer by layer by using RP techniques such as fused deposition modeling (FDM), selective laser sintering (SLS), 3D printing (3D-P) or stereolithography. Now a day RP is an efficient way for generating the scaffolds of desired property, other advantage of this technique is to produce the parts with highly reproducible architecture and compositional variations. RP has advantage over other fabrication techniques, it

has ability to control matrix architecture (size, shape, inter connectivity, branching, geometry and orientation) yielding biomimetic structure, that varying in design and material composition. It has ability to control the mechanical property, biological effects and degradation kinetics of scaffolds (Kai *et al*., 2009, Hutmacher *et al*., 2000). RP technique can easily be integrated with the imaging technique to produce the scaffolds that are customized in size and shape allowing the tissue engineered graft to be modified for particular applications or for individual patient. One of the main drawbacks of this technique is achieved low resolution by current systems and types of polymeric materials that are used for this technique.

1.2.3.3.3.11 Melt molding

A large number of techniques are discussed for the fabrication of scaffolds. These scaffolds fabrication techniques are developed to control the pore interconnectivity and geometry, which are important for the exchange of nutrient/waste from pore to pore. Melt molding process involves the filling of Teflon mold with PLGA powder and gelatin microspheres of specific diameter followed by heating the mold above the glass transition temperature of PLGA while applying pressure to the mixture (Thompson *et al*., 1995a). This action causes the PLGA particle to attach together. Once the mold is removed gelatin microspheres is dissolved by immersing the mixture into water and scaffolds are then dried. Scaffolds produced by this technique assume the shape of the mold. Melt molding process was modified to incorporate short fiber of HA. Uniform distribution of HA fiber throughout the PLGA scaffolds could only be achieved by using the solvent casting technique to prepare the composite material of HA fiber, PLGA matrix and gelatin or salt porogen, which are used in melt molding process (Hou *et al*., 2003).

1.2.3.3.3.12 Phase separation

Phase separation technique for scaffolds designing requires temperature change that separates the polymeric solution in two phases, one having low polymer concentration (polymer lean phase) and other having the high polymer concentration (polymer rich phase). Polymer is dissolved in suitable solvent, followed by dispersion of biologically active molecule in these solutions. By lowering the temperature liquid-liquid phase is separated and quenched to form a two phase solid and the solvent has removed by extraction, evaporation and sublimation (Mikos *et al*., 2004) to give porous scaffolds with bioactive molecules integrated in to that structure (Sachlos and Czernuszka, 2003; Hua *et al*., 2002). Freeze drying technique is use for the fabrication of porous scaffolds (Whang *et*

al., 1995; Schoof *et al*., 2001). This technique is based upon the principle of sublimation. Polymer is first dissolved in a suitable solvent to form a solution of desired concentration. The solution is frozen and solvent is removed by lyophilization under the high vacuum fabricate the scaffold with high porosity and inter connectivity (Mandal and Kundu, 2009a). The pore size can be controlled by the freezing rate and pH; a fast freezing rate produces smaller pores. Controlled solidification in a single direction has been used to create a homogenous 3D-pore structure (Schoof *et al*., 2001). Compared with the electrospinning approach, phase separation holds great potential for fabrication of three-dimensional nano fibrous scaffolds with uniform pore structures through dual or multiple phase separation processes. In addition, phase separation can engineer three-dimensional shapes via several techniques, including solid free-form fabrication, rapid prototyping, and computer-assisted design and manufacture. However, limitations such as limited material selection and inadequate resolution still exist.

Table 1.2: **Merits and demerits of different fabrication techniques**

Methods	Merits	Demerits	References
Solvent casting/ particulate leaching	Control over Porosity, pore size and crystallinity	Limited mechanical property, residual solvents and porogen material	Ma, 2007; Xiang *et al*., 2006
Porogen leaching	Controlled over porosity and pore geometry	Inadequate pore size and pore interconnectivity	Mano *et al*., 2007
Freeze drying	High temperature and separate leaching step not required	Small pore size and long processing time	Boland *et al*., 2004; Mandal and Kundu, 2008
Gas foaming	Free of harsh organic solvents, control over porosity and pore size	Limited mechanical property, inadequate pore interconnectivity	Ikada., 2006
Fiber mesh	Large surface area for cell attachment, rapid nutrient diffusion	Lack the structural stability	Chen *et al*., 2002
Fiber bonding	High surface to volume ratio, high porosity	Poor mechanical property, limited applications to other polymers	Mooney *et al*., 1996
Melt molding	Independent control over porosity and pore size	Required high temperature for non amorphous polymer	Thompson *et al*., 1995 a; b
Membrane lamination	Provide 3D matrix	Lack required mechanical strength, inadequate pore interconnectivity	Maquet and Jerome, 1997
Phase separation	No decrease in the activity of the molecule	Difficult to control precisely scaffold morphology	Smith *et al*., 2006

1.3 Aims and Objectives

Tissue engineering is one of the most significant achievements of modern science. Therefore, the aim of the study was to formulate a suitable scaffold which can be used in animal body, tissue replacement, reconstruction and regeneration without any long-term adverse effects. For this purpose, the objective of this study was set to-

- Optimization and Characterization of Hydroxyapatite, Chitosan, and Alginate (HCA) scaffold
- Fabrication and Characterization of Hydroxyapatite, Collagen and Chitosan (HCC) scaffold
- A comparative study of HCA and HCC scaffold with human bone allograft (HBA)

Materials and Methods

2.1 Working place:

The research work entitled "**Fabrication and Characterization of Hydroxyapatite Based Biocompatible Composite Scaffold for Bone Tissue Engineering**" was designed and carried out in Institute of Tissue Banking and Biomaterial Research (ITBBR), Atomic Energy Research Establishment (AERE), Savar, Dhaka from June 2015 to January 2017. An outline of this study has been depicted in Figure 2.1. All the chemicals and equipment used for this study is given in Appendix Π.

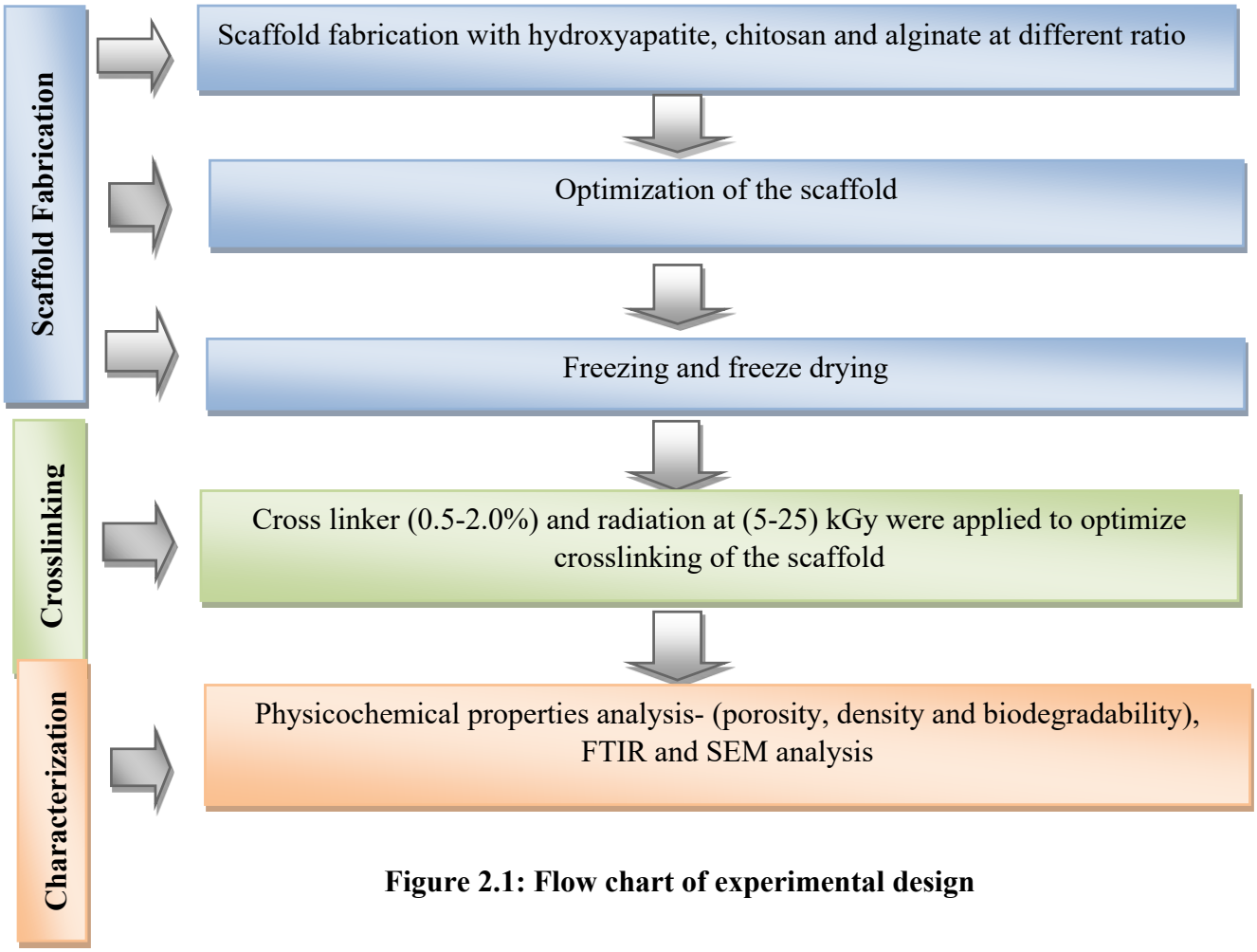

Figure 2.1: Flow chart of experimental design

2.1.1 Fabrication of the HCA scaffold

Scaffolds were fabricated according to the protocol of Xiaoning *et al*., 2014 with simple modification. HCA (hydroxyapatite, Chitosan, Alginate) complex scaffolds with different ratio (1:1 and 1:2) were prepared through in situ co-precipitation technique.

In short, 1:1 ratio (HCA-1), 1.0 g chitosan was dissolved in 1 wt % acetic acid solution under agitation, and 1 g of alginate powder was dissolved and thoroughly mixed in 25mL of deionized water. Then 80 mL of 0.1mol/L $CaCl_2$ solution and 48 mL of 0.1mol/L KH_2PO_4 solution were added to the aqueous chitosan and alginate solutions, respectively.

Again concisely alike HCA-1 sample in 1:2 ratio (HCA-2), 2.0 g chitosan was dissolved in 1 wt % acetic acid solution under agitation, and 2 g of alginate powder was dissolved and thoroughly mixed in 25mL of deionized water. Then 80 mL of 0.1mol/L $CaCl_2$ solution and 48 mL of 0.1mol/L KH_2PO_4 solution were added to the aqueous chitosan and alginate solutions, sequentially.

In the above mentioned methods, the mineral concentration in both samples was constant. After that, alginate solution was mixed with the chitosan solution under continuous stirring in a blender for 1 h at room temperature. Then the samples were frozen at -40℃ for 24 h. The samples were then lyophilized in a freeze dryer at -50˚C for 30h to obtain the HCA composite scaffolds and radiated at 25kGy. The radiated samples were further analyzed to obtain physicochemical properties, e.g., biodegradation, porosity and density.

Table 2.1 Properties of the materials used in this experiment

	Hydroxyapatite	Chitosan	Calcium Alginate	Potassium dihydrogen phosphate	Calcium chloride	Acetic Acid	Hydroxyethyl methacrylate (HEMA)
Chemical Formula	$Ca_{10}(PO_4)_6(OH)_2$	---	$(C_{12}H_{14}CaO_{12})_n$	KH_2PO_4	$CaCl_2$	CH_3COOH	$C_6H_{10}O_3$
Molecular weight (g/mol)	1004.6	---	1170.93	136.086	110.98	60.05	130.1418
Density (g/cm3)	3.14	1.51	----	2.34	----	1.05	1.07

2.1.2 Cross linker

After observing physicochemical properties, the HCA-2 sample found to be more porous and also considering the degradation properties it was selected for further study for adding cross liker. In this experiment, 2-Hydroxyethyl Methacrylate (HEMA) was used as a cross linking agent and 0.5%, 1%, 1.5 % and 2% HEMA was added to HCA-2 sample and radiated at 25kGy, 15kGy, 10kGy and 5kGy. Then the solutions were frozen at -40˚C for 24 h. Then samples were lyophilized in a freeze dryer at –50˚C for 30 h to obtain HCA composite scaffolds.

2.2 Extraction of Collagen and Fabrication of the Scaffold

2.2.1 Collagen Extraction

Soluble type I collagen was extracted from bovine dermis using acid extraction and salt fractionation technique (Trelstad, 1982; Huang-Lee and Nimni, 1993). Bovine dermal tissue was trimmed of hair and excess fat Strips of tissue, weighing 250 g and measuring ∼10 × 50 mm, were defatted in 0.5 L of 50/50 chloroform/methanol by volume for 8 h and washed for 2 h each in 100% methanol, 50% methanol in water by volume, and finally physiological phosphate buffered saline (PBS). Defatted dermal tissue strips were then placed in 0.75 L of 0.5 M acetic acid and blended for 5 min in a commercial blender. Porcine pepsin was added at a concentration of 2 mg/mL to increase the fraction of extractable soluble collagen.

Pepsin preferentially attacks the globular ends of the collagen proteins, breaking crosslinks that bind collagen molecules to each other. Pepsin can increase the extractable yield by 400% and the resulting collagen displays lower immunogenicity compared to collagen not treated with pepsin (Trelstad, 1982). The acid solution was adjusted to a pH of 2.5 with HCl for optimum pepsin activity and incubated at 4 ◦C for 24 h.

After acid extraction, the solution was centrifuged at 5000 g for 1 h to remove all non-soluble collagen fragments. The supernatant contained 4-6 mg/mL of soluble type I collagen. Other minor contaminants likely included residual elastin, type III collagen, and keratin. Type I collagen was separated by adding NaCl to a concentration of 2.5 M to induce precipitation. The precipitated collagen was collected by centrifugation at 7500 g for 1 h, re-dissolved in 0.1 M acetic acid, centrifuged again at 7500 g for 1 h, and the remaining precipitate was discarded. The resulting supernatant was nearly pure type I collagen as demonstrated by sodium dodecyl sulfate polyacrylamide gel electrophoresis (SDS-PAGE) using a 10% acrylamide gel. The final collagen solution was stored at −20 ◦C until further use.

2.2.2 Fabrication of Hydroxyapatite-Collagen-Chitosan Scaffold (HCC):

Hydroxyapatite-Chitosan-Collagen (HCC) scaffolds were fabricated according to Wattanut chariya *et al*., 2014 with simple modification. Briefly 2g of HA was weighed into a flask and added deionized distilled water. The mixture was stirred at room temperature for 5 hours and treated by ultra-sonication until the HA powder was thoroughly dispersed in the water. At the same time, 70

ml of as extracted collagen solution was taken in another flask and stirred at room temperature. Then 2 g of chitosan was added to the collagen solution and stirred at room temperature to form a chitosan-collagen solution. After that, HA slurry was added to the collagen-chitosan solution and stirred for 2 hours to disperse thoroughly. The resultant solution was transferred to petri plates and pre-frozen at -40 ºC for 24 hours, followed by freeze-drying at -55˚ºC using a constant cooling freeze-drying protocol.

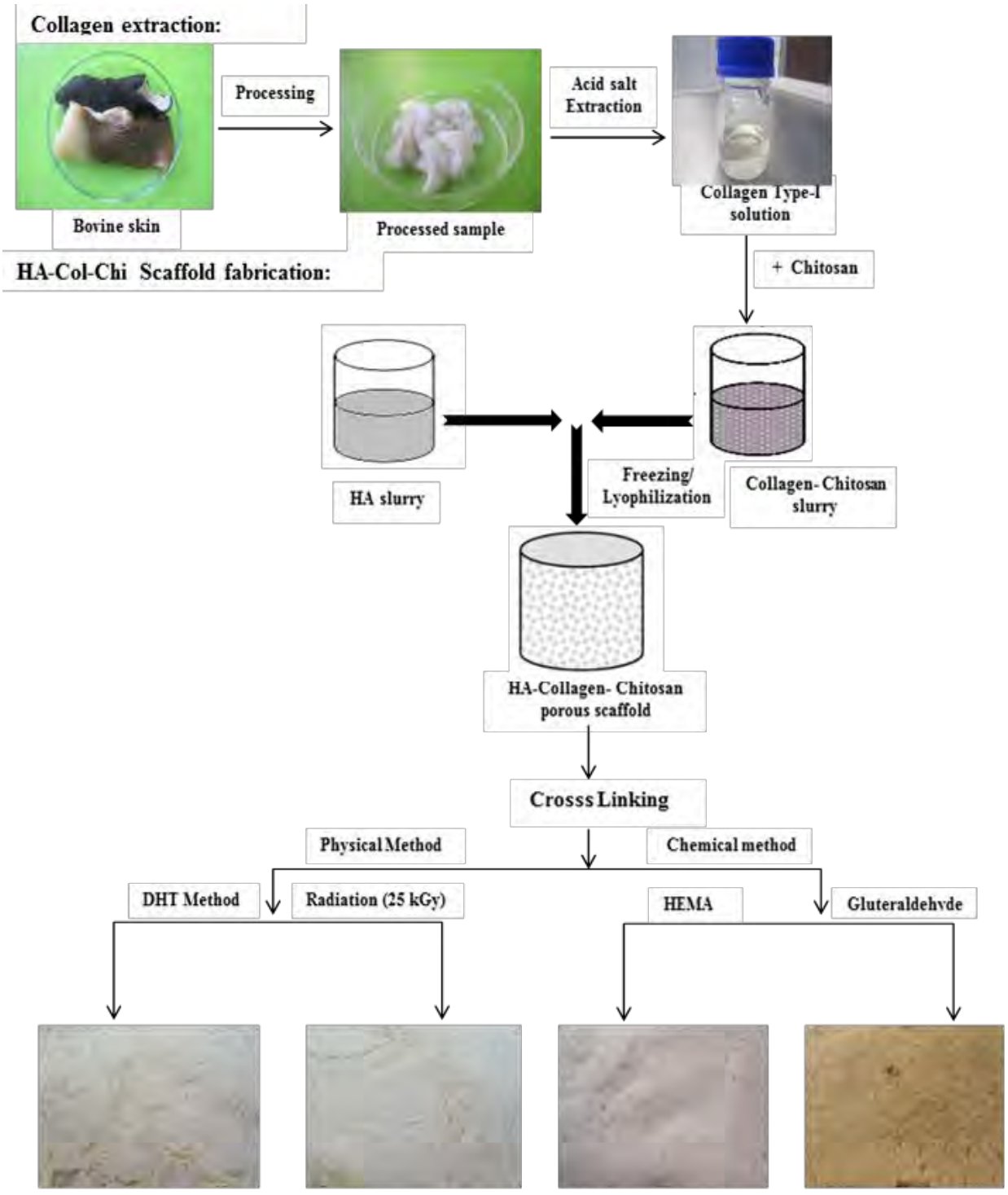

Figure 2.2: Fabrication of hydroxyapatite-collagen-chitosan

2.2.3 Addition of Cross linker:

The lyophilized porous samples were stabilized using different treatment methods: chemical cross-linking with HEMA & Gluteraldehyde solution and physical crosslinking by de-hydrothermal treatment (DHT) and Radiation.

HEMA (2-Hydroxyethyl Methacrylate) and Gluteraldehyde cross-linking were achieved by immersing the scaffolds in a cross-linking solution consisting of 2% HEMA and 2.5 % gluteraldehyde solution consequently. After reaction for 4 h at room temperature, scaffolds were washed with deionized water for another 1 h, changing the water every 30 min. Samples were frozen again, then lyophilized as described above.

For DHT cross-linking, freeze-dried scaffolds were placed under a vacuum at a temperature of 110 ◦C for 24 h. For Radiated cross-linking, fabricated scaffolds were irradiated at 25 kGy.

2.3 Scaffold Characterization

The prepared final materials and resultant structures of the porous bone scaffolds were characterized for analyzing their biological and chemical properties.

2.3.1 Porosity

Porosity of the prepared scaffolds was determined through liquid displacement method according to the methods of Zhang and Zhang (Zhang and Zhang, 2001) using ethanol. The scaffolds were first cut into smaller circular discs measuring 1 cm in diameter and 1 cm thickness. Initial weight (w_0) and the volume (v) of six samples per scaffold were measured prior to immersion. The samples were immersed in ethanol for 48 hours to allow complete saturation after which it is weighed and noted as w_1. The porosity of the scaffold was calculated according to the following formula with ρ representing the density of ethanol

$$\text{Porosity } (\%) = \frac{w_1 - w_0}{\rho^v} \times 100$$

2.3.2 Density

A liquid displacement method was used to measure the porosity and density of 50 wt% HA scaffold (Nazarov R *et al*., 2004 and Zhang R *et al*., 1999). A scaffold of weight W was immersed in a graded cylinder containing a known volume of ethanol (v_1). The cylinder was placed in a vacuum to force the ethanol into the pores of the scaffold until no air bubble emerged from the scaffold. The total volume of the ethanol and scaffold was then recorded as v_2. The volume difference (v_2-v_1) was the volume of the skeleton of the scaffold. The scaffold was removed from the ethanol and the residual ethanol volume was measured as v_3. The total volume of the scaffold, V, was then

$$v = v_2 - v_3$$

The apparent density of the scaffold, ρ was evaluated using,

$$\rho = \frac{w}{v_2 - v3}$$

2.3.3 Swelling tests

The piece of each dried porous scaffold was weighed and then immersed in 5 ml of phosphate buffer saline (PBS, pH = 7.4) for 2, 24, 48 and 72 h at 37 ◦C. At each time point, the scaffolds were taken out from the solution. The water uptake of the scaffolds was assessed using two different methods.

The first measurement was carried out after being removed from PBS, without pressing the soaked samples. After removal from the water or PBS solution, the samples were hung over a table for 1 min until no dripping was observed and then weighed (Wws). In this case we assessed the swelling ability of the scaffold structure with its pore system.

In the second measurement the same swollen samples were pressed between filter paper to remove the excess water remaining in the pores and then weighed (Wwm). In this way the ability of the scaffold material itself to absorb water was assessed. Each value was averaged from three parallel measurements.

The swelling ratio of the scaffold was defined as the ratio of the weight increase (Ww − Wd) to the initial weight (Wd) according to following equation:

$$\text{Swelling ratio}\,(\%) = \left[\frac{W_w - W_d}{W_d}\right] \times 100$$

Where, Ww represents Wws or Wwm.

2.3.4 Biodegradability

Biodegradability of the scaffolds was characterized by in vitro study (H. Shahoon *et al*., 2010). The scaffolds were immersed in Phosphate buffer saline (PBS) medium at 37 °C for 7 days. The initial scaffold weight was denoted as w_0. After 7 days, the scaffolds were washed in deionized water to remove ions adsorbed on the surface and then freeze-dried. The dry weight of the scaffold was denoted as w_t. The degradation of the scaffold was calculated by the equation

$$\text{Biodegradability} = \frac{Wo - Wt}{Wt} \times 100$$

2.3.5 Fourier Transform Infrared Spectroscopy (FTIR) analysis

FTIR Spectroscopy, is an analytical technique used to identify organic, polymeric, and in some cases, inorganic materials. The FTIR analysis method uses infrared light to scan test samples and observe chemical properties. For obtaining FTIR spectra, samples are directly placed in sample holder (Model: IRprestige21, Shimadzu, Japan). FTIR spectra were recorded with FT-IR 8400S Shimadzu Spectrophotometer in the range 4000-700cm-1, Resolution 4 cm-1, No of scan : 20 times. An image of FTIR machine used for this study is shown in Figure 2.3.

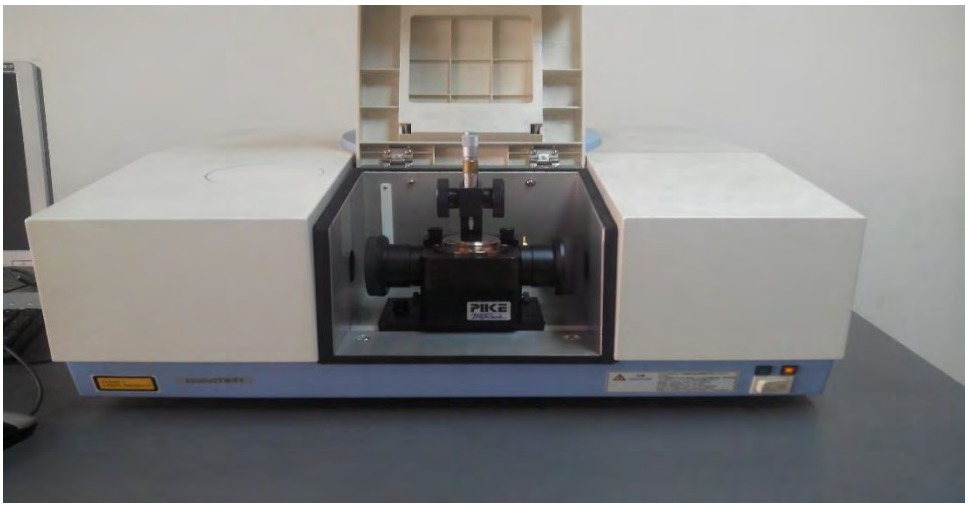

Figure 2.3: Fourier Transform Infrared Spectroscopy

2.3.6 Scanning Electron Microscope (SEM) analysis

Pore structure morphology was examined by scanning electron microscope analysis (SEM). The surface of the scaffolds was platinum coated to render it conductive, and then the sample was placed inside the SEM chamber. An image of SEM machine (JSM-6490LA) used for this study is shown in Figure 2.4.

Figure 2.4: Scanning electron microscope

Result

In tissue engineering realm, bone grafts require an osteogenic cell source and a 3D scaffold capable of supporting tissue regeneration. The combination of chitosan and alginate with synthetic hydroxyapatite is to produce a biomimetic scaffold with chemical similarity to the main structure components of natural bone tissue. The study was therefore planned, to fabricate and characterize of HA based biocompatible scaffold for bone tissue engineering that could be analogous to human bone. In the result section has divided into three parts. Such are-

- Optimization and Characterization of Hydroxyapatite, Chitosan, and Alginate (HCA) scaffold
- Characterization of Hydroxyapatite, Collagen and Chitosan (HCC) scaffold
- A comparative study of HCA and HCC scaffold with human bone allograft (HBA)

3.1 Optimization and Characterization of Hydroxyapatite, Chitosan, and Alginate (HCA) scaffold

3.1.1 Optimization of biopolymers and minerals

In this regard, we mixed different ratio of Ca-alginate (A) and chitosan (C) with fixed amount of di-hydrogen potassium phosphate and calcium chloride to prepare a HA-Chitosan-Ca alginate (HCA) scaffold. Fabricated scaffold were characterized by porosity, density & biodegradation test. Table 3.1 illustrates the optimization of mineral polymer ratio.

.**Table 3.1: Optimization of mineral polymers ratio**

Sample ID		**Minerals polymer ratio**	**Mineral**	**Polymer**	
				Chitosan	**Alginate**
HCA	HCA-1	1:1	2	1	1
	HCA-2	1:2	2	2	2

Figure 3.1: Fabricated scaffolds of HCA

3.1.2 Characterization of Porous Hydroxyapatite-Calcium Chitosan and Alginate (HCA) composites

3.1.2.1 Porosity and Density

Porosity and density of the scaffolds were measured by using liquid displacement method. The highest porosity was found in HCA-2 sample (75%) with the poor density (0.041 g/cm3), whereas highest density was in HCA-1 sample (0.076g/cm^3) with lowest porosity (67%). Table 3.2 shows the porosity and density of HCA scaffold.

Table 3.2: Porosity and density of HCA (HCA-1 and HCA-2) sample

Sample ID		Porosity (%)	Density (g/cm^3)
HCA	HCA-1	67	0.076
	HCA-2	75	0.041

3.1.2.2 Degradation properties

To determine the biodegradability result, HCA-1 and HCA-2 samples were soaked into the PBS buffer solution sequentially for 1, 3 and 7 days. The remaining weight of the scaffold after 7 days for HCA-2 sample found 17.05%, which was comparatively higher than HCA-1 sample which was 13.4%. All samples were analyzed for degradation after sterilization by radiation at 25kGy. The samples having remaining weight with respect to number of days has been shown in the Table 3.3 and Figure 3.2 & 3.3.

Table 3.3: In-vitro degradation properties of HCA (HCA-1 and HCA-2) sample

Sample ID		Biodegradation (%)		
		Day-1	Day-3	Day-7
HCA	HCA-1	77.4	25.06	13.04
	HCA-2	74.05	27.91	17.05

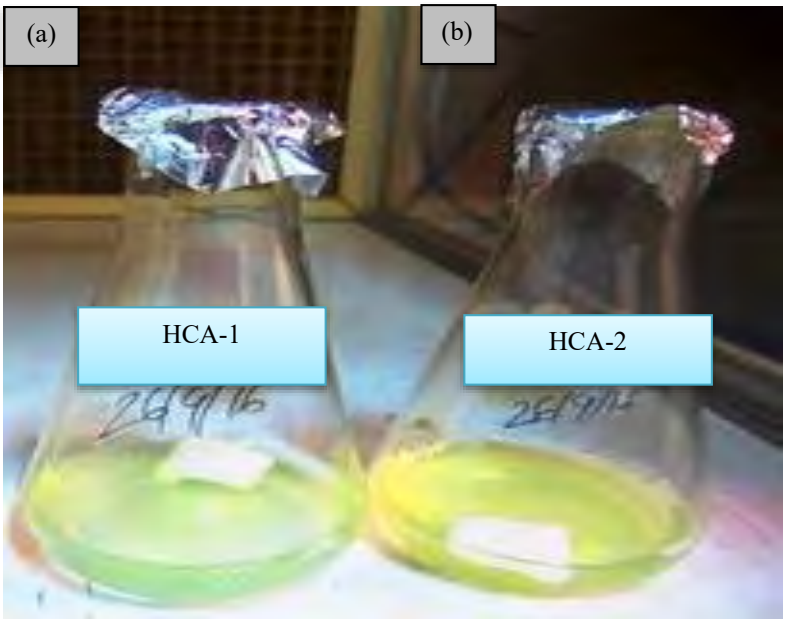

Figure 3.2: Seven (07) days in vitro Biodegradation profile of a) HCA-1 and b) HCA-2 sample

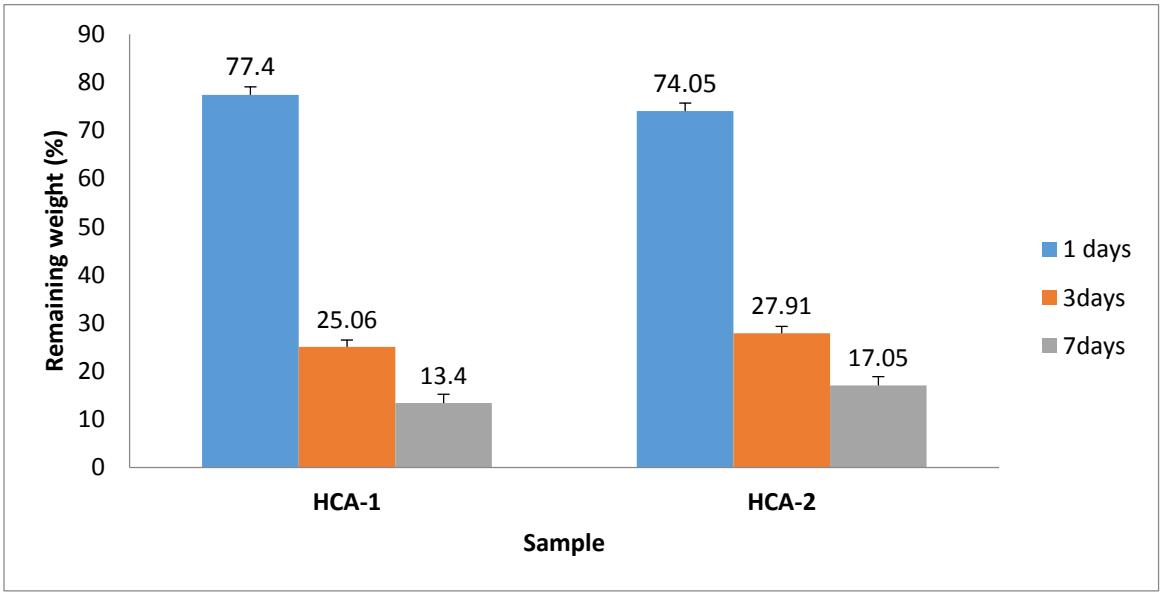

Figure 3.3: In-vitro degradation profile of HCA and HBA

3.1.3 Cross linker and radiation dose optimization

From the HCA (HCA-1 and HCA-2) samples, the HCA-2 sample was selected for further studies (adding cross linker & optimization of radiation dose) on the basis of porosity, density and biodegradation test. In this study, HEMA (2-Hydroxyethyl Methacrylate) was used as a crosslinking agent. At different percentage (0.5%, 1%, 1.5%and 2%) of HEMA was added into the HCA-2 (2:1) solution and radiated at 25kGy, 15kGy, 10kGy, and 5 kGy. But radiated solutions with 25 kGy, 15 kGy and 10 kGy were not dissolved properly and precipitations were formed and the slurry was found attached with the conical flask (Figure 3.4).

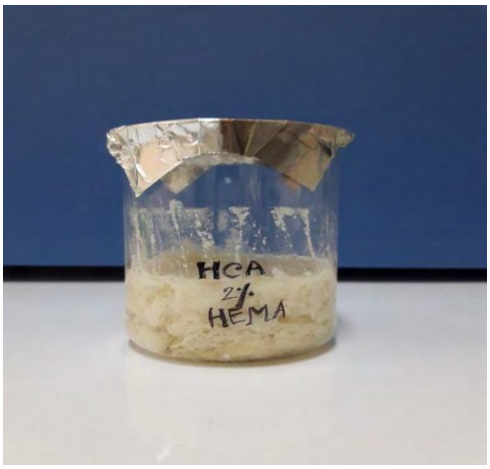

Figure 3.4: Precipitation formed after radiation at 25, 15, and 10 kGy

However, solution radiated at 5kGy, the crosslinking agent, HEMA was dissolved with the HCA-2 solution and then the crosslinked samples were further characterized for analyzing their physiochemical properties. The following Table 3.4 shows the radiated scaffold (5kGy) with the different percentage of HEMA.

Table 3.4: Radiated scaffold (5kGy) with the different percentage of crosslinking agent

Sample ID		**% of Cross linker(HEMA)**
HCA-2	CR5H1	0.5
	CR5H2	1
	CR5H3	1.5
	CR5H4	2

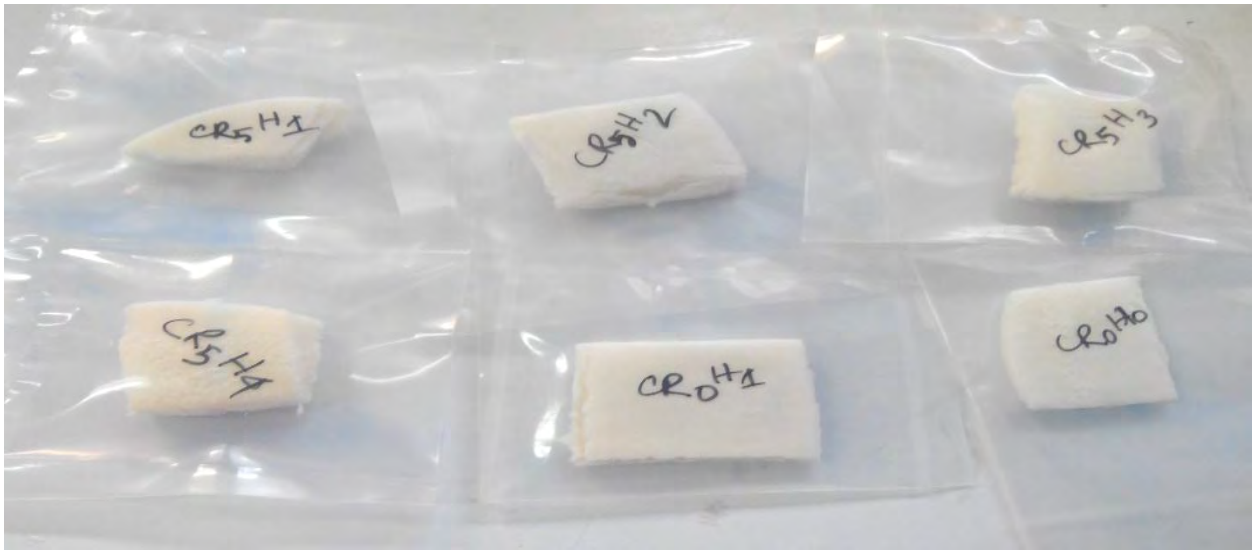

Figure 3.5: Prepared scaffold after radiation at 5kGy with different % of Cross linker

3.1.4 Characterization of the cross-linked scaffold

The physiochemical analysis of the four cross- linked scaffolds (CR5H1, CR5H2, CR5H3 & CR5H4), radiated scaffold without cross-linked (CR5H0) and non-irradiated & without cross-linked scaffold (CR0H0) were showed different and scattered properties.

3.1.4.1 Porosity and Density of scaffold

Among the six scaffolds, CR5H3 was found to be more porous (86%) than the others (Figure-3.6). The porosity results of the CR0H0, CR5H0, CR5H1,CR5H2, CR5H3 and CR5H4 samples were 66, 62, 73, 81, 86 and 75 (%) respectively.

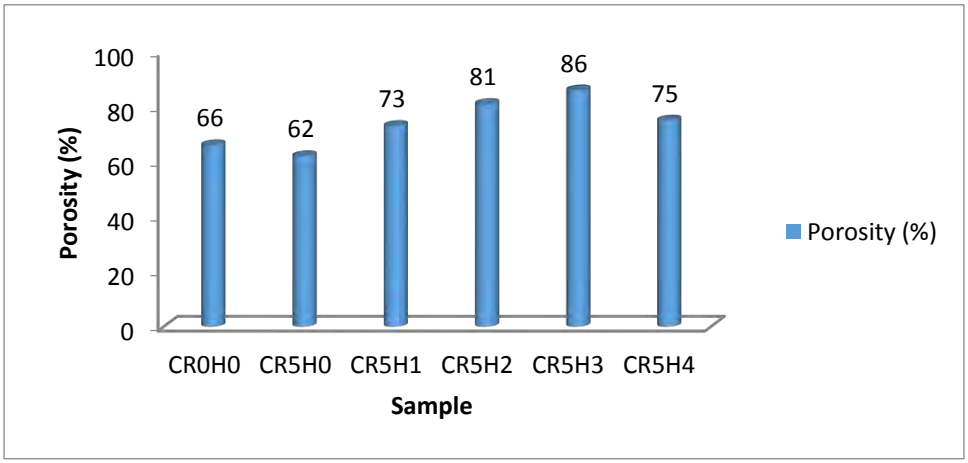

Figure 3.6: Porosity of the cross-linked scaffold with 5 kGy radiation.

Density of the scaffolds was measured by using liquid displacement method. Among the samples the highest density was in CR5H3 sample (0.076 g/cm^3) and the lowest was CR0H0 sample (0.004 g/cm^3) (Figure 3.7).

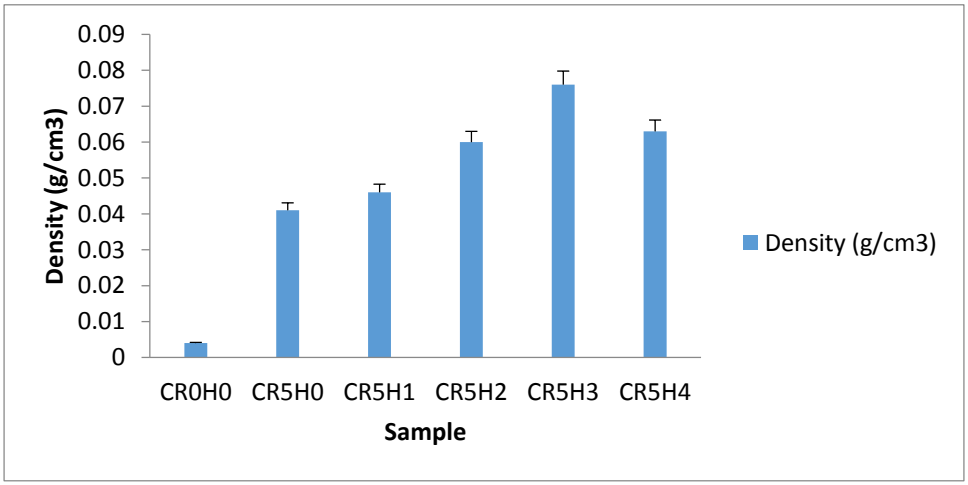

Figure 3.7: Density of the cross-linked scaffold with 5 kGy radiation

3.1.4.2 Biodegradability of scaffold

From Figure 3.8, it illustrates the biodegradation profile at 5 kGy. When the non-irradiated & 5 kGy radiated samples were soaked in PBS solution, after 1 day, among the samples, highest remaining weight (89.4%) was found in sample CR5H4and the lowest remaining weight (50%) was found in sample CR5H2. So, in 1 day degradation result, sample CR5H2 was shown the higher degradation rate.

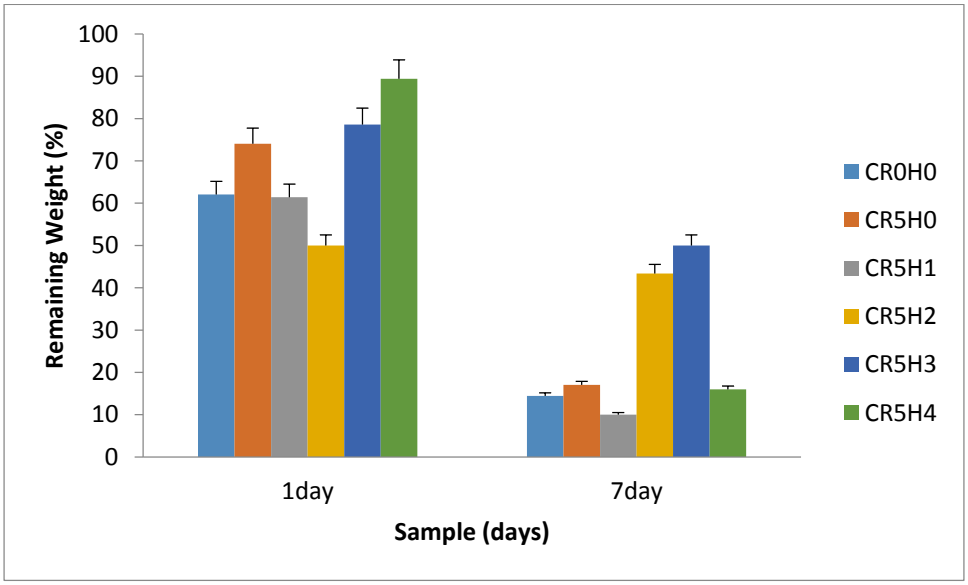

Figure 3.8: Remaining weight (%) of the cross-linked scaffold with 5 kGy radiation sample

On the other hand, when the samples were again soaked in PBS solution, after 7 days the lowest remaining weight ((10%) was found in sample CR5H1 and the highest remaining weight (50%) was found in sample CR5H3. So, after 7 days degradation profile, CR5H1 sample was shown the higher degradation rate (Table 3.5).

Table 3.5: Porosity, density and biodegradability test of the cross-linked scaffold.

Sample ID	Porosity (%)	Density (g/cm^3)	Remaining Weight (%)	
			1day	7day
CR0H0	66	0.004	62.07	14.43
CR5H0	62	0.041	74.05	17.05
CR5H1	73	0.046	61.43	10
CR5H2	81	0.060	50	43.37
CR5H3	86	0.076	78.57	50
CR5H4	75	0.063	89.4	16

3.1.4.3 Fourier Transform Infrared Spectroscopy (FTIR) analysis

In order to illustrate intermolecular interaction between components in systems, FTIR spectroscopy measurements were taken to compare the IR result of pure hydroxyapatite (HA), Chitosan (Chi), Alginate (Alg) composite scaffolds (HA/Chi-Alg).

Hydroxyapatite

Table 3.6 illustrates the FTIR spectrum of HA. It has shown the asymmetric stretching vibration of phosphate (v^1 PO_4), (v^3 PO_4) and (v^4 PO_4) present in HA appeared at 962 cm^{-1}, 570-603 cm^{-1} and 1028-1058 cm^{-1}, respectively. Whereas the band at 877cm^{-1}& 572 cm^{-1} suggests the presence of HPO_4^{2-} group. The characteristic bands for OH^- appeared at 3452, 3782cm^{-1} (Figure 3.9).

Table 3.6: Peaks of infrared spectra assigned to synthesize HA Nano powder

Compound	Name of the assigned group	Infrared frequency (cm^{-1})
HA	PO_4 band V1	962
	PO_4 band V^4(Symmetric stretching vibration)	570,603
	P-O band V^3 (Asymmetric stretching vibration)	1058,1028
	HPO_4^{2-}	875,572
	OH structural	3452,3782

Chitosan

The peaks of infrared spectra Chitosan Scaffold has been showed in Table 3.7. The bands at 2845 cm^{-1} were corresponded to the CH stretching. The broad bands at 1637 and 1543 cm^{-1} were attributed to the presence of amide I and amide II groups. The sharp band at 1408 cm^{-1} was assigned to stretching of carbonyl from COO^{-} group. The low intense bands at 1382 and 1321 cm^{-1} were corresponded to CH bending vibrations of the ring. The characteristics peaks of C-O-C glycosidic linkage were observed in the region of 1153-1021cm^{-1} (Figure 3.9).

Table 3.7: Peaks of infrared spectra assigned to Chitosan

Compound	Name of the assigned group	Infrared frequency (cm^{-1})
Chitosan	Vibrations of CO	1024, 1072,1153
	Vibration of C-H	1321,1382, 2883
	Amide I	1637
	Amide II	1543
	C=O from COO- group	1408

Alginate

The peaks of infrared spectra from Alginate Scaffold have been showed in Table 3.8. The band at 1028 and 1083 cm-1 was corresponded to the C-O-C stretching. The broad band at 1409 and 1597 was attributed to the presence of -COO group. The characteristics peak -CH stretching was observed at of 815cm^{-1} .The characteristic bands for OH^{-} was appeared at 3365cm^{-1} (Figure 3.9)

Table 3.8: Peaks of infrared spectra assigned to alginate

Compound	Name of the assigned group	Infrared frequency (cm–1)
Alginate	-CH stretching	815
	C-O-C stretching	1028,1083
	C-O stretching	1298
	-COO group	1409,1597
	-OH stretching	3365

Different percentages cross-linked scaffolds, radiated at 5kGy:

The peaks of infrared spectra of different concentration HA/Chi-Alg composite have been shown in Table 3.9. When the bands of scaffold were compared with the HA, chitosan and alginate banding pattern, some peak of scaffolds were found to shift from the original peak position due to the formation of new bond among them.

The asymmetric stretching vibration of phosphate (v3 PO4) was found in 1024-1037 cm^{-1} , whereas the characteristic bands for OH^- appeared at 3354 to 3782cm^{-1} in different scaffold, which was indicated in HA (Figure 3.9).

Table 3.9: Peaks of infrared spectra in different percentages of cross-linked scaffolds, irradiated at 5kGy

Name of the assigned group	Infrared frequency (cm^{-1})					
	CR0H0	**CR5H0**	**CR5H1**	**CR5H2**	**CR5H3**	**CR5H4**
P-O band V3	1037	1033	1024	1028	1028	1026
HPO_4^{2-}	896	894	894	894	896	898
Vibrations of CO	1064	1072	1159	1070,1159	1072,1159	1072,1161
Vibration of C-H	1311,2881	1224,1367, 2924	1238, 1373, 2858,2926	1234,1373,2931	1273,1381,2931	1240,1371,2933
Amide I	1641	1643	1643	1641	1641	1645
C=O from COO- group	1529	1710	1454, 1548,1712	1452,1539,1714	1454,1543,1714	1452,1546,1714
-OH stretching	3354	---	3373	3373	3369	3387

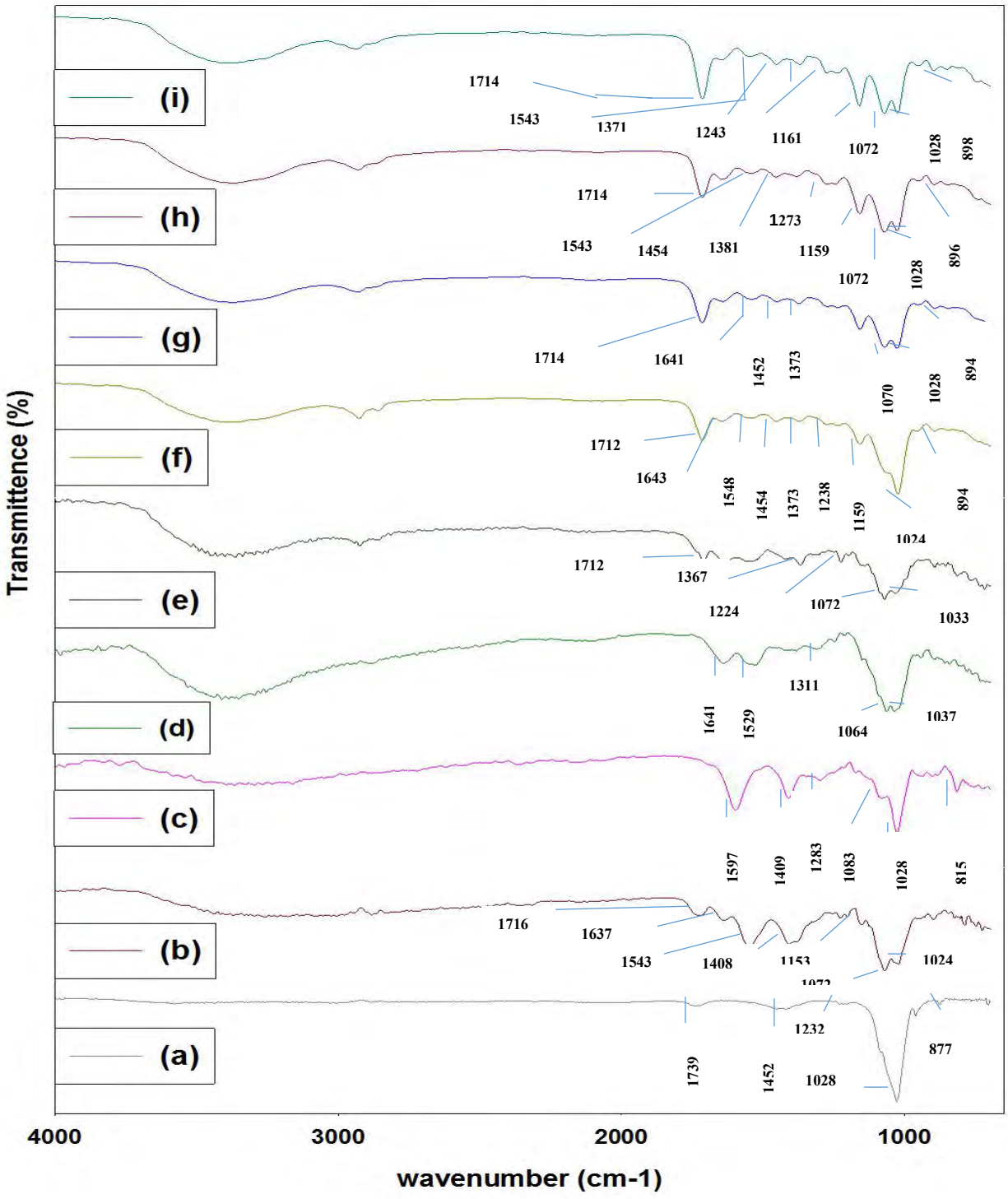

Figure 3.9: FTIR spectra of a) HA, b) Chitosan, c) Alginate, d) CR0H0, e) CR5H0,f) CR5H1, g) CR5H2, h) CR5H3 and i) CR5H4.

The HPO_4^{2-}bands at 875 cm^{-1} was shifted to 894-896 cm^{-1}in different percentages of cross-linked sample. The peak position 1382, 2883 and 2926 cm^{-1} for band of C-H were shifted to 1311-1381, 2858-2881 and 2924-2933 cm^{-1} in different scaffold containing cross-linker sequentially. Peak position 1153 cm^{-1}& 1637 cm^{-1} for band of C=O & amide-I were shifted into 1159-1161 cm^{-1} and 1641-1645 cm^{-1} consequently in different scaffold (Figure 3.9).

Considering the porosity, density, biodegradability and FTIR analysis CR5H3 found more potent to be subjected for further studies to determine pore morphology by SEM analysis.

3.1.4.4 SEM analysis

Scanning electron microscopy (SEM) is one of the most crucial and precise tools that can image bio nanostructure and it can also track bio-materials in nano-materials, and finally measure physical properties and determine composition. SEM images surface with a beam of electrons which produce three-dimensional image of a sample. So SEM micrograph is useful for understanding structure of surface. The surface morphology, pore distribution and pore size of HA/Chi-Alg was directly measured in a scanning electron micrograph, and found to be highly porous with a pore size of 162–510 μm for the CR5H3scaffolds (Figure 3.10 a & b)

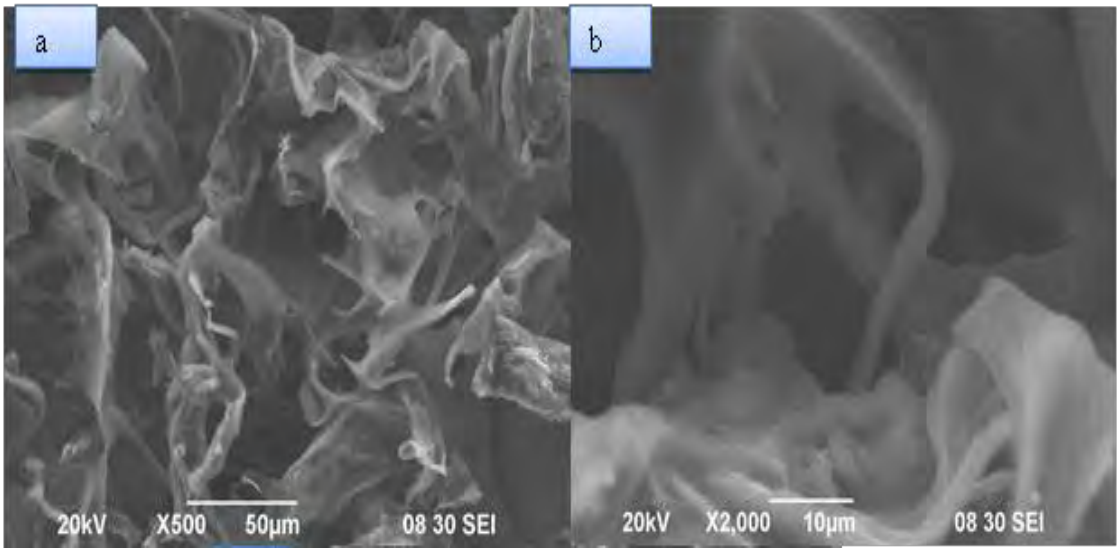

Figure 3.10: SEM micrographs of scaffold (a) CR5H3 (low magnification) (b) CR5H3 (High magnification)

3.2 Characterization of Hydroxyapatite, Collagen and Chitosan (HCC) scaffold

In the previous section, we had got a comparatively ideal ratio to fabricate the scaffold for bone tissue engineering application. In this study, we used this ratio to prepare the HA-Collagen-Chitosan (HCC) scaffold. Fabricated scaffold were characterized by porosity, density, swelling ratio, biodegradability, FTIR and SEM analysis.

3.2.1 Porosity and density

The collagen based scaffolds were prepared by thermally induced phase separation technique showed porosity from 90.64% to 96.21%. Table 3.10 shows that, addition of different types of cross linker into the scaffolds, there was shown alteration in the porosity and density of the composite scaffold. The highest porosity (96.21%) was found with very low density (0.113 g/m^3) in sample S_O where no cross linker was applied, whilst highest density was found in sample S_G that was 0.183g/m^3 in which glutaraldehyde was used as a cross linker but along with the lowest porosity 90.64% comparatively than other scaffolds. From the table 3.10 the variation of porosity with their density profile is visible with the addition of different types of cross linker.

Table 3.10: Porosity and density of the scaffolds

Types of scaffold		Porosity (%)	Density (g/cm^3)
Without cross linker	HCC scaffold (S_O)	96.21	0.113
Physical cross linker	HCC scaffold cross linking with DHT treatment (S_T)	94.24	0.124
	HCC scaffold + 25 kGy radiation (S_R)	95.29	0.115
Chemical cross-linked	HCC scaffold + HEMA (S_H)	92.75	0.157
	HCC scaffold + Gluteraldehyde (S_G)	90.64	0.183

3.2.2 Swelling ratio

The water uptaking ability of the scaffold was determined by the swelling test where cross linked and non-cross linked samples were soaked in to the phosphate buffer saline consequently for 2h, 24h, 48h and 72h. Table 3.11 shows the swelling ability changes with the addition of different cross linker with the sample.

Table 3.11: Swelling percentage of scaffold composition on the overall water uptake at different soaking time

Types of scaffold	2 h	24 h	48 h	72 h
S_O	517.83	524.31	519.15	521.25
S_T	384.81	391.64	379.92	385.18
S_H	320.08	316.92	336.75	329.06
S_G	307.23	311.38	305.49	306.24

Figure 3.11 depicts that lowest water uptaking ability found in sample S_G for different hrs. Whereas highest water absorption rate found in sample S_O where no cross linker were used. It was also shown that there was not any statistical difference of water uptake between time intervals in the individual sample.

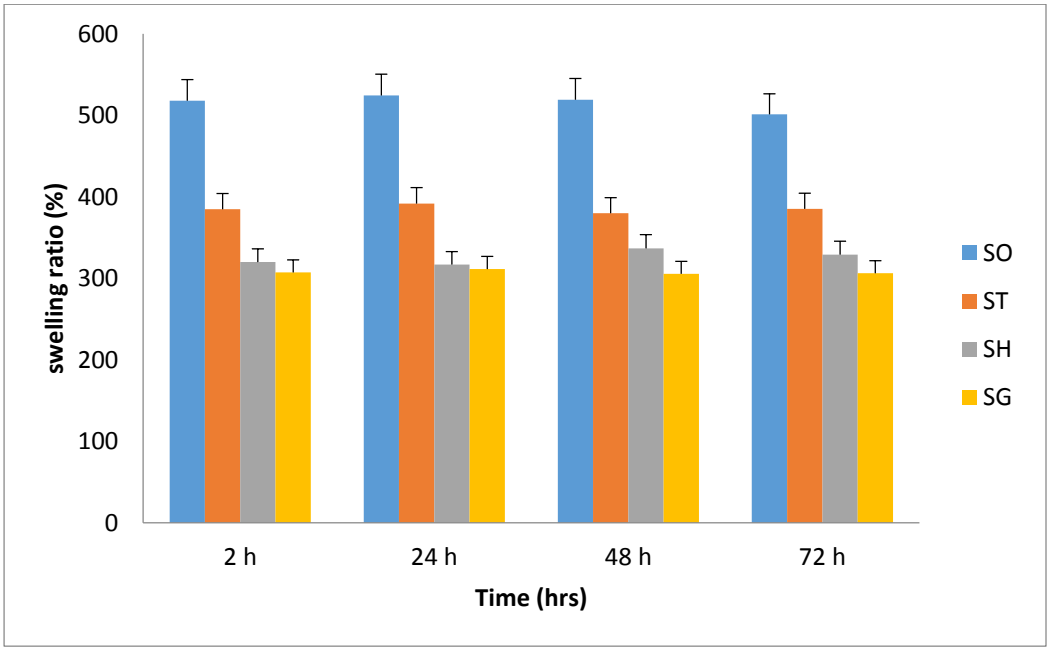

Figure 3.11: Swelling percentage of scaffold composition on the overall water uptake at different soaking time

Table 3.12: Swelling percentage of scaffold material itself at different soaking time

Types of scaffold	2 h	24 h	48 h	72 h
S_O	389.17	316.75	370.11	355.94
S_T	188.76	195.87	191.53	184.05
S_H	234.61	221.54	227.83	219.57
S_G	76.24	74.10	78.03	75.19

From the table 3.12, it can be describes that scaffold crosslinked with glutaraldehyde comparatively showed lowest swelling ability that is 76.24, 74.10, 78.03, 75.19 (%) for 2 , 24 , 48, 72h sequentially. On the other hand scaffold without cross linker showed highest swelling ability. Figure 3.12 represents the variation of swelling ability of different scaffolds.

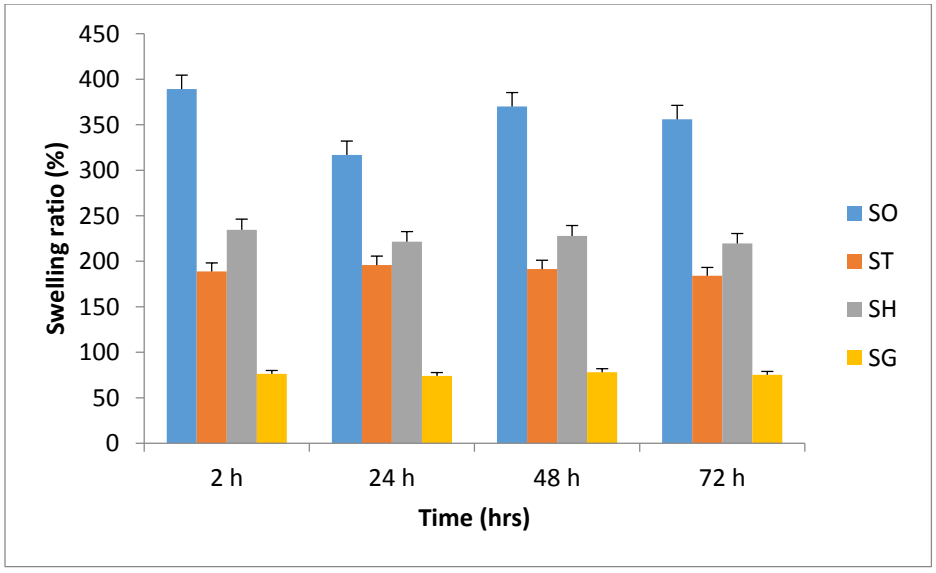

Figure 3.12: Swelling percentage of scaffold material itself at different soaking time

3.2.3 Biodegradation test

Biodegradation is an important factor for biomedical scaffolds. Degradation behaviors of porous scaffolds play an important role in the engineering process of a new tissue. The degradation rate of porous scaffolds affects cell vitality, cell growth, and even host response. The HCC sample mixed with different cross linker and one sample with no cross linker were undertaken for biodegradation test for sequentially 1,3,7, 14 and 21day (table-3.13) .

Table 3.13: In-vitro degradation profile of Scaffold

Types of scaffold	1 d	3 d	7 d	14 d	21 d
S_O	39	43	48	51	55
S_T	16	18	19	20	21
S_H	22	26	31	37	42
S_G	10	11	13	15	16

Biodegradation rate was also varied due to the addition of different cross linker. The lowest degradation rate was found in glutaraldehyde cross-linked sample (S_G). The degradation rate of S_G sample was 10% and 16 % for day 1 and day 21, respectively. On the other hand, without cross linker sample (S_O) was applied showed drastic degradation rate i.e. 39% for 1 day and 55% for 21day. The degradation rate of different sample in 1, 3, 7, 14 and 21 days are illustrated in figure 3.13.

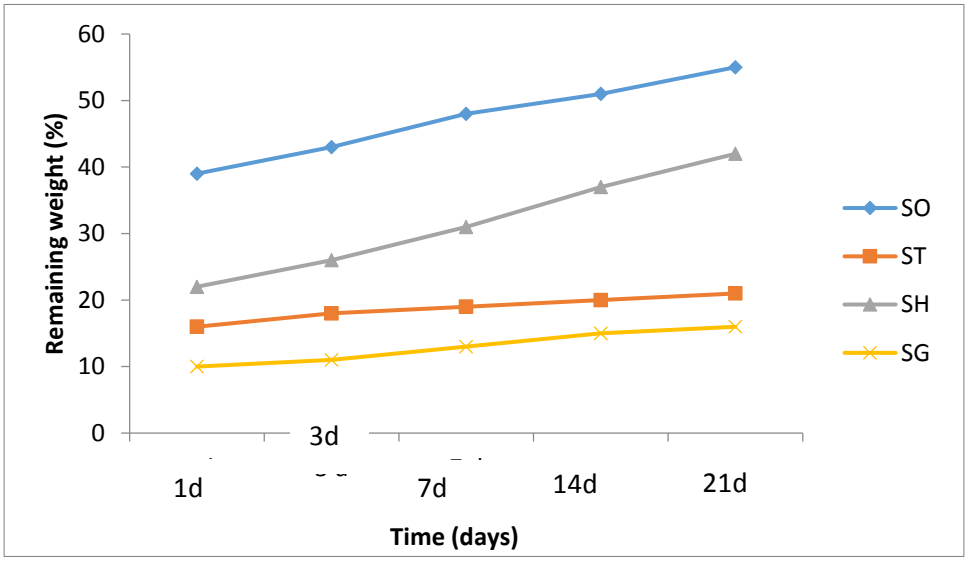

3.2.4 FTIR Analysis

In order to illustrate intermolecular interaction among components in scaffold, FTIR spectroscopy measurements were taken to compare the result of pure hydroxyapatite (HA), Chitosan, Collagen, and HCC based composite cross-linked with different physical and chemical cross linker (S_0, S_T, S_H, S_G).

Hydroxyapatite

Figure 3.14 illustrates the FTIR spectrum of HA. It has shown the asymmetric stretching vibration of phosphate ($v^1 PO_4$), ($v^3 PO_4$) and ($v^4 PO_4$) present in HA appeared at 962 cm^{-1}, 570-603 cm^{-1} and 1028-1058 cm^{-1}, respectively. Whereas the band at 877cm^{-1}& 572 cm^{-1} suggests the presence of HPO_4^{2-} group. The characteristic bands for OH^- appeared at 3452 to 3782cm^{-1}.

Chitosan

The peaks of infrared spectra of Chitosan Scaffold has been shown in figure 3.14. The bands at 2845 cm^{-1} were corresponded to the CH stretching. The broad bands at 1637 and 1543 cm^{-1} were attributed to the presence of amide I and amide II groups. The sharp band at 1408 cm^{-1} was assigned to stretching of carbonyl from COO^- group. The low intense bands at 1382 and 1321 cm^{-1} were corresponded to CH bending vibrations of the ring. The characteristics peaks of C-O-C glycosidic linkage were observed in the region of 1153-1021cm^{-1}.

Collagen type –I

The main absorption bands of collagen are amide A (3299 cm^{-1}), amide B (2950-2919 cm^{-1}) and amide I (1632-1664 cm^{-1}) with N-H stretching signature. In contrast, amide II (1500-1585 cm^{-1}) and amide III (1200-1300 cm^{-1}) were also observed. A free N–H stretching vibration occurs in the range of 3400–3440 cm^{-1} and when the NH group of a peptide is involved in a hydrogen bond, the position is shifted to lower frequencies, usually around 3300 cm^{-1}. The result was indicated that the NH groups of this collagen were involved in hydrogen bonding, probably with a carbonyl group of the peptide chain. The amide B band positions were found at wave numbers of 2919 cm^{-1}, representing the asymmetrical stretch of CH_2.

Table 3.14 Peaks of infrared spectra assigned to collagen type – I

Compound	Name of the assigned group	Infrared frequency (cm^{-1})
Collagen type-I	Amide A	3299
	Amide B	2889
	Amide I	1645
	Amide II	1527
	Amide III	1242
	N–H stretching	3411

Amide I peak (1628 cm^{-1}) is associated with stretching vibrations of carbonyl groups (C=O bond), along the polypeptide backbone and it is the most useful for infrared spectroscopic analysis of the secondary structure of proteins. The amide II peak of the collagens was observed at 1540 cm^{-1}, resulting from N–H bending vibration coupled with the stretching vibration of CN (1536–1544 cm^{-1}). Amide III (1234 cm^{-1}) is related to CN stretching and NH and is involved with the triple helical structure of collagen.

Table 3.15: Peaks of infrared spectra in different cross-linked scaffolds and non-cross linked HCC scaffold.

Name of the assigned group	Infrared frequency (cm^{-1})			
	S_O	S_T	S_H	S_G
carbonate V_2	------	823.6, 869.9	854.47	896.9
CO_3 V_3	1411.89, 1543.05	1402.25, 1560.41	1425.4, 1537.27	1396.46, 1544.98
PO_4^{3-} V_3	1037.7	1026.13, 1085.92	1024.2, 1091.71	1026.13, 1053.13
Asymmetric HPO_4	1149.57	1155.36	1234.44,	------
amide III	------	1325.1	1298.09, 1381.03	1396.46
amide I	1639.49	1643.35	1643.35	1645.28
N–H stretching	3213.41, 3398.57	3265.49	3122.75, 3572.17	3184.48, 3525.88

Figure 3.14 is also depicted that carbonate V_2 found for sample S_T, S_H and S_G at 823.6-869.9 cm^{-1}, 854.47 cm^{-1} and 896.9 cm^{-1} sequentially. Again CO_3 V_3 also found for sample S_0, S_T, S_H and S_G at 1411.89, 1543.05 cm^{-1}; 1402.25, 1560.41 cm^{-1}; 1425.4, 1537.27 cm^{-1}; and 1396.46, 1544.98 cm^{-1} respectively.

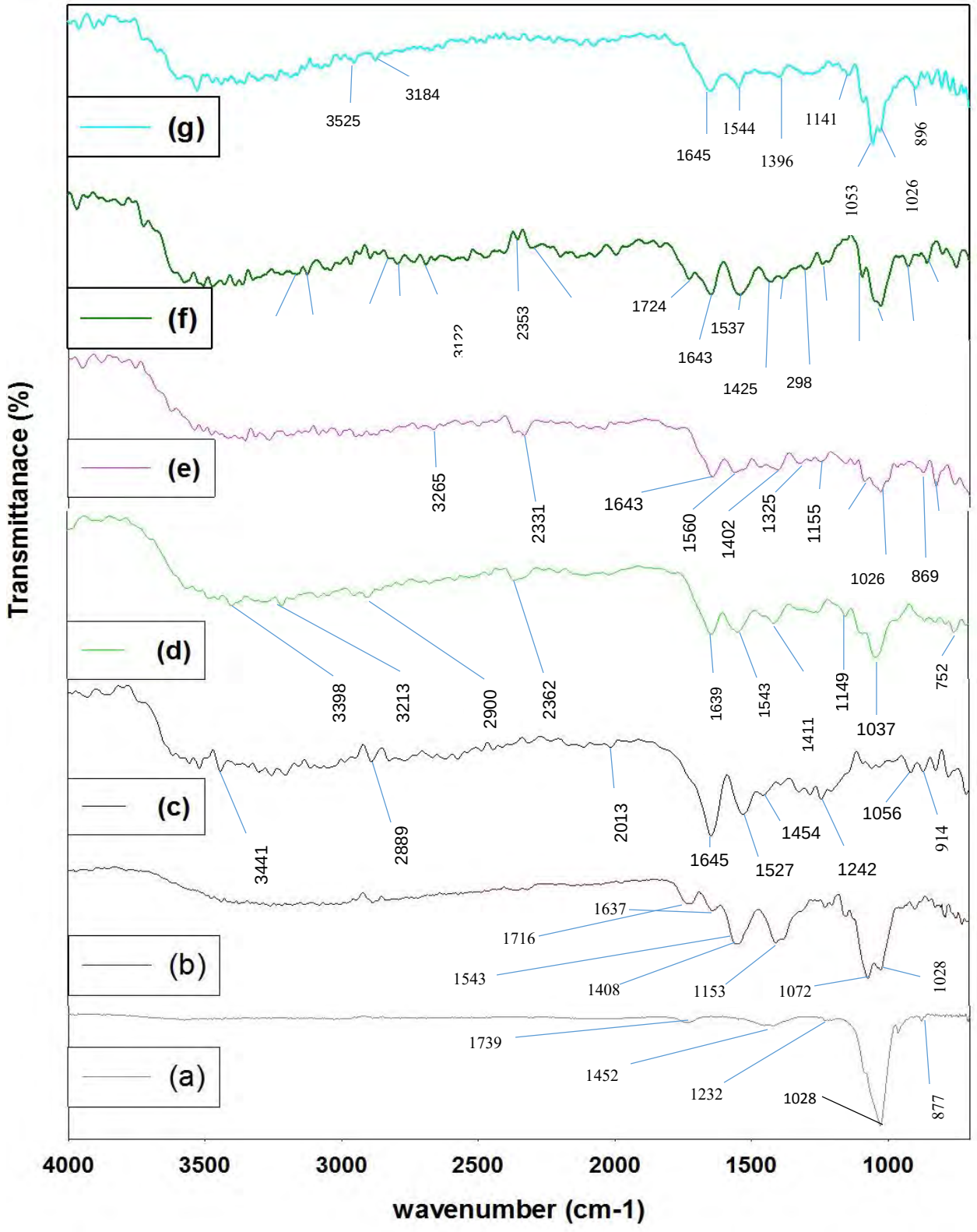

Figure 3.14: FTIR spectra of a) HA, b) Chitosan, c) Collagen, d) S_0, e) S_T, f) S_H, g) S_G

At the same time, amide I also found for sample S_0, S_T, S_H and S_G at 1639.49, 1643.35 cm^{-1}; 1643.35 and 1645.28 cm^{-1} correspondingly. In contrast, the N-H stretching was also shown for sample S_0, S_T, S_H and S_G at 3213.41, 3398.57 cm^{-1}; 3265.49 cm^{-1}; 3122.75, 3572.17 cm^{-1}; and 3184.48, 3525.88 cm^{-1} separately. Besides, other functional groups such as- amide III, PO_4^{3-} v3, asymmetric HPO_4 etc. found at different peak position assigned by various numeric value. From the Table 3.15, we can find the assigned numeric value including their functional group of different scaffold.

3.2.5 SEM analysis:

The porous HCC matrices were fabricated by freeze-drying and cross-linked using physical and chemical way. Scanning electron microscopy (SEM) was used to examine the microstructure of the scaffolds. Figure 3.15 shows SEM images of the horizontal cross section of freeze-dried scaffolds. The porosity of formed scaffolds was quite high. From SEM observations one can see scaffold of HCC with fully inter-connective macro-porosity. SEM results show a structure of irregular interconnected pores with a size of 111.80-212.60 µm.

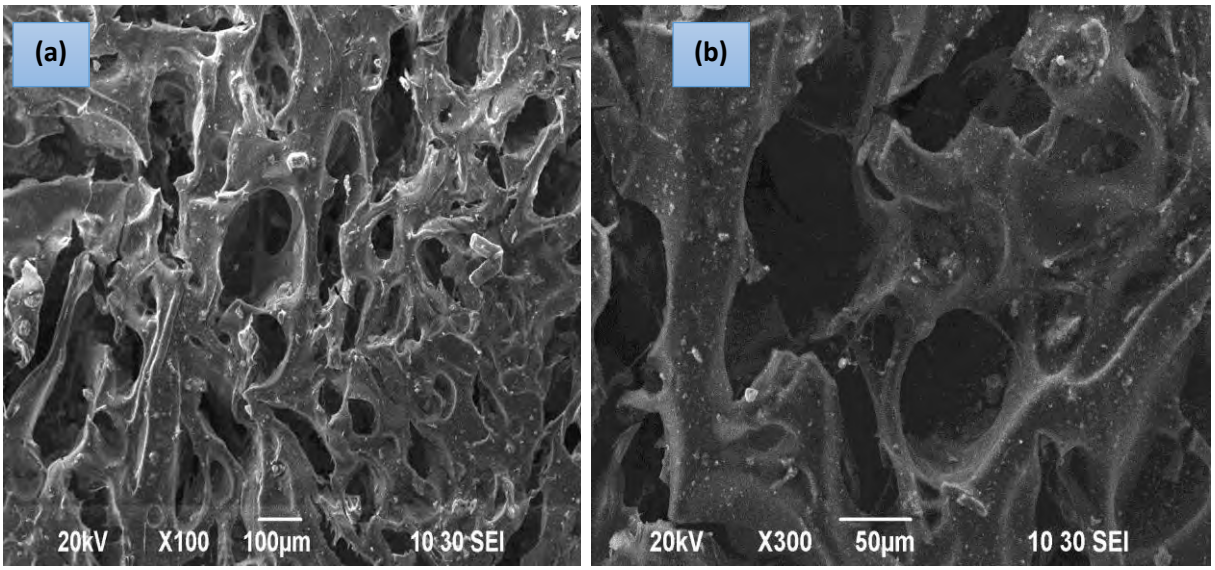

Figure 3.15: SEM micrographs of scaffold (a) HCC (low magnification) (b) HCC (High magnification)

3.3 Comparisons of HCA and HCC scaffold with human bone allograft (HBA)

The use of porous polymer/bio ceramic composites to repair and replace injured bone tissue has been a well-established area of interest. The fabrication of materials that can match both mechanical and biological properties of human bone tissue matrix is a critical concern in orthopedic treatment. Keeping this aforementioned fact in mind, attempts have been made to recreate nanoscale topographical cues from the extracellular environment with improved levels of bio-functionality.

The goal of the study is to fabricate a scaffold that mimic the characteristics of human bone and can be used as a substitute to human bone so it is important to compare our whole study with human bone allograft. In this regard, hydroxyapatite-chitosan-alginate (HCA) and hydroxyapatite-collagen-chitosan (HCC) scaffold were fabricated by freeze drying method and characterized their properties and also compared them with human bone allograft (HBA). Porosity is the key parameter for the scaffold design. A highly porous scaffold plays a critical role in cell seeding, proliferation and new tissue formation in three dimensions (3D). An ideal bone scaffold should have sufficient porosity (such as ≥90%) to accommodate osteoblasts or osteoprogenitor cells. The porosity of human bone allograft found 96% comparing with the other two samples (HCC and HCA), it was found 90.64 % and 86 % which was close enough to the HBA. Then density properties showed huge different i.e. for HBA it showed 0.625g/cm^3 and HCC sample showed 0.183g/cm^3 but HCA sample showed 0.076g/cm^3 which was very poor comparing to the HBA.

Table 3.16: Comparison of Hydroxyapatite-Chitosan-Alginate (HCA) and Hydroxyapatite-Collagen-Chitosan (HCC) scaffold with Human Bone Allograft (HBA)

Sample ID	Porosity (%)	Density (g/cm^3)	Swelling Ratio (%)		Remaining weight (%)	
			Scaffold Water uptake (2 hrs)	Material water uptake(2 hrs)	1day	7day
HBA	96	0.625	51.30	13.68	89	80.82
HCA	86	0.076	354.61	68.64	78.57	50
HCC	90.64	0.183	307.23	76.24	90	87

In the contrast, the water up taking rate varied drastically where HCA showed highest water absorption rate (354.61%) and HCC showed (307.23%) but water absorption rate for HBA found 51.30%. Finally, comparing the degradation properties among HBA, HCA and HCC it was found that the remaining weight of sample HCA and HCC for day 1 & day 7 consequently 90 & 87%; and 78. 57 & 50% for HCA sample; whilst remaining weight of HBA found 89% for day 1 and 80.82% for day 7. The complete comparisons among HBA, HCA and HCC are illustrated in Table 3.15.

Pore morphology analysis:

Scanning electron microscopy (SEM) was used to examine the microstructure of the scaffolds. It is a necessary tool that helps to observe the bio-nanostructure and also tracks the biomaterials in a composite. Moreover the fundamental requirement of a composite i.e. its pore surface structure, pore morphology, pore size and pore distribution, which are basically the prerequisite for cell migration and regeneration can be determined by SEM analysis.

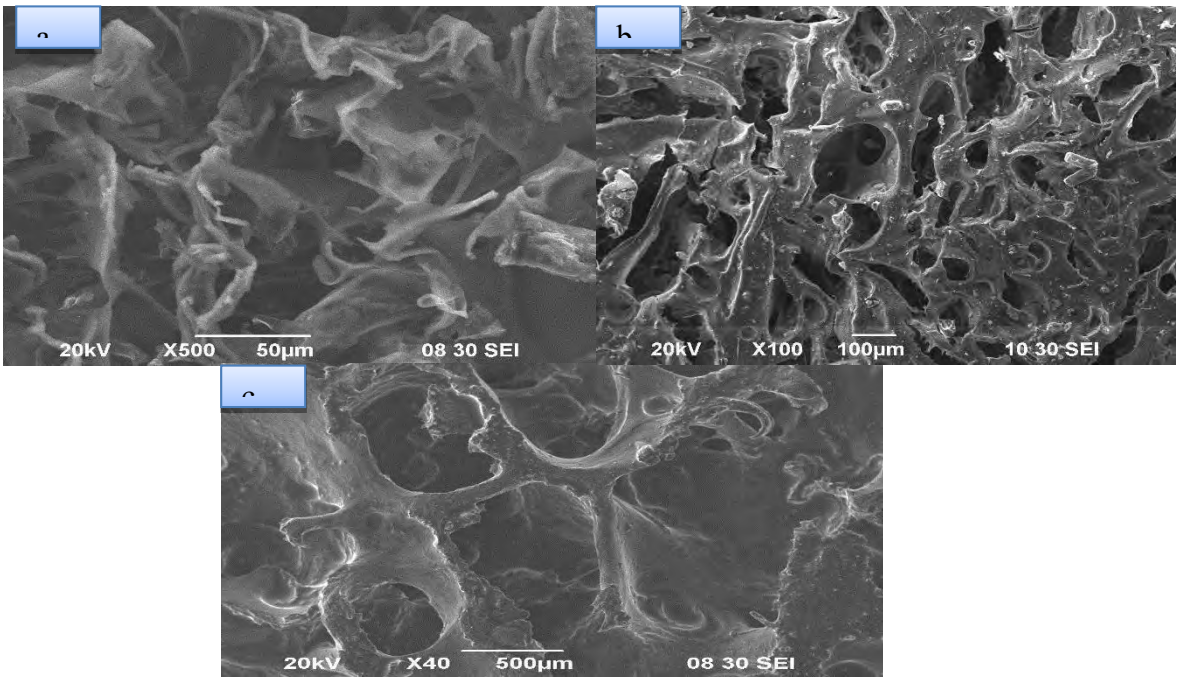

Figure 3.16: SEM analysis of a) HCA, b) HCC, c) HBA

Figure 3.16 shows the comparative SEM images of the horizontal cross section of freeze-dried scaffolds (HCC & HCA) and human bone allograft (HBA) prepared from human femoral head.

In the HCA scaffold, the porosity was 162 to 510 µm (mean: 251 ± 113) (Fig. 3.16 a). The pore size of HCC scaffold was directly measured and found to be moderately porous with an expected pore size of 111.80-212.60 µm (mean: 157 ± 41) (Fig. 3.16 b). Macro pores of HBA ranged from 420 to 623µm and mean pore diameter of HBA was 515 ± 102 µm (Fig. 3.16 c).

Discussion

Tissue engineering represents the alternative or complementary solution to the damaged tissue or organ failure that is addressed by implanting natural biopolymers, synthetic or semi synthetic three-dimensional tissues. For this purpose, investigation of a noble biomaterial found to be most crucial step in the area of bone tissue engineering. In addition, to ameliorate or recover the damaged bone by replacing them with scaffold that mimic human bone with high regenerative capacity scaffold fabrication is the most feasible and significant approach. Scaffold for bone tissue engineering should have some high porous structure. Greater porosity and pore size with high surface area that enables the adherence of the bone cell to the scaffold that promote bone tissue regeneration. The goal of the study was to fabricate a scaffold that mimic the characteristics of human bone and can be used as a substitute to human bone, so it is important to compare our whole study with human bone allograft. In this regard, hydroxyapatite-chitosan-alginate (HCA) and hydroxyapatite-collagen-chitosan (HCC) scaffold were fabricated by freeze drying method and characterized their properties and also compared them with human bone allograft (HBA).

Hydroxyapatite-Chitosan-alginate scaffold:

From a biomimetic basis, we constructed (HA/Chi-Alg) composite scaffolds that comprised of constant ratio of synthetic HA and different ratio of the polymers. The prepared materials and resultant structures of the porous scaffolds were further characterized to analyse their composition, biodegradability, morphology, porosity, density which was compared with human cancellous bone allograft (HBA). In this study, scaffold were prepared at two different ratio where mineral's ratio was constant for both composite scaffold but the polymer's ratio were altered (1:1and 1:2).

The total porosity and density of scaffold were measured by using liquid displacement method. The highestand lowest porosity value was measured respectively at sample HCA-2 (75%) and HCA-1(67%). Highest density was found in sample HCA-1 (0.076 g/cm^3) and the lowest density was found in sample HCA-2 (0.041 g /cm^3) [Table-3.2]. The density value increased from 0.041 to 0.076 g /cm^3 due to the denser packing of polymer network and as expected led to a decrease in porosity. (Sehaqui *et al*., 2010 and Sehaqui *et al*., 2011).

To determine the biodegradability result, HCA (HCA-1, HCA-2) samples were soaked into the PBS buffer solution for sequentially 1, 3 &7 days, the remaining weight of the scaffold after 7 days for sample HCA-2 were found 17.05%, which was comparatively higher than sample HCA-1 that was 13.4%. Whilst after 1day the remaining weight for sample HCA-1 and HCA-2 found 77.4% and 74.05% respectively. The change in degradation properties is visible from Table 3.3.

Based on porosity, density and biodegradability test, from the HCA (HCA-1 and HCA-2) samples, Scaffold sample HCA-2 was selected and crossed linked with HEMA (2-Hydroxyethyl Methacrylate), at different percentages (0.5%, 1%, 1.5% and 2%) and also irradiated at different doses (25 kGy, 15 kGy, 10 kGy, and 5 kGy). At the beginning it found difficult to dissolve components in the presence of HEMA and slurry was continuously formed when the solutions were irradiated at 25 kGy, 15 kGy, and 10 kGy [Figure 3.4]. But when the components were dissolved after irradiation at 5 kGy in the presence of HEMA, wefound the optimum radiation dose for dissolving components in the presence of cross linker HEMA. So, it can be hypothesized from this analysis, that the increased radiation dose (>5 kGy) might be effecting the cross linker for better dissolving with the components that subjected to the chemical bond breakdown of the cross linker. After that, the crosslinked samples were washed with ethanol 2-3 times for sterilization and the removal of residual nonbinding components.

The physiochemical analysis of the six crosslinked scaffolds, sample CR5H3 was found to be more porous (86%) than others (62-81%) [Table 3.4]. The results showed that at the same ratio (1:2) of mineral-polymer and radiation dose (5 kGy), by increasing the percentage of crosslinking agent, the porosity of scaffold were found to increase and the optimum value was determined at 1.5% among the cross-linked scaffold. When the percentage of crosslinking agent is increased that is more than 1.5%, the porosity of scaffold were found to decrease. Meanwhile among the samples the highest density was found in sample CR5H3 (0.076 g/cm^3) and the lowest was in sample CR5H0 (0.041 g/cm^3).

FTIR analysis is an important tool to determine the chemical changes at molecular level. The width and intensity of spectral bands as well as position of peaks are all sensitive to chemical changes and to conformations of macromolecule. Infrared absorption spectra of the scaffold are summarized in Figure 3.9.

The absorption bands at 3540 cm^{-1}, 3487 cm^{-1} and 633 cm^{-1} represent the stretching and vibration of the lattice OH^- ionsrespectively, while the bands of absorbed water are shown at 3287 cm^{-1} and 3163 cm^{-1}. Also, low intense band of adsorbed water (stretching) is present at 1642 cm^{-1} (Chen *et al.*, 2004). The characteristic bands for HPO_4^{2-} is shown at 1133 cm^{-1}, 1064 cm^{-1}, 989 cm^{-1}, 875 cm^{-1}, 577 cm^{-1}, 527 cm^{-1}. The magnitude of these bands became weaker with the development of in situ hydration and finally disappeared (Koumoulidis *et al.*, 2003). The characteristic band for PO_4^{3-} is observed at 963 cm^{-1} for the ν1 mode (Tang *et al.*, 2008; Olad and Azhar, 2014). The signal became clearly as the hydration processing. The observation of the ν3 symmetric P-O stretching vibration at 1032-1042 cm^{-1} as a distinguishable peak, together with the bands 566-602 cm^{-1} corresponds the ν4 bending vibration and indicates the presence of HA in the scaffold.

In the pure chitosan spectrum, band corresponding to N–H stretching is observed at 3400 cm^{-1} (Katti *et al.*, 2008). The bands at 2920 and 2845 cm^{-1} corresponded to the CH stretching. The broad bands at 1643 and 1546 cm^{-1} represented the presence of amide I and amide II groups. The sharp band at 1404 cm^{-1} assigned to stretching of carbonyl from COO− group. The low intense bands at 1375 and 1321 cm^{-1} corresponded to CH bending vibrations of the ring. The characteristics peaks of C-O-C glycosidic linkage were observed in the region of 1153-1021 cm^{-1} . The absorption band corresponding to the CH deformation vibration of β-pyranose was observed at 897 cm^{-1} (Chang and Tanaka, 2002).

The alginate spectrum shows the characteristic peak at 1298 cm^{-1}, which corresponds to the carboxylate group (C=O). In addition, a strong intense peak was observed at 3365 cm^{-1}, corresponding to the –OH group. The symmetric stretching frequency of the carboxyl group was observed at 1409 cm^{-1}, whereas 1028–1083 cm^{-1}shows the asymmetric stretching frequency.

On the other hand, in the case of Chi-Alg, an intense peak was observed at 1161 and 1641 cm^{-1}, corresponding to the superposition of the bands assigned to the carboxylate group of alginate and the amine group of chitosan respectively. The interaction from electrostatic interaction between the carboxylate group of alginate and the amine group of chitosan forms a polyelectrolyte complex (Ho *et al.,* 2009). The lower stretching frequency in –OH was observed from 3354cm^{-1} to 3387 cm^{-1}. This suggests that intermolecular hydrogen bonds exist in the chitosan-alginate system (Zhang *et al.,* 2000).

In the HA/chitosan-alginate composite spectrum, the amide-I peak shifted from 1641 to 1645cm^{-1}, and the peak of the amino group (1173 cm^{-1}) was absent. These changes suggest the formation of the chitosan-alginate copolymer complex, as a result of the ionic interaction between the negatively charged carbonyl group (–COOH) of alginateand the positively charged amino group (–NH_2) of chitosan (Li *et al.,* 2005). The broad bands around 3354 to 3782cm^{-1} represent the absorbed water or contained water in the scaffold (Zhang and Zhang, 2002).

The surface morphology, pore distribution and pore size of HCA scaffold was examined using scanning electron microscopy analysis (Figure 3.10). The depicted pore size enables the scaffolds to allow for cell adhesion, proliferation and also nutrient supply, which will enable proper bone tissue growth. The optical microscopic images inferred that the dispersion of the components is uniform within the scaffolding network for the HCA scaffolds.

Hydroxyapatite- Collagen- Chitosan Scaffold:

Following the previous ratio pattern (HCA scaffold mineral-polymer ratio) of hydroxyapatite-chitosan-collagen based scaffold were fabricated by freeze drying method and cross linked using two types of cross linker (physical and chemical). In the physical cross linker de-hydrothermal treatment (DHT) and another is radiation. On the other hand, glutaraldehyde and calcium chloride were used as a chemical cross linker.

Porosity is the key parameter for the scaffold design. A highly porous scaffold plays a critical role in cell seeding, proliferation and new tissue formation in three dimensions (3D). An ideal bone scaffold should have sufficient porosity (such as ≥90%) to accommodate osteoblasts or osteoprogenitor cells (Liu *et al*., 2004 and Sabir *et al*., 2002) In this study, the collagen based scaffolds prepared by freeze-drying showed porosity from 90.64 to 96.21%. After dehydro-thermal treatment (S_T) and irradiated sample (S_R) of HCC scaffold showed porosity 94.24 % and 95.29% respectively. At the same time, sample treated with chemical cross likers S_H and S_G showed 92.75% and 90.64% porosity. But highest porosity was found in sample S_O that is 96.21% where no cross linker was applied. Analyzing the density report, the highest and lowest density was measured 0.183 and 0.113 g/m_3^{-1} in sample S_G and S_O. It has already found that density and porosity reversely equal. When density is increased, at same time porosity is decreased in scaffolds. Other density values have been described in Table 3.10.

The ability of a scaffold to retain water is an important index to evaluate its efficacy for tissue engineering (Ma *et al*., 2003 and Shanmugasundaram *et al*., 2001). Scaffold swelling properties have been shown to significantly influence cell behaviors such as adhesion, growth and differentiation (Park *et al*., 2003). In this study each value of swelling test was averaged from three parallel measurements. Analyzing the swelling test we were able to find out the best water uptaking ability of a scaffold. Cross-linked and non-cross-linked scaffold were soaked in the PBS sequentially for 2h, 24h, 48, 72h. After soaking the highest water uptaking ability found in sample S_O and the lowest water up taking ability found in sample S_G [Table 3.11]. Again the swelling ability measured by removing the water from the scaffold by pressing it with blotting paper as well as it could be done. Then the considerable result found in sample S_G [Table 3.12]. The swelling test showed that the water uptake of the scaffold was higher for without cross-linked scaffold samples and decreased with glutaraldehyde content. This may be due to the HA formed crosslink between the collagen chains and resulted in decreasing the hydrophilicity of collagen by binding calcium and phosphate to the hydrophilic COOH or NH_2 groups.

Biodegradability is another important factor for biomedical scaffolds. Degradation behaviors of porous scaffolds play an important role in the engineering process of a new tissue. The degradation rate of porous scaffolds affects cell vitality, cell growth, and even host response (She *et al*., 2008 and Tan *et al*., 2007). Biodegradation is an important and foremost factor in scaffold fabrication. Observing the in vitro degradation profile we were able to find out the most eligible composite. Degradation test was run sequentially for 1d, 3d, 7d, 14d and 21 d. The lowest degradation pattern (10-16%) found in sample S_G and the highest degradation pattern (39-55%) found in sample S_O for the above mentioned days. It also can be concluded that the average degradation pattern was found in sample S_G. Degradation pattern for other sample are shown in Table 3.13 (Sionkowska *et al*., 2013) also found highest degradation rate in uncross-linked scaffold.

FTIR is another crucial analysis that helps us to understand the network and binding capacity among the components of the scaffold. It is not possible to find out the accurate form of binding position but the numeric values or wave number that resemble the functional group and results of a specific bonding among the chemical components of the scaffold. Figure 3.14

Combination of absorption bands absorption bands of CO_3 v_3 groups at 1418 cm^{-1} and 1458 cm^{-1} , as well as at 875 cm^{-1}, proves substitution of "B-type" PO_4 groups with CO_3 groups in the HA crystal lattice (Barinov *et al*., 2006 and Siva Rama Krishna *et al*., 2007). These locations of absorption bands of the functional groups explicitly indicate forming of atypical HA structure in the synthesized samples (Nilen & Richter, 2008; Siva Rama Krishna *et al*., 2007; Kothapalli, *et al*., 2004; Landi, *et al*., 2000; Lioua, *et al*., 2004).

In the pure chitosan spectrum, band corresponding to N–H stretching is observed at 3400 cm^{-1} (Katti *et al*., 2008). The bands at 2920 and 2845 cm^{-1} corresponded to the CH stretching. The broad band's at 1643 and 1546 cm^{-1} represented the presence of amide I and amide II groups. The sharp band at 1404 cm^{-1} assigned to stretching of carbonyl from COO− group. The low intense bands at 1375 and 1321 cm^{-1}corresponded to CH bending vibrations of the ring. The characteristics peaks of C-O-C glycosidic linkage were observed in the region of 1153-1021 cm^{-1} The absorption band corresponding to the CH deformation vibration of β-pyranose was observed at 897 cm^{-1}(Chang and Tanaka, 2002).

In the pure collagen spectrum, the main absorption bands of amide A (3299 cm^{-1}), amide B (2950-2919 cm^{-1}), amide I (1632-1664 cm^{-1}) N-H stretching signature also seen respectively, amide II (1500-1585 cm^{-1}) and amide III (1200-1300 cm^{-1}). According to Doyle *et al*. (Doyel *et al*., 1975), a free N–H stretching vibration occurs in the range of 3400–3440 cm^{-1} and when the NH group of a peptide is involved in a hydrogen bond, the position is shifted to lower frequencies, usually around 3300 cm^{-1}. The result indicated that the NH groups of this collagen were involved in hydrogen bonding, probably with a carbonyl group of the peptide chain. The amide B band positions were found at wave numbers of 2919 cm^{-1}, representing the asymmetrical stretch of CH_2 (Muyonga *et al*., 2004). Amide I peak (1628 cm^{-1}) is associated with stretching vibrations of carbonyl groups (C=O bond), along the polypeptide back bone (Eklouh-Molinier *et al*., 2014) and it is the most useful for infrared spectroscopic analysis of the secondary structure of proteins (Surewicz *et al*., 1988). The amide II peak of the collagens was observed at 1540 cm^{-1}, resulting from N–H bending vibration coupled with the stretching vibration of CN (1536–1544 cm^{-1}) (Krimm and Bandekar, 1986). Amide III (1234 cm^{-1}) is related to CN stretching and NH and is involved with the triple helical structure of collagen.

In this study, carbonate v_2 found for sample S_T, S_H and S_G at 823.6-869.9 cm^{-1}, 854.47 cm^{-1} and 896.9 cm^{-1} sequentially. Again CO_3 V_3 also found for sample S_0, S_T, S_H and S_G at 1411.89, 1543.05 cm^{-1}; 1402.25, 1560.41 cm^{-1}; 1425.4, 1537.27 cm^{-1}; and 1396.46, 1544.98 cm^{-1} respectively. In this study, amide I also found for sample S_0, S_T, S_H and S_G at 1639.49, 1643.35 cm^{-1}; 1643.35 and 1645.28 cm^{-1} correspondingly. Another study shows that, the major amide I band of the cross-linked Hydroxyapatite/collagen sample is centered at 1653 cm^{-1} and minor bands are assigned at 1636 and 1663 cm^{-1}. In animal bone the intensity of the band at 1685 cm^{-1} is sensitively dependent upon the extent of collagen cross-linking, which is extremely important for the mineralization process (Boskey *et al*.,1999).The cross-linking effect of the collagen structure (Epaschalis *et al*., 2001) can be analyzed as a peak height ratio of 1685/1653 cm^{-1}. In contrast, the N-H stretching was also shown for sample S_0, S_T, S_H and S_G at 3213.41, 3398.57 cm^{-1}; 3265.49 cm^{-1}; 3122.75, 3572.17 cm^{-1}; and 3184.48, 3525.88 cm^{-1} separately. We can suppose that the spectral feature is affected by both of the cross-linking and other factors. As one of the other factors we consider the characteristic microstructure development of the HCC composite samples, which is induced by the cross-linking (Chang *et al*., 2001 and Chang *et al*.,)Besides, other functional group such as amide III, PO_4^{3-} v_3, asymmetric HPO_4 etc found at different peak position assigned by various wave number. FTIR analysis revels that using the cross linker in the scaffold helped to form better network. The bonding pattern found to be stronger than the scaffold having no cross linker. More specifically the scaffold that cross linked with gluterldehyde found to be well connected with the components applied to form scaffold.

SEM is another important tool that helps to understand the pore morphology such as pore size, pore density etc. To understand the pore surface morphology HCC sample was examined. The pore sizes of the scaffolds were directly measured in a scanning electron micrograph, and all the prepared scaffolds were found to be highly porous with a pore size of 111.80-212.60 μm for HCC scaffold (Figure 3.15). The optimum pore size for bone tissue engineering remains unclear; however, investigations that sought to identify the optimum pore size for bone tissue engineering found pore sizes ranging from 100 to 500 μm to be viable (Fisher and Reddi, 2003).

Comparison of Hydroxyapatite-Chitosan-Alginate and (HCA) Hydroxyapatite-Collagen-Chitosan (HCC) scaffolds with Human bone allograft (HBA):

A comparative study of human bone, HCA and HCC sample helps to find the best composite that mimic human cancellous bone properties and can be used as a substitute of HBA in future. The porosity of human bone allograft found 96% comparing with the other two samples (HCC and HCA) it was found 90.64 % and 86 % which was close enough to the HBA. But in some reports it is also found that the trabecular enclose larger voids (macro pores), providing 55–70% interconnected porosity (Innocentini *et al*., 2010). Then density properties showed huge difference i.e. for HBA it showed 0.625g/cm^3 and HCC sample showed 0.183 g/cm^3 but HCA sample showed 0.076 g/cm. The apparent density of trabecular bone ranges from 0.14 to 1.10 g/cm^3. However we can say that the density of sample HCC was close enough to HBA though further investigation is needed to find a method to increase the density of the scaffold. The swelling kinetics of both HCC and HCA sample were very high comparative to human bone [Table 3.16]. Observing the degradation properties it can be depicted that reaming weight of sample HCC was closer to sample HBA than HCA. Finally from the SEM analysis, it was found that the average pore size of HBA, HCA and HCC samples were 420 to 623 µm, 162 to 510 µm and 111.80 to 212.60 µm respectively. Considering the porosity, density, swelling kinetics, degradation and SEM analysis it was found that sample HCC was more prominent and potent to the substitute of HBA.

A large number of bone grafts are required annually for clinical treatment of severe bone fracture. The limitations in autograft and allograft restricted their clinical application. Alternatively, tissue engineering approach may offer a new solution to produce bone grafts for clinical use. Over the last twenty years, tissue engineering of the bone has made remarkable progress, although the problems of translating into clinical application still remain.

The use of biomaterials and development of scaffolds are especially important for engineering bone grafts, because they need to provide mechanical support during bone repair and bioactive aspect for bone formation. In order to obtain optimal mechanical properties, and high biocompatibility, numerous composite materials were designed to acquire integrated properties from the individual components. Recently, more stringent requirements brought forth in the scaffold design for complete bone healing efficacy, such as inducing neo-vascularization during the formation of bone.

The achievements in engineering bone tissue so far are encouraging, while new challenges and opportunities are bringing the perspective of bone tissue engineering to a new height in clinical application. In the near future, tissue engineering approaches will achieve new dimension for clinical transplantation and engineered bone graft will be mature osseous tissue regeneration.

The study showed that it is possible to vary properties like density, porosity, biodegradability for optimization of artificial bone scaffold formation and thus develop suitable graft for through tissue engineering for use in regeneration of mineralized tissue for the transplantation of bone. Further studies with the two biomimetic Hydroxyapatite/Chitosan-Alginate (HCA) and Hydroxyapatite /Collagen-Chitosan (HCC) scaffolds with different combination of crosslinking polymers would result in development of scaffolds nearly similar to human bone allograft for use potential bon substitute to be used in reconstructive surgery.

Conclusion

In this study, two different types of three dimensional, open cells, porous scaffold were prepared through freeze dried technique and cross-linked with different types of cross-linker and also compared their properties with Human Bone Allograft (HBA). Firstly, Hydroxyapatite/Chitosan-alginate (HCA) scaffold was fabricated by in-situ co-precipitation method. Different percentages of 2-Hydroxylmethacrylate (HEMA) were applied as a crosslinking agent; meantime radiation dose was also revealed for proper mixing of components in the presences of HEMA. Among the different percentages of HEMA, 1.5% was optimum concentration at 5 kGy radiation dose for proper mixing. The results showed that, the prepared scaffolds are porous, with porosity about 86% and biodegradability of the scaffold was decreased with increasing of polymer concentration. Scanning Electron Microscope (SEM) analysis showed an open pore structure of scaffolds appropriate for blood supply and cell attachment and pores ranging from 162 to 510 μm. Fourier transform infrared spectroscopy (FTIR) results showed intermolecular interaction between components in scaffold.

Based on the selected mineral-polymer ratio of HCA scaffold, another scaffold was fabricated through thermal induced phase separation technique and cross-linked with physical (Dehydrothermal and radiation) and chemical (HEMA and glutaraldehyde) cross-linker. Among the prepared scaffolds, cross linked with glutaraldehyde found to be more eligible for bone replacement due to its acceptable porosity, density, biodegradability and swelling ability. Considering the scanning electron microscope analysis of HCC, it was also found that the scaffold were porous and fair for cell migration and regeneration. In addition, Fourier transform infrared spectroscopy data showed the proper inter molecular interaction among the component of the scaffold. Finally, comparison among the HBA, HCC, and HCA reveal that HCC composite that was crosslinked with glutaraldehyde partially fulfilled most of the criteria needed to present in a scaffold and mimic the characteristics of HBA. However, further investigation is needed to find out the technique for the development of suitable pore size with increased mechanical strength of the scaffolds.

REFERENCE

Agrawal, C.M., and Ray, R.B. (2001). Biodegradable polymeric scaffolds for musculoskeletal tissue engineering. *Journal of Biomedical Materials Research*, 55(2): 141- 150.

Agrawal, P., Strijkers, G.J., and Nicolay, K. (2010). Chitosan-based systems for molecular imaging. *Advanced Drug Delivery Reviews*, 62: 42-58.

Ajir, H., Takahashi, Y., Akashi, M., and Fujiwara, T. (2012). Polylactide block copolymers using trimethylene carbonate with methoxyethoxy side groups for dual modification of hydrophilicity and biodegradability. *Macromolecular Biosciences*, 12: 1315-1320.

Altman, G.H., Diaz, F., Jakuba, C., Calabro, T., Horan, R.L., Chen, J., Lu, H., Richmond, J., and Kaplan, D.L. (2003). Silk based biomaterials. *Biomaterials*, 24: 401–416.

Andersen, R.E., and Lim, D.A (2014). An ingredient for the elixir of youth. *Cell Research*, 24: 1381.

Aubin, J.E., and Liau, F. (1996). Principles of Bone Biology. 1st edition, ed.; Academic: San Diego, CA, 51.

Azhar, F.F., Olad, A., and Salehi, R. (2014). Fabrication and characterization of chitosan–gelatin/nanohydroxyapatite–polyaniline composite with potential application in tissue engineering scaffolds. *Designed Monomers and Polymers,* 17(7): 654-667.

Babensee, J.E., Anderson, J.M., McIntire, LV., and Mikos, A.G. (1998). Host response to tissue engineered devices. *Advanced Drug Delivery Reviews*, 33(1- 2): 111- 139.

Babensee, J.E., McIntire, L.V., and Mikos, A.G. (2000). Growth factor delivery for tissue engineering. *Pharmaceutical Research*, 17: 497-504.

Baker, B.M., Gee, A.O., Metter, R.B., Nathan, A.S., Marklein, R.A., Burdick, J.A., and Mauk, R. (2008). The potential to improve cell infiltration in composite fiber-aligned electrospun scaffolds by the selective removal of sacrificial fibers. *Biomaterials*, 29: 2348-2358.

Barakat, N.A.M., Khalil, K.A., Sheikh, F.A., Omran, A.M., Gaihre, B., Khil, S.M., and Kim, H.Y. (2008). Physiochemical characterization of hydroxyapatite extracted from bovine bones by three different methods: Extraction of biologically desirable Hap. *Materials Science and Engineering,* 28: 1381-7.

Barinov, S.M., Rau, J.V., and Cesaro, S.N. (2006). Carbonate release from carbonated hydroxyapatite in the wide temperature range. *The Journal of Materials Science*, 17: 597–604.

Barry, F.P. (2003). Biology and clinical applications of mesenchymal stem cells. *Birth Defects Research*, 69: 250-256.

Ben-Nissan, B., Milev, A., and Vago, R. (2004). Morphology of sol-gel derived nano-coated coralline hydroxyapatite. *Biomaterials*, 25: 4971-5.

Bhattarai, N., Edmondson, D., Veiseh, O., Matsen, F.A., and Zhang, M.Q. (2005). Electro spun chitosan-based nanofibers and their cellular compatibility. *Biomaterials,* 26: 6176-6184.

Bhattarai, N., Gunn, J., and Zhang, M.Q. (2010). Chitosan-based hydrogels for controlled, localized drug delivery. *Advanced Drug Delivery Reviews,* 62: 83-99.

Boland, E.D., Espy, P.G., and Bowlin, G.L. (2004). Tissue engineering scaffolds. In Encyclopedia of Biomaterials and biomedical engineering. *Taylor & Francis Group*, 1633-1635.

Boskey, A.L., Wright, T.M., and Blank, R.D. (1999). Collagen and bone strength. *Journal of Bone and Mineral Research*, 14: 330–335.

Browning, W.D., Cho, S.D., and Deschepper, E.J. (2012). Effect of a nano-hydroxyapatite paste on bleaching‐related tooth sensitivity. *Journal of Esthetic and Restorative Dentistry*, 24: 268-76.

Cai, X., Tong, H., Shen, X., Chen, W., Yan, J., and Hu, J. (2009). Preparation and characterization of homogeneous chitosan-polylactic acid/ hydroxyapatite nanocomposite for bone tissue engineering and evaluation of its mechanical properties. *Acta Biomaterialia*, 5: 2693-703.

Centres for disease control and prevention (CDC) Update. Allograft-associated bacterial infections: United States, 2002, 51: 207–10.

Chang, E., Chang, W.J., Wang, B.C., and Yang, C.Y. (1997). Plasma spraying of zirconia‐reinforced hydroxyapatite composite coatings on titanium: Part I: Phase, microstructure and bonding strength. *Journal of Materials Science: Materials in Medicine*, 8: 193‐200.

Chang, M.C., Ikoma, T., Kikuchi, M., Tanaka, J. (2001). Preparation of a porous hydroxyapatite/collagen nanocomposite using glutaraldehyde as a cross-linkage agent. *Journal of Materials Science Letters*, 20: 1109–201.

Chang, M.C., Ikoma, T., Kikuchi, M., Tanaka, J. (2002). The cross-linkage effect of hydroxyapatite/collagen nanocomposites on a selforganization phenomenon, *Journal of Materials Science: Materials in Medicine*, 13(10): 993-7.

Chang, M.C., and Tanaka, J. (2002). FT-IR study for hydroxyapatite/collagen nanocomposite cross-linked by glutaraldehyde. *Biomaterials*, 23(24): 4811-8.

Chen, G., Ushida, T., and Tateishi, T. (2002). Development of biodegradable porous scaffolds for tissue engineering. *Journal of Materials Science Engineering C*, 17: 63–69.

Chen, G.C., Gajowniczek, P., and Settleman, J. (2004). Rho-LIM kinase signaling regulates ecdysone-induced gene expression and morphogenesis during Drosophila metamorphosis. *Current Biology*, 14(4): 309-313.

Chen, L., Jiang, W., Huang, J., He, B.C., Zuo, G.W., Zhang, W., and Bone, M.J (2010). TGFβ/BMP Type I Receptors ALK1 and ALK2 Are Essential for BMP9-induced Osteogenic Signaling in Mesenchymal Stem Cells. *Journal of Biological Chemistry*, 25: 2447.

Chew, S.Y., Wen, J., Yim, E.K., and Leong, K.W. (2005). Sustained release of proteins from electrospun biodegradable fibers. *Bio macromolecules*, 6: 2017-2024.

Cho, K.Y., Moon, J.Y., Lee, Y.W., Lee, K.G., Yeo, J.H., Kweon, H.Y., Kim, K.H., and Cho, S.C. (2003). Preparation of self-assembled silk sericin nanoparticles. *International Journal of Biological Macromolecules*, 32: 36-42.

Conrad, E.U., Gretch, DR., Obermeyer, KR., Moogk, MS., Sayers, M., and Wilson, J.J. (1995). Transmission of the hepatitis-C virus by tissue transplantation. *Journal of Bone and Joint Surgery*, 77, 214–24.

Cowin, S.C., Van Buskirk, W.C., Chien, S., “Properties of Bone”, In: Skalak, R. and Chien, S. (1989). (ed.s) Handbook of Bioengineering. New York and McGraw-Hill, 21-27.

Cunningham, N.S., Jenkins, N.A., Gilbert, D.J., Copeland, N.G., Reddi, A.H., and Lee, S.J. (1995). Growth/differentiation factor-10: a new member of the transforming growth factor-beta superfamily related to bone morphogenetic protein-3. *Growth Factors*, 12: 99.

Dezawa, M., Ishikawa, H., Itokazu, Y., Yoshihara, T., Hoshino, M., Akeda, S., Ide, C., and Nabeshima, Y. (2005). Bone marrow stromal cells generate muscle cells and repair muscle degeneration. *Science*, 309: 314-317.

Dhandayuthapani, B., Yoshida, Y., Maekawa, T., and Kumar, D.S. (2011). Polymeric Scaffolds in Tissue Engineering Application: A Review. *International Journal of Polymer Science*, 1-19.

Doshi, J., and Reneker, D.H. (1995). Electrospinning process and application of electrospun fibers. *Journal of Electrostatics*, 35: 151-160.

Doyle, B.B,, Bendi,. E.G., and Blout, E.R. (1975). Infrared spectroscopy of collagen and collagen-like polypeptides. *Biomaterials*, 14(5): 937-57.

Ducy, P., Schinke, T., and Karsenty, G. (2000). The osteoblast: A sophisticated fibroblast under central surveillance. *Science*, 289: 1501-1504.

Eberli, D., Freitas, F.L., Atala, A., and Yoo, J.J. (2009). Composite scaffolds for the engineering of hollow organs and tissues. *Methods*, 47(2): 109-115.

Einhorn, T., O'Keefe, R., and Buckwalter, JA. (2007). Form and function of bone. In Orthopaedic Basic Science: Foundations of Clinical Practice. *Rosemont*, IL, 129-174.

Eklouh-Molinier, C., Happillon, T., Bouland, N., Fichel, C., Diebold, M.D., Angiboust, J.F., Manfait, M., Brassart-Pasco, S., and Piot, O. (2014). Investigating the relationship between changes in collagen fiber orientation during skin aging and collagen/water interactions by polarized-FTIR microimaging. *Analyst,* 140: 6260-6268.

- Epaschalis, E.P., Verdelis, K., Dotty, S.B., Boskey, A.L., Mendelsohn, R., and Yamauchi, M. (2001). Spectroscopic characterization of collagen crosslinks in bone. *Journal of Biomedical Materials Research*, 16: 1821–8.

Evans, L.A., Macey, D.J., and Webb, J. (1992). Calcium bio mineralization in the regular teeth of the chiton, acanthopleura hirtosa. *Calcif Tissue Int.*, 51: 78-82.

Falconnet, D., Csucs, G., Michelle Grandin, H., and Textor, M. (2006). Surface engineering approaches to micropattern surfaces for cell- based assays. *Biomaterials*, 27(16): 3044- 3063.

Fisher, J. P., and Reddi, A. H. (2003). Functional tissue engineering of bone: signals and scaffolds. *Journal of Tissue Engineering and Regenerative Medicine,* 1: 1-29.

Flemming, R.G., Murphy, C.J., Abrams, G.A., Goodman, S.L., and Nealey, P.F. (1999). Effects of synthetic micro- and nano- structured surfaces on cell behavior. *Biomaterials*, 20(6): 573-588.

Florida and Louisiana. (2001). Centers for disease control and prevention. Septic arthritis following anterior cruciate ligament reconstruction using tendon allografts, 50: 1081–3.

Gaalen S. (2008). Tissue engineering of bone. In: van Blitterswijk (ed), Tissue Engineering. Elsevier Academic Press, San Diego, 559-610.

Garg, T., Singh, O., Arora, S., and Murthy, R. (2012). Scaffold: anovel carrier for cell and drug delivery. *Critical Reviews in Therapy Drug Carrier Systems*, 29: 1-63.

Garg, T., Singh, O., Arora, S., and Murthy, R. (2012). Scaffold: a novel carrier for cell and drug delivery. *Critical Reviews in Therapeutic Drug Carrier Systems*, 29: 1-63.

Gautschi, O.P., Frey, S.P., and Zellweger, R. (2007). Bone morphogenetic proteins in clinical applications. *ANZ Journal of Surgery*, 77: 626.

Glantz, P.O. (1987). Comment. In: Williams DF (ed) Progress in biomedical engineering. Definitions in biomaterials. *Elsevier*, 4: 24.

Gong,Y., Ma, Z., Gao, C., Wang, W., and Shen, J. (2005). Especially Elaborated Thermally Induced Phase Separation to Fabricate Poly (L-lactic acid) Scaffolds with Ultra Large Pores and Good Interconnectivity. *Journal of Applied Polymer Science*, 101: 3336–3342.

Hartgerink, J.D., Beniash, E., and Stupp, S.I. (2002). Peptide-amphiphile nanofibers: a versatile scaffold for the preparation of self-assembling materials. *Proceeding of the National Academy of Sciences*, 99: 5133–8.

Herbert, S.P., and Stainier, D.Y. Rev, Nat. (2011). Molecular control of endothelial cell behaviour during blood vessel morphogenesis. *Molecular Cell Biology*, 12: 551.

Hollister, S.J. (2005). Porous scaffold design for tissue engineering. *Nature materials*, 4: 518-524.

Hou, Q.P., Grijpma, D.W., and Feijen, J. (2003). Porous polymeric structures for tissue engineering prepared by coagulation, compression moulding and salt leaching technique. *Biomaterials*, 24: 1937–1947.

Houssine,S., Salajková,M., Zhou, Q., and Berglund, L.A. (2010). Mechanical performance tailoring of tough ultra-high porosity foams prepared from cellulose I nanofiber suspensions. *Soft Matter*, 8: 1824–1832.

Hua, F.J., Kim, G.E., Lee, J.D., Son, Y.K., and Lee, D.S. (2002). Macroporous poly (l- lactide) scaffold 1. Preparation of a macroporous scaffold by liquid-liquid phase separation of a PLLA-dioxane- water system. *Journal of Biomedical Materials Research*, 63: 61-167.

Huang, S., Gao, S., Cheng, L., and Yu, H. (2011). Remineralization potential of nano-hydroxyapatite on initial enamel lesions: An in vitro study. *Caries Research*, 45: 460-8.

Huang, S., Gao, S., Cheng, L., Yu, H. (2010). Combined effects of nano-hydroxyapatite and Galla chinensis on remineralisation of initial enamel lesion in vitro. *Journal of Dentistry*, 38: 811-9.

Huang, Y.C., and Mooney, D.J. (2005). Gas foaming to fabricate polymer scaffolds in tissue engineering. In: Scaffoldings in tissue engineering, Ma X P., Elisseeff J., (Ed.), PP 159, Taylor and Francis group. *CRC press*, 206: 61-72.

Huaping, Tan., Constance, R. Chu., Karin, A. Payne., and Kacey, G. Marra.(2007). Injectable in situ forming biodegradable chitosan–hyaluronic acid based hydrogels for cartilage tissue engineering. *Biomaterials,* 30(13): 2499-2506.

Hutmacher, D.W. (2000). Scaffolds in tissue engineering bone and cartilage. *Biomaterials*, 21(24): 2529-2543.

Hutmacher, D.W. (2001). Scaffold design and fabrication technologies for engineering tissues state of the art and future perspectives. *Journal of Biomaterials*, 12: 107- 124.

Ikada, Y. (2006). Scope of tissue engineering In: Tissue engineering: fundamental and applications, Ikada Y. (Ed.). *Academic press*, USA, 29.

Innocentini, M. D. M., Faleiros, R. K., Pisani Jr. R., Thijs I., Luyten J., and Mullens, S. (2010). Permeability of porous gelcast scaffolds for bone tissue engineering. *Journal of Porous Materials,* 17(5): 615-627.

Ito, Y., Zheng, J., and Imanishi, Y. (1997). Enhancement of cell growth on a porous membrane co-immobilized with cell- growth and cell adhesion factors. *Biomaterials*, 18(3): 197- 202.

Jayakumar, R., Prabaharan, M., Nair, S.V., and Tamura, H. (2010). Novel chitin and chitosan Nano fibers in biomedical applications. *Biotechnology Advances,* 28: 142-150.

Jin, H.J., Chen, J., Karageorgiou, V., Altman, G.H., and Kaplan, D.L. (2004). Human bone marrow stromal cell responses to electrospun silk fibroin mats. *Biomaterials*, 25: 1039–1047.

Joshi, K.B., Singh, P., and Verma, S. (2009). Fabrication of platinum nanopillers on peptidebased soft structure using a focused ion beams. *Biofabrication* 1, 025002.

Kai, H., Wang, X., Madhukar, K.S., Qin, L., Yan, Y., Zhang, R., Wang, X. (2009). Fabrication of two-level tumor bone repair biomaterial based on rapid prototyping technique. Biofabrication. *Iop Science,* 1(2): 025003.

Kannan, R.Y., Salacinski, H.J., Sales, K., Butler, P., and Seifalian, A.M. (1976). The roles of tissue engineering and vascularization in the development of micro- Dunn GA, Heath JP. A new hypothesis of contact guidance in tissue cells. *Experimental Cell Research*, 101(1): 1- 14.

Karageorgiou, V., and Kaplan, D. (2005). Porosity of 3D biomaterial scaffolds and osteogenesis. *Biomaterials*, 26: 5474- 5491.

Karande, T.S., Ong, J.L., and Agrawal, C.M. (2004). Diffusion in musculoskeletal tissue engineering scaffolds: Design issues related to porosity, permeability, architecture, and nutrient mixing. *Annals of Biomedical Engineering*, 32(12): 1728- 1743.

Katti, D.S., Robinson, K.W., Ko, F.K., and Laurencin, C.T. (2004). Bioresorbable nanofiber-based system for wound healing and drug delivery: optimization of the fabrication parameters. J. Biomed. Mat. Res. Part B. *Applied Biomaterials*, 70B: 286–296.

Katti, K. S., Katti, D. R., and Dash, R. (2008). Synthesis and characterization of a novel chitosan/montmorillonite/hydroxyapatite nanocomposite for bone tissue engineering. *Biomedical Material*, 3: 034122.

Kean, T., and Thanou, M. (2010). Biodegradation, bio distribution and toxicity of chitosan. *Advanced Drug Delivery Reviews*, 62: 3-11.

Kempen, D.H.R., Kruyt, M.C., Lu, L., Wilson, C.E., Florschutz, A.V., Creemers, L.B., Yaszemski, M.J., and Dhert, W.J.A. (2009). Effects of composite formulation on the mechanical properties of biodegradable poly (propylene fumarate)/bone fiber scaffolds. *Tissue Engineering*, Part A, 15: 587.

Khan, M.N., Islam, J.M., And Khan, M.A. (2012). Fabrication and characterization of gelatin-based biocompatible porous composite scaffold for bone tissue engineering. *Journal of Biomedical Materials Research A*, 100: 3020-3028

Kim, B.S., Baez, C.E., and Atala, A. (2000). Biomaterials for tissue engineering, *World Journal of Urology*, 18: 2–9.

Kim, I.Y., Seo, S.J., Moon, H.S., Yoo, M.K., Park, I.Y., Kim, B.C., and Cho, C.S. (2008). Chitosan and its derivatives for tissue engineering applications. *Biotechnology Advances*, 26: 1-21.

Kim, M.S., Kim, J.H., Min, B.H., Chun, H.J., Han, D.K., and Lee, H.B. (2011). Polymeric Scaffolds for Regenerative Medicine. *Polymer Reviews*, 51: 23-52.

KoHF, Sfeir, C., and Kumta, P.N. (2010). Novel synthesis strategies for natural polymer and composite biomaterials as potential scaffolds for tissue engineering. *Philosophical Transactions of the Royal Society A*, 368: 1981-1997.

Koumoulidis, G.C., Katsoulidis, A.P., Ladavos, A.K., Pomonis, P.J., Trapalis, C.C., Sdoukos, A.T., and Vaimakis, T.C. (2003). Preparation of hydroxyapatite via microemulsion route. *Journal of colloid and interface science*, 259(2): 254-60.

Kretlow, J.D., and Mikos, A.G. (2008). From material to tissue: Biomaterial development, scaffold fabrication, and tissue engineering. *AIChE Journal*, 54(12): 3048- 3067.

Krimm, S., and Bandekar, J. (1986). Vibrational spectroscopy and conformation of peptides, polypeptides, and proteins. *Advances in Protein Chemistry,* 38:181-364.

Kuen Yong, Lee, and David, J., and Mooney. (2012). Alginate: properties and biomedical applications. *Progress in Polymer Science*, 37: 106–126.

Kuo, C.K., and Ma, P.X. (2001). Ionically crosslinked alginate hydrogels as scaffolds for tissue engineering: Part 1. Structure, gelation rate and mechanical properties. *Biomaterials,* 22: 511–521.

Kweh, S.W., Khor, K.A.,and Cheang, P. (1999). The effect of processing parameters on the characteristics of plasma sprayed hydroxyapatite (HA) coatings. *Journal of Materials Process Technology*, 89: 373.

Lakshmi, S., and Nair Cato, T. (2007). Biodegradable polymers as biomaterials. *Laurencin*, 32, 755-1134.

Lee, K., Silva, E.A., and Mooney, D.J. (2011). Growth factor delivery-based tissue engineering: general approaches and a review of recent developments. *Journal of the Royal Society Interface*, 8: 153.

Lee, K.Y., Jeong, L., Kang, Y.O., Lee, S.J., and Park, W.H. (2009). Electrospinning of polysaccharides for regenerative medicine. *Advanced Drug Delivery Reviews,* 61: 1020-1032.

Lee, S.H., Kim, B.S., Kim, S.H., Kang, S.W., and Kim, Y.H. (2004). Thermally produced biodegradable scaffolds for cartilage tissue engineering. *Macromolecular Biosciences*, 4: 802–810.

Leong, M.F., Rasheed, M.Z., Lim, T.C., and Chian, K.S (2008). In vitro cell infiltration and in vivo cell in filtration and vascularization in fibrous highly porous poly (D, L-Lactic acid) scaffold fabrication by electro spinning technique. *Journal of Biomedical Research*, 91: 231-240.

Li, L., Pan, H., Tao, J., Xu, X., Mao, C., and Gu, X. (2008). Repair of enamel by using hydroxyapatite nano particles as the building blocks. *Journal of Materials Chemistry*, 18: 4079-84.

Li, W., Li, Y., Gao, F.B. (2005). Abelson, enabled, and p120 catenin exert distinct effects on dendritic morphogenesis in Drosophila. *Developmental Dynamic*s, 234 (3): 512-522.

Li, W.J., and Tuan, R.S. (2009). Fabrication and application of nanofibrous scaffolds in tissue engineering. *Current Protocols in Cell Biology*, 25 Unit 25.2

Li, Z., Leung, M., Hopper, R., Ellenbogen, R., and Zhang, M. (2010). Feeder-free self-renewal of human embryonic stem cells in 3D porous natural polymer scaffolds. *Biomaterials*, 31: 404-412.

Liang, D., Hsiao, B.S., and Chu, B. (2007). Functional electrospun nanofibrous scaffolds for biomedical applications. *Advanced Drug Delivery Reviews*, 59: 1392–1412.

Lin, L.; Ju, S.; Cen, L.; Zhang, H. & Hu, Q. (2008). Fabrication of porous, TCP scaffolds by combination of rapid prototyping and freeze drying technology. Yi Peng, Xiaohong Weng (Eds.), pp. 88–91APCMBE 2008, IFMBE Proceedings 19, Springer-Verlag, Berlin Heidelberg.

Liu, C., Wang, W., Shen, W., Chen, T., Hu, L., and Chen, Z. (1997). Evaluation of the biocompatibility of a nonceramic hydroxyapatite. *Journal of Endodontics*, 23: 490‐3.

Liu, C., Xia, Z., and Czernuszka, J.T. (2007). Design and Development of Three- Dimensional Scaffolds for Tissue Engineering. *Chemical Engineering Research and Design,* 85(7): 1051-1064.

Liu, G.J., Ding, J.F., Qiao, L.J., Guo, A., Dymov, B.P., Gleeson, J.T., Hashimoto, T., and Saijo, K. (1999). Polystyrene block- poly (2-cinnamoylethyl methacrylate) nanofibers: Preparation, characterization, and liquid crystalline properties. *Chemistry European Journal*, 5: 2740-2749.

Liu, G.J., Qiao, L.J., and Guo, A. (1996). Diblock copolymer nanofibers. *Macromolecules*, 29.

Lu, P., and Ding, B. (2008). Applications of electrospun fibers. *Recent Patents on Nanotechnology*, 2(3): 169-82.

Ma, L., Gao, C., Mao, Z., Zhou, J., Shen, J., Hu, X., and Han, C.(2003). Collagen/chitosan porous scaffolds with improved biostability for skin tissue engineering. *Biomaterial,* 24(26): 4833-41.

Ma, P.X. (2008). Biomimetic materials for tissue engineering. *Advanced Drug Delivery Reviews*, 60: 184– 98.

Ma, P.X., and Langer, R. (1999). Fabrication of biodegradable polymer foams for cell transplantation and tissue engineering. *In Tissue Engineering Methods and Protocols*, 47.

Ma, Z., Kotaki, M., Inai, R., and Ramakrishna, S. (2005). Potential of nanofiber matrix as tissueengineering scaffolds. *Tissue Engineering*, 11: 101–109.

Madurantakam, P.A., Cost, C.P., Simpson, D.G., and Bowlin, G.L (2009). Science of nano fibrous scaffold fabrication: strategies for next generation tissue-engineering scaffolds. *Nanomedicine*, 4(2): 193-206.

Mandal, B.B., and Kundu, S.C. (2008). Non-bioengineered high strength three-dimensional gland fibroin scaffolds from tropical non-mulberry silkworm for potential tissue engineering applications. *Macromolecular Bioscience*, 8: 807-818.

Mandal, B.B., and Kundu, S.C. (2008). Non-bioengineered silk gland fibroin protein: characterization and evaluation of matrices for potential tissue engineering applications. *Biotechnology and Bioengineering*, 100 (6): 1237 – 50.

Mano, J.F., Silva, G.A., Azevedo, H.S., Malafaya, P.B., Sousa, R.A., Silva, S.S., Boesel, L.F., Oliviera, J.M., Santos, .T.C., Marques, A.P., Neves, N.M., and Reis, R.L. (2007). Natural origin biodegradable systems in tissue engineering and regenerative medicine: present status and some moving trends. *Journal of Royal Society Interface*, 4: 999–1030.

Maquet, V., and Jerome, R. (1997). Design of macroporous biodegradable polymer scaffolds for cell transplantations. *Materials Science Forum*, 250: 15-24.

Martins, A.M., Pham, Q.P., Malafaya, P.B., Sousa, R.A., Gomes, M.E., Raphael, R.M., Kasper, F.K., Reis, R.L., and Mikos, A.G (2009). The Role of Lipase and alphaAmylase in the Degradation of Starch/Poly (varepsilon-Caprolactone) Fiber Meshes and the Osteogenic Differentiation of Cultured Marrow Stromal Cells. *Tissue Engineering Part A*, 15(2): 295-305.

Matthews, J.A., Wnek, G.E., Simpson, D.G., and Bowlin, G.L. (2002). Electrospinning of collagen nanofibers. *Bio macromolecules*, 3: 232-238.

McKay, I.A., and Leigh, I. (1993). Growth Factors: A Practical Approach. IRL Press: Oxford.

McPherron, A.C., Lawler, A.M., and Lee, S.J. (1997). Regulation of skeletal muscle mass in mice by a new TGF-p superfamily member. *Nature*, 387: 83

Meffert, R.M., Thomas, J.R., Hamilton, K.M., and Brownstein, C.N. (1985). Hydroxylapatite as an alloplastic graft in the treatment of human periodontal osseous defects. Twelve month reentry results. *Journal of Periodontology*, 56: 540‑7.

Mikos, A.G., Bao, Y., Cima, L.G., Ingber, D.E., Vacanti, J.P., and Langer, R. (1993). Preparation of Poly (glycolic acid) bonded fiber structures for cell attachment and transplantation. *Journal of Biomedical Materials Research*, 27: 183-189.

Mikos, A.G., Lu, L., Temenoff, J.S., and Temmser, J.K. (2004). Synthetic Bioresorbable polymer scaffolds. In: An introduction to material in medicine, Ratner B D, Hoffman A S, Schoen F J, Lemons J E, (Ed.). *Elsevier Academic Press*. USA, 743

Mikos, A.G., Sarakinos, G., Leite, S.M., Vacanti, J.P., and Langer, R. (1993). Laminated three dimensional biodegradable foams for use in tissue engineering. *Biomaterials* 14: 323-330.

Mikos, A.G., Sarakinos, G., Vacanti, J.P., Langar, R.S., and Cima, L.G. (1996). Biocompatible polymer membranes and methods of preparation of three dimensional membrane structures. *Mikos* , U.S. patent 5, 514, and 378.

Mitragotri, S., and Lahann, J. (2009). Physical approaches to biomaterial design. *Nat Mater*, 8(1): 1523.

Miyazaki, M., Akiyama, I., Sakaguch, M., Nakashima, E., Okada, M., Kataoka, K., and Huh, N.H. (2002). Improved conditions to induce hepatocytes from rat bone marrow cells in culture. *Biochemical and Biophysical Research Communications*, 298: 24-30.

Mooney, D.J., McNamara, K., Hern, D., Vacanti, J.P., and Langer, R (1996). Stabilized polyglycolic acid fibre-based tubes for tissue engineering. *Biomaterials*, 17: 115–124.

Moore, M.J., Jabbari, E., Ritman, E.L., Lu, L.C., Currier, B.L., Windebank, A.J and Yaszemski, M.J.(2004). Quantitative analysis of interconnectivity of porous biodegradable scaffolds with micro computed tomography. *Journal of Biomedical Materials Research Part A*, 71: 258–267.

Moroni, L., De, Wijn J.R., Van, Blitterswijk C.A. (2008). Integrating novel technologies to fabricate smart scaffolds. Journal of Biomaterials. Science- *Polymer Edition*, 19(5): 543- 572.

Moroni, L., Hamann, D., Paoluzzi, L., Pieper, J., de Wijn, J.R., and van Blitterswijk, C.A.(2008). Regenerating articular tissue by converging technologies. *PLOS One*, 3(8): 30-32.

Muhammad Iqbal Sabir, Xiaoxue Xu and Li Li. (2002). A review on biodegradable polymeric materials for bone tissue engineering applications. *Journal of Materials Science,* 44(21): 5713–5724

Munting, E., Verhelpen, M., Li, F., and Vincent, A. (1990). Contribution of hydroxyapatite coatings to implant fixations. Handbook of Bioactive Ceramics. Vol. 2. Boca Raton, FLA, USA: CRC Press. *International Journal of Biomaterials*, 143-8.

Muyonga, J., Cole, C. and Duodu, K. (2004). Extraction and physicochemical characterization of Nile perch (Lates niloticus) skin and bone gelatin. *Food Chemistry,* 86: 325-332.

Naderi, H., Matin, M.M., and Bahrami, A.R. (2015). Critical Issues in Tissue Engineering: Biomaterials, Cell Sources, Angiogenesis, and Drug Delivery Systems. *Journal of Biomaterials Applications*, 26: 383-417.

Nagai, M.K., and Embil, JM. (2002). Becaplermin: recombinant platelet derived growth factor, a new treatment for healing diabetic foot ulcers. *Expert Opinion of Biological Therapy*, 2, 211.

Narayana, R.P., Melman, G., Letourneau, N.J., Mendelson, N.L., and Melman, A. (2012). Photo degradable iron (III) cross-linked alginate gels. *Bio macromolecules,* 13: 2465–2471.

Nazarov, R., Jin, H.J., and Kaplan, D.L (2004). Porous 3-D scaffolds from regenerated silk fibroin. *Biomacro molecules,* 5(3): 718-26.

Nilen, R. W. N., and Richter, P. W. (2008). The thermal stability of hydroxyapatite in biphasic calcium phosphate ceramics. *Journal of Materials Science: Materials in Medicine,* 19(4): 1693–1702.

Ohkawa, K., Cha, D., Kim, H., Nishida, A., and Yamamoto, H. (2004). Electrospinning of Chitosan. *Macromolecular Rapid Communications*, 5: 1600-1605.

Oliveira, M., and Mansur, H.S. (2007). Synthetic tooth enamel: SEM characterization of a fluoride hydroxyapatite coating for dentistry applications. *Materials Research*, 10: 115‑ 8.

Ozgur, N.E., and Cuneyt Tas, A. (1999). Manufacture of macroporous calcium hydroxyapatite and tri‑ calcium phosphate bioceramics. *Journal of European Ceramic Society*, 19: 2569.

Papenburg, B.J., Vogelaar, L., Bolhuis- Versteeg, L.A.M., Lammertink, R.G.H., Stamatialis, D., and Wessling, M. (2007). One- step fabrication of porous micropatterned scaffolds to control cell behavior. *Biomaterials*, 28(11): 1998- 2009.

Park, S.N., Lee, H.J., Lee, K.H., and Suh, H. (2003). Biological characterization of EDC-crosslinked collagen-hyaluronic acid matrix in dermal tissue restoration. *Biomaterials,* 24(9): 1631-41.

Piecuch J.F. (1986). Augmentation of the atrophic edentulous ridge with porous replamineform hydroxyapatite (Interpore‐ 200). *Dental Clinics of North America*, 30: 291-305.

Plikk, P., Målberg, S., and Albertsson, A.C. (2009). Design of resorbable porous tubular copolyester scaffolds for use in nerve regeneration. *Biomacromolecules*, 10(5): 1259-64

Poncin-Epaillard, F., Shavdina, O., and Debarnot, D. (2013). Elaboration and surface modification of structured poly (L-lactic acid) thin film on various substrates. *Materials Science and Engineering C: Materials for Biological Applications*, 33: 2526-2533.

Prabhakaran, M.P., Venugopal, J.R., and Ramakrishna, S. (2009). Mesenchymal stem cell differentiation to neuronal cells on electrospun nanofibrous substrates for nerve tissue engineering. *Biomaterials*, 30: 4996-5003.

Raafat, D., von, Bargen K., Haas, A., and Sahl, H.G. (2008). Insights into the mode of action of chitosan as an antibacterial compound. *Applied and Environmental Microbiology*, 74, 3764-3773.

Ramli, R.A., Adnan, R., Bakar, M.A., and Masudi, S.M. (2011).Synthesis and characterization of pure nanoporous hydroxyapatite. *Journal of Physical Science*, 22: 25‐ 37.

Reneker, D.H., and Chun, I. (1996). Nanometer diameter fibres of polymer, produced by electrospinning Nanotechnology. *PLOS ONE*, 216-223.

Reya, T., Morrison, S.J., Clarke, M.F., and Weissman, I.L. (2001). Stem cells, cancer, and cancer stem cells. *Nature*, 414: 05-111.

Rigo, E.C., Boschi, A.O., Yoshimoto, M., Allegrini, Jr S., Kong, Jr B., and Corbani, M.J. (2004). Evaluation in vitro and in vivo of biomimetic hydroxyapatite coated on titanium dental implants. *Materials Science Engineering*, C 24-647.

Sachlos, E., and Czernuszka, J.T. (2003). Making tissue engineering scaffolds work. Review on the application of solid free from fabrication technology to the production of tissue engineering scaffolds. *European cells and materials*, 5: 29-40.

Salgado, A.J., Coutinho, O.P., and Reis, R.L. (2004). Bone tissue engineering: State of the art and future trends. *Macromolecular Bioscience*, 4: 743-765.

Schmelzer, E., Deiwick, A., Bruns, H., Fiegel, H.C., Bader, A., and Gastroenterol, EurJ . (2008). Deficiency in Thrombopoietin Induction after Liver Surgery Is Associated with Postoperative Liver Dysfunction. *Hepatology*, 20: 209.

Schoof, H., Apel, J., Heschel, I., and Rau, G. (2001). Control of pore structure and size in freezedried collagen sponges. *Journal of Biomedical Materials Research*, 58: 352–7.

Sehaqui, H., Salajkov´a, M., Zhou Q., and Berglund, L. A. (2010). Mechanical performance tailoring of tough ultra-high porosity foams prepared from cellulose I nanofiber suspensions . *Soft Matter*, 6: 1824–1832.

Sehaqui, H., Zhou Q., and Berglund, L. A. (2011). Strong and tough cellulose nanopaper with high specific surface area and porosity. *Bio macromolecules*, 12(10): 3638-44.

Shanmugasundaram, N ., Ravichandran, P., Reddy, P.N,, Ramamurty, N., Pal, S., and Rao, K.P.(2001). Collagen-chitosan polymeric scaffolds for the in vitro culture of human epidermoid carcinoma cells. *Biomaterials*, 22(14): 1943-51.

She, Z., Zhang, B., Jin, C., Feng, Q., and Xu, Y. (2008). Preparation and in vitro degradation of porous three-dimensional silk fibroin/chitosan scaffold. *Polymer Degradation and Stability,* 93(7): 1316-1322.

Shi, C., Zhu, Y., Ran, X., Wang, M., Su, Y., and Cheng, T. (2006). Therapeutic potential of chitosan and its derivatives in regenerative medicine. *Journal of Surgical Research*, 133: 185-192.

Sikavitsas, V.I., Temenoff, J.S., and Mikos, A.G. (2001). Biomaterials and bone mechano transduction. *Biomaterials*, 22: 2581-2593.

Silva, J.R., Van, Den., Hurk, R., van Tol, H.T., Roelen, B.A., Figueiredo, J.R., and Reprod Mol. (2005). Expression of growth differentiation factor 9 (GDF9), bone morphogenetic protein 15 (BMP15), and BMP receptors in the ovaries of goats. *Dev*, 70: 11.

Sionkowska, A., and Kozłowska, J. (2013). Properties and modification of porous 3-D collagen/hydroxyapatite composites. *International Journal of Biological Macromolecules*, 52: 250-259.

Siva Rama Krishna, D., Siddharthan, A., and Seshadri, S. K. (2007). A novel route for synthesis of nanocrystal line hydroxyapatite from eggshell waste. *J. Mater., Sci. Mater, and Med*, 18: 1735-1743.

Skjak-Braerk, G., Grasdalen, H., and Smidsrod, O. (1989). Inhomogeneous polysaccharide ionic gels. *Carbohydrate Polymer*, 10: 31–54.

Smith, L.A., Beck, J.A., and Ma, P.X. (2004). Nano fibrous scaffolds and their biological effects. In: Tissue Cell and Organ Engineering. *Colloids and surfaces B: Bio Interfaces,* 39(3): 125-131.

Sommerfeldt, D.W., and Rubin, C.T. (2001). Biology of bone and how it orchestrates the form and function of the skeleton. *European Spine Journal,* 10: S86-S95.

Stevens, M.M., Qanadilo, H., Langer, R., and Shastri, V.P. (2004). A rapid-curing alginate gel system: Utility in periosteum-derived cartilage tissue engineering. *Biomaterials,* 25: 887–894.

Sukigara, S., Gandhi, M., Ayutsede, J., Micklus, M., and Ko, F. (2003). Regeneration of Bombyx mori silk by electrospinning—part 1: processing parameters and geometric properties. *Polymer*, 44: 5721–5727.

Surewicz, W. K., and Mantsch, H. H. (1988). *New insight into protein secondary structure from resolution-enhanced infrared spectra*. *Biochimica et Biophysica Acta (BBA)/Protein Structure and Molecular, 952*(C): 115-130.

Tambralli, A., Blakeney, B., Anderson, J., Kushwaha, M., Andukuri, A., Dean, D., and Jun, H.W. (2009) A hybrid biomimetic scaffold composed of electrospum Polycaprolactone nanofibers and self-assembled peptide amphiphile nanofibers. *Biofabrication* 1, 025001, 11.

Tang, H., Kambris, Z., Lemaitre, B., and Hashimoto, C. (2008). A serpin that regulates immune melanization in the respiratory system of Drosophila. *Developmental Cell*, 15 (4): 617-626.

Thompson, R. C.; Yaszembksi, M. J.; Powers, J. M.; Harrigan, T. P. & Mikos, A. G (1995b). Poly (a-hydroxy ester)/short fiber hydroxyapatite composite foams for orthopaedic applications. In: Polymers in Medicine and Pharmacy, Vol 394. Mikos AG, Leong KW, Yaszemski MJ, (Ed.). pp. 25-30. *Materials Research Society Symposium Proceedings*, Pittsburgh USA

Thompson, R.C., Wake, M.C., Yaszemski and Mikos, A.G. (1995) Biodegradable polymer scaffolds to regenerate organs. *Advanced Polymer Science*, 122: 245-274.

Thompson, R.C., Wake, M.C., Yaszemski and Mikos, A.G. (1995). Biodegradable polymer scaffolds to regenerate organs. *Advanced Polymer Science*, 122: 245-274.

Thompson, R.C., Yaszembksi, M.J., Powers, J.M., Harrigan, T.P., and Mikos, A.G.(1995). Poly (a-hydroxy ester)/short fiber hydroxyapatite composite foams for orthopaedic applications. In: Polymers in Medicine and Pharmacy. *European cells and materials*, 5: 394.

Tschoppe, P., Zandim, D.L., Martus, P., and Kielbassa, A.M. (2002). Enamel and dentine remineralization by Kong LB, Ma T, Boey F. Nanosized hydroxyapatite powders derived from coprecipitation process. *Journal of Materials Science*, 37: 1131.

Ulloa-Montoya, F., Verfaillie, C.M., and Hu, W.S. (2005). Culture systems for pluripotent stem cells. *Journal of Bioscience and Bioengineering*, 100: 12-27.

Vacanti, J.P., and Langer R. (1999). Tissue engineering: the design and fabrication of living replacement devices for surgical reconstruction and transplantation. *Lance*t, 354: SI32-SI34.

Vachiraroj, N., Ratanavaraporn, J., Damrongsakkul, S., Pichyangkura, R., Banaprasert, T., and Kanokpanont, S. (2009). A comparison of Thai silk fibroin-based and chitosan-based materials on in vitro biocompatibility for bone substitutes. *International Journal of Biological Macromolecules*, 45: 470-7.

Vasita, R., and Katti, D.S. (2006). Growth factor-delivery systems for tissue engineering: a materials perspective. *Expert Review of Medical Devices*, 3: 29-47.

Vecchio, K.S., Zhang, X., Massie, J.B., Wang, M., and Kim, C.W. (2007). Conversion of bulk seashell to biocompatible hydroxyapatite for bone implants. *Acta Biomaterialia*, 3: 910-8.

Venugopal, J., Prabhakaran, M.P., Low, S., Choon, A.T., Zhang, Y.Z., Deepika, G., and Ramakrishna, S. (2008). Nanotechnology for nanomedicine and delivery of drugs. *Current Pharm Design*, 14(22): 2184-200.

Vepari, C., and Kaplan, D.L. (2007). Silk as a Biomaterial. *Progress Polymer Science*, 32(8-9): 991-1007.

Williams, D.F.(2008) On the mechanisms of biocompatibility. *Biomaterials*, 29(20): 2941- 2953.

Wilson-Hench, J. (1987). Osteoinduction. In: Williams DF Progress in biomedical engineering. Definitions in biomaterials. *Elsevier*, 4: 29.

Wolach, B., van der Laan, L.J., Maianski, N.A., Tool, T.A., VanBruggen, R., Roos, D., and Kuijpers (2007). Granulocyte concentrates: prolonged functional capacity during storage in the presence of phenotypic changes. *Experimental Hematology*, 35(4): 541

Woodfield, T.B., Guggenheim, M., von Rechenberg, B., Riesle, J., van Blitterswijk, C.A., and Wedler V. (2009). Rapid prototyping of anatomically shaped, tissue engineered implants for restoring congruent articulating surfaces in small joints. *Cell Proliferation*, 4: 485-97.

Xiang, Z., Liao, R., Kelly, M.S., and Spector, M. (2006). Collagen–GAG scaffolds grafted onto myocardial infarcts in a rat model: a delivery vehicle for mesenchymal stem cells. *Journal of Tissue Engineering*, 12: 2467–2478.

Xiaohua, Liu., and Peter X, Ma.(2004). Polymeric Scaffolds for Bone Tissue Engineering. *The Journal of the Biomedical Engineering Society,* 32(3): 477–486.

Xu, J., McCarthy, S.P., Gross, R.A., and Kaplan, D.L. (1996). Chitosan film acylation and effects on biodegradability. *Macromolecules*, 29: 3436-3440.

Yamazaki, C.M., Kadoya, Y., Hozumi, K., Okano-Kosugi, H., Asada, S., Kitagawa, K., Nomizu, M., and Koide, T. (2010). A collagen-mimetic triple helical supramolecule that evokes integrin-dependent cell responses. *Biomaterials*, 31(7): 1925-34.

Yang, F., Murugan, R., Wang, S., and Ramakrishna, S. (2005). Electrospinning of nano/micro scale poly (L-lactic acid) aligned fibers and their potential in neural tissue engineering. *Biomaterials*, 26: 2603–2610.

Yi, H., Wu, L.Q., Bentley, W.E., Ghodssi, R., Rubloff, G.W., Culver, J.N., and Payne, G.F. (2005). Biofabrication with Chitosan. *Bio macromolecules*, 6: 2881–2894.

Zanetti, A.S., Sabliov, C., Gimble, J.M., and Hayes, D.J. (2013). Human adipose-derived stem cells and three-dimensional scaffold constructs: a review of the biomaterials and models currently used for bone regeneration. *Journal of Biomedical Materials Research*, 101: 187-199.

Zanetti, A.S., Sabliov, C., Gimble, J.M., and Hayes, D.J. (2013). Human adipose-derived stem cells and three dimensional scaffold constructs: a review of the biomaterials and models currently used for bone regeneration. *Journal of Biomedical Materials Research Part B Applied Biomaterials*, 101: 187-199.

Zarkoob, S., Eby, R.K., Reneker, D.H., Hudson, S.D., Ertley, D., and Adams, W.W. (2004). Structure and morphology of electrospun silk nanofibers. *Polymer*, 45: 3973–3977.

Zeng, Q., Li, X., Beck, G., Balian, G., and Shen, F.H. (2007). Growth and differentiation factor-5 (GDF-5) stimulates osteogenic differentiation and increases vascular endothelial growth factor (VEGF) levels in fat-derived stromal cells *in vitro*. *Bone*, 40: 374.

Zhang, S. (2003). Fabrication of novel biomaterial through molecular self-assembly. *Nature Biotechnology*, 21: 1171-1178.

Zhang, Y., Bell, A., Perlman, P.S., and Leibowitz, M.J. (2000). Pentamidine inhibits mitochondrial intron splicing and translation in Saccharomyces cerevisiae. *RNA*, 6(7): 937-51.

Zhang,Y., Kihara,D., and Skolnick, j. (2002). Local energy landscape flattening: Parallel hyperbolic Monte Carlo sampling of protein folding. *Proteins: Structure, Function, and Bioinformatics,* 48: 192 (2002).

Zhang. S., Zhao, X., and Spirio L. (2006). Pura matrix: self-assembling peptide nanofiber scaffolds. In "scaffolding in tissue Engineering "(P.X. Ma and J Elisseeff eds.). *International Journal of Nanomedicine*, 217-236.

Zhou, J., Xu, C., Wu, G., Cao, X., Zhang, L., Zhai, Z., Zheng, Z., Chen, X., and Wang, Y. (2011). In vitro generation of osteochondral differentiation of human marrow mesenchymal stem cells in novel collagen-hydroxyapatite layered scaffolds. *Acta Biomateralials*, 7: 3999-4006.

Appendix - I

List of Abbreviations (Symbol)

%	Percentage
°C	Degree Centigrade
g/cm^3	Gram per centimeter cube
=	Equal
~	Proportional
G	Gram
cm^{-1}	Per centimeter
mol/L	Mole per milliliter
H	Hour
U/ml	Unit per milliliter
&	And
et.al	And others
Etc	Etcetera
Fig	Figure
M	Molar
ml	Milliliter
mg	Milligram
(+)Ve	Positive
(-)Ve	Negative
µm	Micrometer

kGy	Kilogray
V	Volume

List of Abbreviations (General Terms)

nHA	Nano-Hydroxyapatite
Chi	Chitosan
Alg	Alginate
HBA	Human Bone Allograft
BTE	Bone tissue engineering
TE	Tissue engineering
PBS	Phosphate buffered saline
SEM	Scanning electron microscope
FTIR	Fourier transform infrared spectroscopy
ESC	Embryonic stem cell
ASC	Adult stem cell
Ang	Angiopoietin
BMP	Bone morphogenetic protein
EGF	Epidermal growth factor
EPO	Erythropoietin
FGF	Fibroblast growth factor
G-CSF	Granulocyte-colony stimulating factor

GM-CSF	Granulocyte-macrophage colony-stimulating factor
HGF	Hepatocyte growth Factor
IGF	Insulin-like growth Factor
GDF	Growth and differentiation Factor
NGF	Nerve growth factor
PDGF	Platelet-derived growth factor
TGF	Transforming growth factor
TGF	Thrombopoietin
VEGF	Vascular endothelial growth factor
GAG	Glycosaminoglycan
ECM	Extracellular matrix
PLLA	Poly(L-lactic acid)
PGA	Phosphoglyceric acid
PA	Peptide ampholites
RP	Rapid prototyping
CAD	Computer added design
FDM	Fused deposition modeling
SLS	Selective laser sintering
PLGA	Poly lactic-*co*-glycolic acid
ATR	Attenuated total reflection
SDS	Sodium Dodecyl Sulfate
PAGE	Polyacrylamide gel electrophoresis

Appendix-II

Equipments:

- Hot air oven (Salvis Lab, Switzerland)
- Autoclave (HYSC, Model: AC-100, Korea)
- Magnetic Stirrer (Phoenix Instrument, RSM-0.2HD)
- Sonicator bath (Power Sonic-420)
- pH meter (pH-98107)
- Freeze (Lab Cold, Model: RLHE0845, UK)
- Freeze Dryer (Alpha1-4LD, CHRIST)
- Weighting balance (EP 420A, SWISS)
- Deionized water machine (ELGA, Reservoir 40L)
- Fourier Transform Infrared Spectroscopy (FTIR, IRPrestige21, Japan)
- Scanning Electron Microscope (SEM, JSM-6490LA)

Glassware and Other accessories:

- Beakers: 250 ml, 500 ml, 1000 ml
- Conical flasks: 100 ml, 250 ml, 500 ml
- Measuring cylinder: 50 ml, 500 ml, 1000 ml
- Pipettes: 10 ml
- Pipette holder
- Petri dishes
- Scissors
- Forceps
- Sterile cotton
- Sterile aluminum foil
- Filter paper
- Glass rod
- Sterile cotton
- Tissue paper

Materials

Components:

1. Alginate (Alginic acid calcium salt form, brown algae, CAS: 9005-35-0)
2. Chitosan (chitosan, deacetylate chitin CAS: 9012-76-4)

Cross linker:

1. HEMA (2-Hydroxyethyl Methacrylate, Sigma USA)
2. Glutaraldehyde (Sigma, USA)
3. Dehydrothermal (DHT)

Solvents:

1. Acetic acid (Essigsaure 99.100%, (1048-1054) reinst)
2. Deionized water
3. Methanol

Minerals:

1. Calcium chloride ($CaCl_2$)
2. Dihydrogen potassium phosphate (KH_2PO_4)
3. Sodium chloride (NaCl)

Peptide:

Porcine pepsin

Appendix- III

Chemical composition:

1% Acetic Acid Solution

Acetic Acid	1 ml
Distilled water	99 ml

50% methanol solution

Methanol	50 ml
Distilled water	50 ml

Porcine pepsin

Porcine pepsin	2 mg
Distilled water	100 ml

3.5 M NaCl solution

NaCl	142.5 g
Distilled water	1L

Phosphate Buffered Saline (500 ml)

Potassium Chloride	0.10 g
Sodium Chloride	4.00 g
KH_2PO_4	0.10 g
Na_2HPO_4	0.717 g
Distilled water	500 ml
P^H	7.4

2% NaOH Solution

NaOH	2 g
Distilled water	98 ml

0.5%, 1%, 1.5% and 2% HEMA solution

0.25ml (0.5%)	50 ml
0.5ml (1%)	50 ml
0.75ml (1.5%)	50 ml
1ml (2%)	50 ml

*1ml = 1000 µl